

**DESIGN, FABRICATION AND NOVEL CALIBRATION
TECHNIQUES FOR HEAT TRANSFER GAUGES
DURING SHORT-DURATION TRANSIENT
MEASUREMENT**

A Thesis

*Submitted in Partial Fulfillment of the Requirements for
the Award of the Degree of*

DOCTOR OF PHILOSOPHY

By

Rakesh Kumar



**DEPARTMENT OF MECHANICAL ENGINEERING
INDIAN INSTITUTE OF TECHNOLOGY GUWAHATI
GUWAHATI – 781039**

INDIA

JANUARY 2014



Dedicated to My Parents
Shri Damodar Prasad and Mrs. Savitri Devi,
brother Shri Rajeev Kumar and his family,
brother Dr. Ravi Ranjan

CERTIFICATE

It is certified that the work contained in the thesis entitled **Design, Fabrication and Novel Calibration Techniques for Heat Transfer Gauges during Short-Duration Transient Measurement** by **Rakesh Kumar**, a student in the Department of Mechanical Engineering, Indian Institute of Technology Guwahati, India, for the award of the degree of the **Doctor of Philosophy**, has been carried out under my supervision and that this work has not been submitted elsewhere for the degree.

Dr. Niranjana Sahoo

Associate Professor

Department of Mechanical Engineering

Indian Institute of Technology Guwahati

Guwahati – 781039, Assam, India

Acknowledgements

I am deeply indebted to my supervisor, **Dr. Niranjan Sahoo**, for their invaluable guidance and steady encouragement throughout my Ph. D. program. The vigour and attention bestowed by them in taking my research ahead in difficult times will never be forgotten. Starting from formulating the problems to the final experimental results and their physical interpretations, he remained deeply involved in my thesis work. He provided me with most innovative ideas, helpful books and journals that were very helpful in successfully completing the present thesis. I have immensely benefited from each and every moment of my associated with him. As my supervisor, his personal character with Great Spirit and enthusiasm will remain a source of inspiration for the rest of my life. I am highly inspired by his intellectual prowess and exemplary professionalism.

I am extremely grateful to **Dr. Vinayak Kulkarni** for their support and guidance to carry out a part of my research work. The thing which likes me about **Dr. Kulkarni** is the way he approaches and handles the problem. It is simply unsurpassed. I would also like to thank for providing the sensor materials and necessary instrumentation.

I am thankful to my doctoral committee members, namely, **Prof. Anoop Kumar Dass, Dr. Anugrah Singh** and **Dr. Vinayak Kulkarni** for providing insightful comments and valuable suggestions during the annual progressive seminars and on other occasions too. Their suggestions helped me work in a focused manner and improve my communication skills. I am grateful to all of them. I would like to express my sincere thanks to the highly skilled workshop personnel for making components in time and making the experiments a success. I would like to express my sincere thanks to **Prof. U. S. Dixit, Prof. S. C. Mishra, Prof. P. Mahanta, Prof. U. K. Saha** and **Prof. S. K. Dwivedy** and other faculty members of the Department of Mechanical

Engineering for their encouragement and support. I am also thankful to the all **Scientific Officer, Lab Assistant** and **Administrative Staff** of IIT Guwahati who directly and indirectly helped me to complete the thesis work.

I am sincerely thankful to **Biplab Kumar Debnath, Ravi Kumar Peetala** and **Bipin John** was a helping hand and an academic partner in many discussions ranging from the basis of heat transfer measurement analysis. In the same way **Dr. Ranjan Das, Dr. V. K. Pantangi, Dr. B. B. Sahoo, Dr. R. Chopdae, Dr. Ratnakar Das, Dr. Sachine Singh, Mohit Lal, Perumalla Janaki Ramula, Pallekonda Ramesh Babu, Srikant Prasad, Niraj Kumar Mishra, Daya Shankar, Bharat Kawale, Sandip Chavan, Jayesh Kanayi, Varun Karthik, Himanshu Shekhar Jha, Searjul Haque Faizi, Kuntal Deka** and **Rajesh Ranjan** gave me remarkable moral support without which it would have been difficult for me to stay 1000km from home. **Sumit Agarwal** indeed played the role of the friend in need. The company of my friends in IIT Guwahati made me “complete.” Because of them, I really “lived a life” here. Everybody of them deserves a special thank for being with me when I was in distress and when I was happy.

I am extremely thankful to all of my family members for their patience and the enormous trust they repose in my abilities. Without their moral support and wishes it would have been difficult for me to reach this position.

And last, but not least, I would like to extend my sincere thanks to who are all helped me directly and indirectly for the successful completion of the thesis.

January 2014
IIT Guwahati

Rakesh Kumar

List of Publications from this Thesis Work

1. R. Kumar, N. Sahoo and V. Kulkarni (2010) Design, Fabrication and Calibration of Heat Transfer Gauges for Transient Measurement, **ASME International Mechanical Engineering Congress & Exposition**, November 12-18, Vancouver, British Columbia, Canada, IMECE2010: 40253.
2. R. Kumar and N. Sahoo (2010) One Dimensional Heat Flux Analysis of Heat Transfer Thin Film Gauges for Transient Measurement, **5TH International Conference on Theoretical, Applied Computational and Experimental Mechanics**, December 27-29, IIT Kharagpur, India, ICTACEM2010: 109-111.
3. R. Kumar, N. Sahoo, V. Kulkarni and A. Singh (2011) Laser Based Calibration Technique for Thin Film Sensors for Short Duration Transient Measurements, **ASME Journal of Thermal Science and Engineering Applications**, 3 (4): 44504-44509.
4. R. Kumar and N. Sahoo (2011) Enhancement of Thermal Properties for Platinum Thin Film Heat Transfer Gauges with Nanofluids, **28TH International Symposium on Shock Waves**, July 17-22, The University of Manchester, UK, ISSW28 - 2179.
5. R. Kumar and N. Sahoo (2011) Property Analysis of Mixtures of High Conducting Platinum and Grapheme Materials, **International Conference on Advances in Materials and Materials Processing**, December 9-11, IIT Kharagpur, India, ICAMMP2011: 178-179.
6. R. Kumar, N. Sahoo and V. Kulkarni (2012) Conduction Based Calibration of Handmade Platinum Thin Film Gauges for Transient Measurements, **International Journal of Heat and Mass Transfer**, 55: 2707-2713.
7. R. Kumar, P. Jayesh and N. Sahoo (2012) Analysis of One Dimensional Inverse Heat Conduction Problem: A Review, **International Journal of Mechanical & Industrial Engineering**, 2(1): 2231:2239.
8. R. Kumar and N. Sahoo (2013) Design, Fabrication and Sensitivity Analysis of the Resistance Temperature Detector Thin Film Sensors, **International Journal of Mechanical and Industrial Engineering**, 2(4): 20-25.
9. R. Kumar and N. Sahoo (2013) Dynamic Calibration of a Coaxial Thermocouple for Transient Measurements, **ASME Journal of Heat Transfer**, 135: 124502-1.

ABSTRACT

Measurement of transient surface temperature and heat flux is the major requirement in many scientific and engineering applications such as design of combustion chamber in internal combustion engines, design of systems/sub-systems like heat exchanger, steam/gas turbines and thermal protection systems for high speed flight vehicles. In each of the cases, the technique used for accurate heat fluxes measurement must be suited for transient conditions and must have a fast enough response time to trace variations caused by rapidly change in flow conditions. Moreover, there are certain practical situations in which it may not be feasible to keep the thermal sensors exactly on the surface rather they are measured at some interior points inside the medium. For any case, the surface heat fluxes are mostly predicted from the measured temperature histories. The surface heat transfer mapping technique uses very fast response sensors to capture the transient temperature variations and subsequently, the heat fluxes are obtained through appropriate heat transfer modelling. Thus, the estimation of proper temporal nature of heat load and precise quantification of heat fluxes are the roots of a typical temperature sensor during transient measurements.

Thin film gauges (TFGs) and coaxial thermocouples are resistance temperature detector sensors, suitable in measuring highly transient surface temperatures because the response time of these sensors are in the range of microseconds. The transient measurement of temperatures is usually performed by mounting these sensors embedded inside the heated material surface. The surface heat fluxes are then estimated from the measured temperature history through one-dimensional analytical heat transfer modelling. Thin film heat transfer gauges are generally made out of temperature sensitive materials (platinum/nickel/silver) and deposited on an insulated substrate material (pyrex/quartz/macor). The temperature sensing materials are normally

available in the form of paste/ink form and are used to prepare thin film on the substrate material. Moreover, their resistances are extremely sensitive to temperature that varies linearly with temperature. The importance of thin film sensors for prediction of transient heat flux measurement have been highlighted by many researchers. However, when it is desired to have measurement of small order of magnitude of heat flux ($\sim 1 \text{ W/m}^2$), the accuracy becomes an issue. It is mainly because of the limitations in thermal properties of gauge material and its sensitivity. With recent advances in nano-technology, it is possible to enhance the thermal properties by mixing nano-particles into the gauge materials i.e. platinum/nickel/silver. Dispersion or suspension of nano-particles of high thermal conductivities into base materials gives rise to higher thermal conductivity of the mixtures thereby increasing the heat transfer coefficient. Carbon nano tubes (CNTs) are a new form of materials are found to be most effective nano-particles because of their unique thermal conductivity (3000 W/mK), chemical stability, excellent electrical conductivity, high surface area and strong mechanical strength associated with high aspect ratio (~ 2000). So, the substantial thermal property enhancement is expected when CNT materials (typically sizes of 1-100nm) are added to the base material (platinum/nickel/silver).

In coaxial thermocouples, two dissimilar metals are joined together to form a junction and when exposed to a temperature gradient, a corresponding voltage is generated (Seebeck effect). This is in contrast to the thin film gauges which require a current source to record the voltage change and thus considered as passive devices. The coaxial thermocouples are generally fabricated by one thermocouple element is swaged over the second element with an insulating material in between with a typical thickness of about in micrometers. The thermocouple junction is simply formed by grinding its front surface with sandpaper. The micro-scratches generated by

this process form the active junction of the thermocouple and it represents a very small amount of active mass resulting in a short response time. The voltage difference generated can then be measured and related to the corresponding temperature gradient with respect to a known reference temperature.

The present work mainly involves the design, fabrication and analysis of different types of heat transfer gauges in the laboratory. In this work, three type's thermal sensors (platinum material based, platinum/nano materials based and coaxial thermocouple) have been fabricated. In case of thin films, the high conducting (sensing element) platinum material is deposited as a film over the surface of pyrex and macor (low conducting substrate material). The thermal conductivity plays an important role in the development of heat transfer sensors. So, this work also involves re-fabrication of thin film gauges by mixing high thermal conducting CNTs nano materials into the base fluid (i.e platinum) material of the heat transfer gauge. The effective thermal conductivity of the mixtures calculated from the empirical equation and it is found that thermal conductivity of the base material improves significantly. After successful fabrications of heat transfer gauges these sensors are calibrated for temperature as well as and heat fluxes in different types of simple laboratory instruments. An oil bath experimental setup is used to check linearity between changes in voltage with change in temperature and calculate thermal coefficient of resistance as well as sensitivity of each handmade thermal sensor. In radiation and conduction based dynamic calibration technique, step heat loads of known input wattage are applied on the sensing area of the gauges. Then, outputs from the gauges are measured with the help of transient temperature signal measuring instruments. For the known heating load, temperature signal are also predicted using one dimensional transient heat conduction solver using ANSYS. The temperature histories obtained using experimental, numerical and analytical

analysis showed almost same results. However, minor difference is observed when the simulated temperature signals are compared with the experiments. It could be due to the use of standard thermal properties for platinum and pyrex materials during simulation. Recorded transient temperature data is processed for estimation of input heat fluxes using various numerical and analytical models. The average value of uncertainty between input heat flux and measured heat fluxes calculated for platinum TFGs, nanomaterial based platinum TFGs and coaxial thermocouple are found to be 1.6%, 2.4% and 4.1%, respectively.

The measurement of stagnation point heating rates is also very important because it is a point where maximum amount of heat fluxes are generated compared to the other locations when the flow is brought to rest by any obstructing medium. An experimental setup is fabricated for this purpose to generate heated air jet moving at sonic speed. Also, separate stagnation probes with thin film gauges with necessary instrumentations are designed and fabricated. All the handmade gauges prepared are exposed to this flow environment and the corresponding temperature histories are captured and subsequently the surface heat fluxes are calculated. Also, the numerical technique (FLUENT CFD) is used to compare the experimental results with reasonable accuracy ($\pm 4\%$). Thus, the handmade heat transfer gauges can be very useful in the laboratory experiments. Being small in sizes, all the gauges can be flush-mounted on the experimental surfaces. High precision, sensitivity and rapid response times are some of the important advantages that justifies the use of these heat transfer gauges in short duration transient measurements.

Contents

Title		Page No.
Cover Page		i
Certificate		iii
Acknowledgements		iv
List of Publications from this Thesis Work		vi
Abstract		vii
Contents		xi
List of Figures		xiv
List of Tables		xviii
Nomenclature		xix
Abbreviations		xx
Chapter - 1	Introduction	1
1.1	Heat transfer	2
1.1.1	Conduction heat transfer	3
1.1.2	Convection heat transfer	3
1.1.3	Radiation heat transfer	5
1.2	Transient state of heat transfer	6
1.3	Transient state temperature measuring device	7
1.3.1	Thermocouple	7
1.3.2	Thin film gauge	9
1.3.3	Coaxial thermocouple	10
1.3.4	Liquid crystal thermography	12

1.3.5	Infrared thermography	13
1.4	Nanoparticles	13
1.5	Nanofluids	15
1.6	Objective of the present investigation	16
1.7	Thesis organization	19
Chapter - 2	Literature Review	21
2.1	Literature review on heat transfer gauges	22
2.2	Literature review on transient heat transfer measurement techniques	32
2.3	Literature review on nanomaterials and nanofluids	40
Chapter - 3	Design and Fabrication of Heat Transfer Gauges	49
3.1	Introduction	50
3.2	Design and fabrication of heat transfer gauges	55
3.2.1	Platinum thin film gauges	55
3.2.2	Platinum-CNT thin film gauges	59
3.2.3	Fabrication of K-type coaxial thermocouple sensor	62
3.3	Preliminary analysis of the heat transfer gauges	63
3.3.1	Thermal property analysis of Platinum-CNT mixtures	63
3.3.2	Surface morphology of the platinum-CNT sensor	66
3.3.3	Effective thermal properties for sensors	67
3.3.4	Analysis of heat transfer sensors thickness	68
3.4	Surface temperature analysis	70
3.5	Summary	74
Chapter - 4	Static Calibration of the Heat Transfer Gauges for Transient	75

	Measurement	
4.1	Introduction	76
4.2	Working principle of the heat transfer gauges	79
4.3	Sensitivity analysis of heat transfer gauges	81
4.4	Static calibration of heat transfer gauges	82
4.5	Results and Discussions	84
4.6	Summary	89
Chapter - 5	Dynamic Calibration of Heat Transfer Gauges for Transient Heat Flux Measurement	90
5.1	Introduction	91
5.2	Dynamic calibration experiments and computational analysis	94
5.2.1	Radiation based experimental calibration technique	94
5.2.2	Conduction based experimental calibration technique	100
5.2.3	Finite element simulation	107
5.2.4	Determination of temperature history from analytical formulation	115
5.3	One dimensional heat conduction theory	116
5.4	Summary	128
Chapter - 6	Stagnation Point Heat Flux Measurement With Heat Transfer Gauges	130
6.1	Introduction	131
6.2	Measurement of stagnation point heat fluxes	133
6.2.1	Theoretical analysis	133
6.2.2	Experimental investigation	135
6.2.3	Numerical analysis	137

6.2.4	Experimental results and discussions	143
6.3	Summary	150
Chapter - 7	Conclusions and Scope for Future Research	152
	Conclusions	152
	Scope of Future Work	155
References		157
Appendix		172
Appendix - I		172
Appendix - II		177
Appendix - III		177
Appendix - IV		180

List of Figures

Fig. No.	Figure Title	Page No.
1.1	Modes of heat transfer	2
1.2	Schematic diagram of the thermocouple	8
1.3	Schematic diagram of thin film heat transfer gauge	10
1.4	Schematic diagram of coaxial thermocouple	12
1.5	SEM diagram of the nanofluids	16
3.1	Platinum thin film heat transfer gauges or thermal sensors when pyrex or macor as a substrate material	58
3.2	Photograph of a platinum/CNT thin film heat transfer gauge	61
3.3	Photograph of a coaxial thermocouple sensor	63

3.4	Variation of effective thermal conductivity with CNT mass fractions	65
3.5	Variation of effective thermal diffusivity with CNT mass fractions	65
3.6	Surface morphology (SEM image) of thin film sensors	66
3.7	Gauge material thickness of (a) platinum and (b) platinum/CNT sensor	69
3.8	Heat conduction analysis of heat transfer gauge	71
3.9	Determination of substrate thickness for semi-infinite assumptions with pyrex substrate	72
3.10	Determination of substrate thickness for semi-infinite assumptions with macor substrate	72
3.11	Determination of substrate thickness for semi-infinite assumptions with chromel substrate	73
3.12	Determination of substrate thickness for semi-infinite assumptions with alumel substrate	73
4.1	Laboratory setup of constant current source and thermal sensor	81
4.2	Laboratory set up of oil bath type calibration	86
4.3	Schematic diagram oil bath type calibration	86
4.4	Typical temperature-voltage signal measured from platinum thin film heat transfer gauge	87
4.5	Typical temperature-voltage signal measured from platinum/CNT thin film heat transfer gauge	87
4.6	Typical temperature-voltage signal measured from K-type coaxial thermocouple heat transfer sensor	88
4.7	Comparison of sensitivity between different types of heat transfer sensors	88
5.1	Schematic diagram of radiation or laser based experimental setup for dynamic calibration of heat transfer gauges	96
5.2	Laboratry setup for radiation or laser based experiment	96

5.3	Transient (a) original and (b) filter voltage signal for platinum thin film sensor at radiation based step load	97
5.4	Transient (a) original and (b) filter voltage signal for platinum/CNT thin film sensor at radiation based step load	98
5.5	Transient (a) original and (b) filter voltage signal for coaxial thermocouple at radiation based step load	99
5.6	Comparison of temperature histories for various types of heat transfer gauges at radiation based step heat loads	100
5.7	Schematic diagram of an experimental setup for conduction based calibration of heat transfer gauges	101
5.8	Laboratry set up for (a.) Constant heat flux type heater and (b.) PC based data acquisition system	102
5.9	Heater plate surface	102
5.10	Transient temperature signals for platinum thin film gauge at conduction based step heat load	104
5.11	Transient temperature signals for platinum/CNT thin film gauge at conduction based step heat load	105
5.12	Transient temperature signals for coaxial thermocouple sensor at radiation and conduction based step heat load	107
5.13	Schematic diagram of thin film gauge used for computational study	108
5.14	Geometric configuration of the coaxial thermocouple sensor	108
5.15	Geometric configuration of the platinum film mounted on a pyrex substrate	110
5.16	Geometric configuration of the coaxial thermocouple (a) computational model of the thermocouple elements (b) sensing junction and substrate material (c) vertical enlarged view to show the finite element mesh	111
5.17	Typical time heat flux signal obtained from numerical inverse analysis	111
5.18	Contours of total temperature distribution of (a) platinum thin film gauge for 10ms duration (b) platinum thin film gauge for 10s duration	

	(c) platinum/CNT thin film gauge for 10ms duration and (d) coaxial thermocouple sensor for 10ms duration	112
5.19	Comparison of transient temperature signals for platinum thin film gauge at radiation based step heat load	114
5.20	Schematic diagram of the one dimensional semi-infinite body	116
5.21	Comparison of heat fluxes histories for various types of heat transfer gauges at radiation based step heat loads	121
5.22	Transient heat flux signals for platinum thin film sensor at conduction based step heat load	123
5.23	Transient heat flux signals for platinum/CNT thin film sensor at conduction based step heat load	124
5.24	Transient heat flux signals for coaxial thermocouple sensor at radiation and conduction based step heat load	126
5.25	Comparison of transient heat flux signals for platinum thin film sensor at radiation based step heat load	128
6.1	Laboratory setup for insulated solid cylinder with pressure gauge, heater and thermocouple	135
6.2	Thin film based heat transfer gauge over a blunt shaped bodies with macor as substrate material	136
6.3	Fabrication of coaxial thermocouple in the laboratory	137
6.4	Computational model of a flow field	139
6.5	Contour of velocity distribution along the direction of flow field	139
6.6	Contour of pressure distribution along the direction of flow field	140
6.7	Computational model of a blunt shaped spherical sensor in a flow field	141
6.8	Finite element mesh for the flow field with blunt shaped spherical sensor	141
6.9	Contour of velocity distribution along the direction of flow field	142
6.10	Contour of total pressure distribution along the direction of flow field	142

6.11	Contour of static pressure distribution along the direction of flow field	143
6.12	Schematic diagram of the insulated solid cylinder with signal measuring source meter	145
6.13	Comparison of temperature histories for different types of heat transfer gauges	147
6.14	Comparison of heat fluxes histories for different types of heat transfer gauges	149
6.15	Comparison of numerical and experimental heat fluxes measured by different types of heat transfer sensors at stagnation point	150
A1	Pyrex substrate material	172
A2	Thin film gauge materials (a) platinum and (b) silver	172
A3	Digital temperature controlled furnace	173
A4	Highly conducting materials (a) platinum paste (b) thinner and (c) CNT power	173
A5	Mixture of platinum/CNT material in a beaker	174
A6	Experimental set up of the tip sonicator	174
A7	Coaxial thermocouple wires and instrument (Grinding machine) used in this work	175
A8	Sensor thickness measurement analysis by using (a) experimental setup of profilometry and (b) Dial-type Vernier Caliper	176

List of Tables

Table No.	Table Title	Page No.
1	Thermal properties of gauge and substrate materials	177
2	Thermal properties of nano materials	177
3	Thermal properties of alumel and chromel materials at different	178

	temperatures	
4	The mean value of thermal product at different temperatures	179
5	Uncertainty values of handmade heat transfer gauges	181

Nomenclature

R	Initial thin film gauge resistance (Ω)
ΔV	Change in voltage (V)
I	Current flow through the thin film gauges (A)
q_s	Heat transfer rate (W)
K	Thermal conductivity ($W / (mK)$)
α	Thermal diffusivity (m^2 / s)
ΔT	Change in temperature (K)
q''	Surface heat flux (W / m^2)
α_0	Thermal coefficient of resistance (K^{-1})
ρ	Density (Kg / m^3)
S	Sensitivity ($\mu V / ^\circ C$)
β	Effective thermal product ($J / m^2 S^{0.5} K$)
l_1	Sensing junction material thickness (m)
l_2	Sensor thickness (m)
h	Heat transfer coefficient ($W / (m^2 K)$)
t	Time in seconds (s)
c	Specific heat ($J / (kgK)$)
A	Area (m^2)

0	Initial condition
∞	Free stream

Abbreviations

MWCNT	Multi-walled carbon nanotube
IHCP	Inverse heat conduction problem
RTD	Resistance temperature detector
CCS	Constant current source
CCD	Charge coupled device
EMF	Electromotive force
DAS	Data acquisition system
TLC	Thermo-chromic liquid crystal
NDE	Non destructive evaluation
IRT	Infrared thermography
CNT	Carbon nano tube
IR	Infrared
UV	Ultra violet

Chapter - 1

Introduction

Heat transfer is a discipline of thermal engineering that concerns the generation, conversion and exchange between physical systems. The modes of heat transfer include conduction, convection and radiation. The quantity of heat transferred between some processes can either be directly measured or indirectly determined with appropriate modeling. Again the measurements may be steady or unsteady depending on the nature of process. There are many classical steady/unsteady modeling techniques for each of the modes of heat transfer in steady/unsteady cases. In all cases, the temperature measurement is the most vital which in turn used to predict the heat fluxes. In fact, all the processes in nature changes with time. So, obtaining the transient temperatures in most of the heat transfer problems is a challenge because of the nature of complication involved in it. For instance, if it is desired to predict at some interior part of a medium, it may not always be possible to design a temperature probe that can exactly be exposed to the flow rather the same can be mounted on the surface and appropriate heat transfer modeling technique can be used to predict the unknown heat fluxes. The overall objective of this research is to design and fabricate heat transfer gauges having very short response time. Subsequently, appropriate heat transfer modeling techniques can be used to predict the heat fluxes. Application of these heat transfer gauges are intended for short duration high speed flows such as shock tunnels, gun tunnels and wind tunnels. In this chapter, a brief historical background and some classical measurement techniques are discussed. Also, the research objectives of the present investigation are highlighted followed by overall organization of the entire thesis to meet these objectives.

1.1 Heat Transfer

The word *heat transfer* is mainly concerned with temperature and flow of heat. The temperature represents the amount of thermal energy available, while the heat flow represents the movement of thermal energy from place to place by virtue of temperature difference. In thermodynamic sense, it is one of the modes of energy transfer and is mainly governed by three fundamental laws. The *zeroth law* states that ‘no heat transfer’ takes place when two bodies are in thermal equilibrium i.e. the bodies are at same temperature. The *first law of thermodynamics* considers the law of conservation of energy and provides the basic of studying various forms of energy transfer and the energy interaction through work or heat. If it is desired to have heat transfer from a low temperature body to a high temperature body using a cyclic device, then the net effect is to add energy to the device in the form of work (second law of thermodynamics).

Heat is transferred by three mechanisms: conduction, convection and radiation. Conduction is the transfer of energy from more energetic particles of a substance to the adjacent less energetic ones as a result of interaction between particles. Convection is the transfer of energy between a solid surface and the adjacent moving fluid. Radiation is the transfer of energy due to electromagnetic wave or photon. All forms of heat transfer may occur in some systems (Bakken et al. 1974) at the same time as shown in Fig. 1.1.

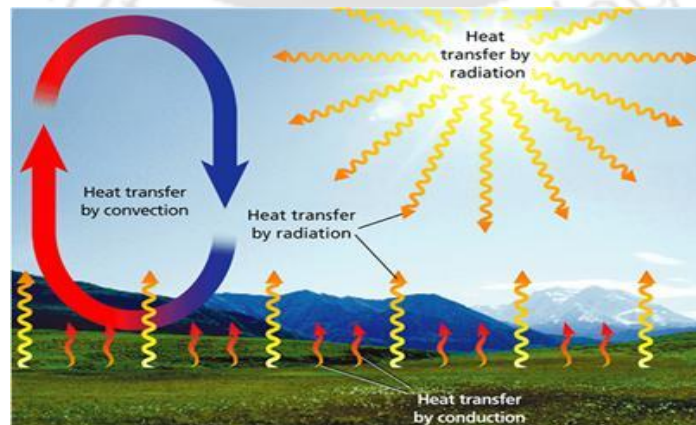


Fig. 1.1: Modes of heat transfer (Bakken et al. 1974)

1.1.1 Conduction Heat Transfer

Conduction is the transfer of thermal energy between neighboring molecules in a substance due to a temperature gradient. It always takes place from a region of higher temperature to a region of lower temperature and acts to equalize temperature differences as shown in Fig. 1.1. Conduction takes place in all forms of matter means solids, liquids, gases and plasmas but does not require any types of bulk motion of matter. In solids, it is due to the combination of vibrations of the molecules in a lattice and the energy transport by free electrons. In gases and liquids, conduction is due to the collisions and diffusion of the molecules during their random motion. Conduction is greater in solids (copper, platinum, gold etc.) because the network of relatively fixed spatial relationships between atoms helps to transfer energy between them by vibration. This is due to the way that metals are chemically and bonded in a metallic bonds (as opposed to covalent or ionic bonds) which have free moving electrons and able to transfer thermal energy rapidly through the metal. The electron fluid of a conductive metallic solid conducts nearly all of the heat flux through the solid. Electrons also conduct electric current through conductive solids and the thermal and electrical conductivities of most metals have about the same ratio. A good electrical conductor, such as copper, usually also conducts heat well. The See-beck effect exhibits the propensity of electrons to conduct heat through an electrically conductive solid. Thermoelectricity is caused by the relationship between electrons, heat fluxes and electrical currents. Heat conduction within a solid is directly analogous to diffusion of particles within a fluid, in the situation where there are no fluid currents.

1.1.2 Convection Heat Transfer

Heat energy transfers between a solid and a fluid when there is a temperature difference between the fluid and the solid, is known as convection heat transfer. Generally, convection heat transfer

cannot be ignored when there is a significant fluid motion around the solid. The temperature of the solid due to an external field such as fluid buoyancy can induce a fluid motion. It cannot take place in solids, since neither bulk current flows nor significant diffusion can take place in solids. Convection is one of the major modes of heat transfer and mass transfer. Convective heat and mass transfer take place through both diffusion random *Brownian motion* of individual particles in the fluid and by advection, in which matter or heat is transported by the larger scale motion of currents in the fluid. There are many forms of convection such as natural, forced, gravitational, granular, thermo magnetic, combustion and capillary action effects. Natural or free convection occurs due to temperature differences which affect the density and thus relative buoyancy of the fluid. Heavier (more dense) components will fall while lighter (less dense) components rise, leading to bulk fluid movement. Natural convection can only occur in a gravitational field as shown in Fig. 1.1. A common example of natural convection is a pot of boiling water in which the hot and less dense water on the bottom layer moves upwards in plumes and the cool and denser water near the top of the pot likewise sinks. Natural convection will be more likely and more rapid with a greater variation in density between the two fluids, a larger acceleration due to gravity that drives the convection and a larger distance through the convection medium.

In forced convection (also called heat advection), the fluid movement results from external surface forces such as a fan or pump. Forced convection is typically used to increase the rate of heat exchange. Many types of mixing also utilize forced convection to distribute one substance within another. Forced convection also occurs as a byproduct to other processes such as the action of a propeller in a fluid or aerodynamic heating. The familiar examples of forced convection are, fluid radiator systems, heating/cooling of parts of the body due to blood circulation etc. The forced convection produces results more quickly than free convection. For

instance a convection oven works by forced convection as a fan which rapidly circulates hot air forces heat into food faster than would naturally happen due to simple heating without the fan.

1.1.3 Radiation Heat Transfer

Thermal radiation is the emission of electromagnetic waves from all matter that has a temperature greater than absolute zero. It represents a conversion of thermal energy into electromagnetic energy. Thermal energy is the collective mean kinetic energy of the random movements of atoms and molecules in matter. Atoms and molecules are generally composed of charged particles i.e. protons and electrons. Their oscillations result in the electro dynamic generation of coupled electric and magnetic fields resulting in the emission of photons, radiating energy and carrying entropy away from the body through its surface boundary. Electromagnetic radiation or light does not require the presence of matter to propagate and travels in the vacuum of space infinitely far if unobstructed. The characteristics of thermal radiation depend on various properties of the surface it is emanating from including its temperature, spectral absorptive and spectral emissive power as expressed by *Kirchhoff's law*. Examples of thermal radiation include visible light emitted by an incandescent light bulb, infrared radiation emitted by animals and detectable with an infrared camera and the cosmic microwave background radiation.

Thermal radiation is different from convection and conduction. A person near a raging bonfire feels radiant heating from the fire even if the surrounding air is very cold. Sunlight is thermal radiation generated by the hot plasma of the sun. Earth also emits thermal radiation but at a much lower intensity and different spectral distribution because it is cooler. The Earth's absorption of solar radiation followed by its outgoing thermal radiation is the two most important processes that determine the temperature of the Earth. If a radiation emitting object meets the physical characteristics of a black body in thermodynamic equilibrium, the radiation is called

blackbody radiation. *Planck's law* describes the spectrum of blackbody radiation which depends only on the object's temperature. *Wien's displacement law* determines the most likely frequency of the emitted radiation while the *Stefan Boltzmann law* gives the information of radiant intensity. In engineering, thermal radiation is considered one of the fundamental methods of heat transfer although a physicist would likely consider energy transfer through thermal radiation a case of one system performing work on another via electromagnetic radiation and say that heat is a transfer of energy that does no work.

1.2 Transient State of Heat Transfer

Heat transfer is the exchange of thermal energy from a body at a high temperature to another body at a lower temperature. This transfer of thermal energy may occur under steady or unsteady state conditions. Under steady state conditions the temperature within the system at any particular point does not change with respect to time. Conversely, under unsteady or transient state conditions the temperature within the system does vary with time. Most of the heat transfer analysis is based on steady state measurements for which the experiments are performed and the initial transient is normally neglected. But, if the measurement time scale is small, then system dynamics becomes important. So, the measurement and prediction of heat transfer/temperature becomes crucial. Transient heat transfer is used in a variety of broad areas of applications such as internal combustion engines, gas turbines, aircrafts and aerospace industries etc.

In a non-generating system, the study of conduction heat transfers depends on the temperature that varies from point to point in the system and but it also undergoes a continuous change with time at any local point in the system. So, the temperature is a function of time and space coordinate and is expressed mathematically by the following equation;

$$T = f(x, y, z, t) \quad (1.1)$$

The process of transient, three-dimensional thermal heat conduction for a stationary, incompressible, continuous medium is generally expressed as;

$$\frac{\partial^2 T}{\partial x^2} + \frac{\partial^2 T}{\partial y^2} + \frac{\partial^2 T}{\partial z^2} = \left(\frac{\rho c}{k} \right) \frac{\partial T}{\partial t} \quad (1.2)$$

Where ρ , c and k are density, specific heat and thermal conductivity of the body and temperature (T) varies with time (t) in x , y and z coordinate. The solutions of the heat equation are characterized by a gradual smoothing of the initial temperature distribution by the flow of heat from warmer to colder areas of an object. Generally, many different states and starting conditions will tend toward the same stable equilibrium.

1.3 Transient State Temperature Measuring Device

In general, most of the transient devices measure the temperature history during the measurement time scale and the heating rates are subsequently predicted from these measurements. Some of these temperature sensors are discussed in this section.

1.3.1 Thermocouple

A thermocouple is a junction between two different metals that produces a voltage related to a temperature difference as shown in Fig.1.2. They are widely used as the temperature sensor for measurement/control where the heat energy is converted to electric power. They are quite inexpensive and are suitable for wide range of temperatures. The main limitation is the accuracy because it is difficult to achieve the system errors of less than one kelvin (K). Any junction of dissimilar metals will produce an electric potential related to temperature. So, they are called *active devices* because no other instruments are required to supply the power. Thermocouples for

practical measurement of temperature are junctions of specific alloys which have a predictable and repeatable relationship between temperature and voltage. Different alloys are used for different temperature ranges. Thermocouples measure the temperature difference between two points, not absolute temperature. To measure a single temperature, one of the junctions normally the cold junction is maintained at a known reference temperature and the other junction is at the temperature to be sensed. A junction of known temperature, while useful for laboratory calibration, is not convenient for most measurement and control applications. Hence, the voltage from a known cold junction can be simulated and the appropriate correction applied. This is known as "cold junction compensation". Practical instruments (Data Acquisition System and Oscilloscope) use electronic methods of cold-junction compensation to adjust for varying temperature at the instrument terminals for specific thermocouple types (K, T, E). Properties such as resistance to corrosion may also be important when choosing a new type of thermocouple. Where the measurement point is far from the measuring instrument, the intermediate connection can be made by extension wires which are less costly than the materials used to make the sensor. Thermocouples are widely used in science and industry; applications include temperature measurement for gas turbine exhaust, diesel engines, and other industrial processes. For wide range of temperatures, a conventional thermocouple is capable of measuring steady-state temperatures.

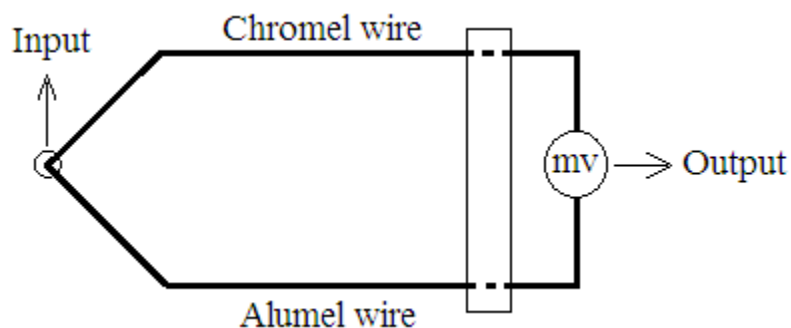


Fig. 1.2: Schematic diagram of the thermocouple

1.3.2 Thin Film Gauge

A thin film gauges (TFG) is a resistance temperature detector which is the combination of a high conducting (sensor) and lower conducting materials (substrate). It operates on the simple principle that penetration of heat pulse from the high conducting material to the low conduction one is very small during the time span of the measurement. The thin film (thickness of gauge film is negligible) is made out of temperature sensitive materials such (platinum/nickel/silver) and is deposited on an insulated substrate material (pyrex/macor/quartz) as shown in Fig. 1.3. Since the response time is very small, it allows the measurement of highly transient surface temperatures, typically, wind tunnel models in impulse facilities, change of the cylinder wall temperature during one cycle of a piston engine, all types of industrial applications and research-oriented work where the registration of highly transient temperatures is of importance. The response time of the TFGs has been proven to be in the range of microseconds. It is important to note that this strongly depends on the dynamic capabilities of the electronic equipment (amplifier, A/D conversion, etc.) of the measuring line which usually limits the achievable response time.

The TFGs are also suitable to measure constant temperatures with time but their superior field of application is in transient measurements. Given by the physics for highly transient processes the output of all gauges represents the time dependent temperature of its measuring part which in this case may significantly deviate from the temperature of the gauge surrounding heating or cooling environment. For example, in a piston engine a flush wall mounted temperature gauge registers with its typical response time the variation of the cylinder wall temperature and not the variation of the average gas temperature within the cylinder. The measured time dependent surface temperature of the gauge and its known thermal properties

allow to recalculate the time-dependent heat flux from the heating environment onto the gauge which caused the temperature change of the gauge. This is accomplished by the theory of heat conduction into a semi-infinite body.

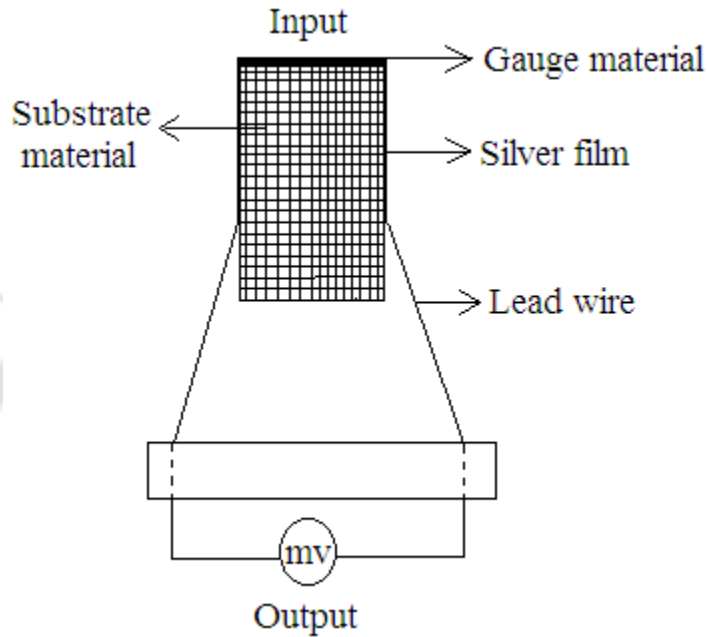


Fig. 1.3: Schematic diagram of thin film heat transfer gauge

1.3.3 Coaxial Thermocouple

Heat transfer plays an important role where experimental transient temperature data is needed to support the design effort. The need of coaxial thermocouple is felt for measuring transient temperatures in a short time duration flow (few microseconds). It arises in numerous heat transfer investigations particularly in internal combustion engine cylinder walls, aerodynamics facilities, gun barrels and in boiling experiments. Because of their simplicity and comparatively rapid response, fine wire thermocouples are usually employed. However, in certain applications fine wire thermocouples are unsatisfactory because of their lack of strength and difficulties in positioning the junction at the point of interest. Furthermore, the minimum size of the junction, which affects the rate of response, usually is limited to the wire diameter. Coaxial thermocouples

of E-type and K-type are available for different standard sizes. The special feature results from its unique design as shown in Fig. 1.4. Here, one thermocouple element is swaged over the second element with an electrical insulation in between with a typical thickness of about 10 μ m. The thermocouple allows a mounting through the wall which is important for the accurate measurement of a rapidly changing surface temperature. For some applications the wall temperature is of direct interest. In this case the probe material should have thermal properties which match those of the surrounding wall as close as possible. This is not a necessary requirement for determining convective heating rates by performing a fast surface temperature measurement with the help of a coaxial thermocouple. Usually the thermocouple is fixed in the wall by gluing at the rear part of the element. Installation by a thread is also possible which is recommended for higher operating temperatures. It is also possible to have a blind hole in the test wall to measure the internal material temperature at a known location. There is teflon based insulation is necessary between the thermocouple and the surrounding wall. Usually, the thermocouple junction is simply formed by grinding its front surface with sandpaper. The micro-scratches generated by this process form the active junction of the thermocouple and therewith, it represents a very small amount of active mass resulting in a short response time. The grinding of the front surface allows to perfectly fitting it into curved walls.

This method of forming the thermocouple junction makes the gauge very robust and suitable for the application in harsh environmental conditions. As an example, the impact of high speed particles transported by a fluid has in general no influence on the operation of the thermocouple. In case of a failure, grinding of the front surface again activates the thermocouple. Coaxial thermocouples are one order of magnitude less sensitive as compared to thin film gauges. But, due to their design, they are, very robust, easy to operate, able to withstand harsh

environmental conditions in extremely high heat fluxes. This thermocouple can be flush mounted with the wall surface for the rapidly changing surface temperature. Usually, the thermocouples are fixed in the wall by gluing at the rear part of the element by a thread is also possible for higher operating temperatures.

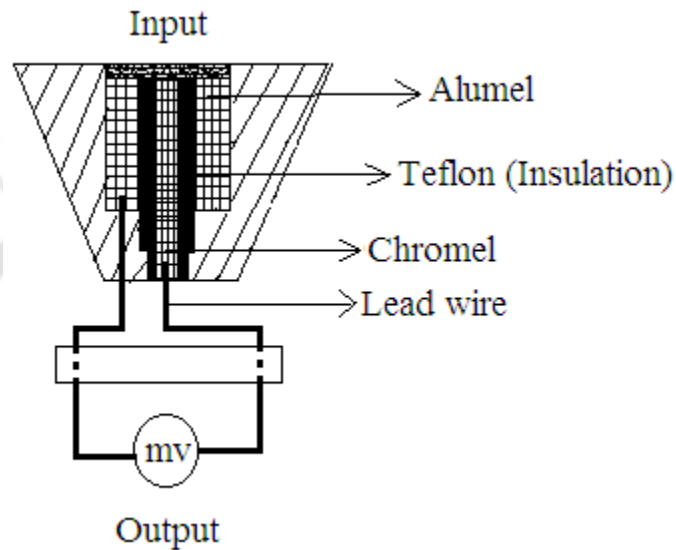


Fig. 1.4: Schematic diagram of coaxial thermocouple

1.3.4 Liquid Crystal Thermography

Thermo chromic liquid crystals (TLC) are materials that change their reflected color as a function of temperature, when illuminated by white light. Hence, they reflect visible light at different wavelengths. Thermo chromic means thermo-temperature and chromic-color. A bright and stable white light source is required to obtain accurate and reliable reflected light intensity from a (TLC) coated surface. The light source must be void of infrared (IR) and ultra-violet (UV) radiation. Any energy content in the incident light in IR, will cause radiant heating of the test surface. Extended exposure to UV radiation can cause rapid deterioration of the TLC surface. This causes the surface to produce unreliable color-temperature response performance.

Consistent light source settings and lighting viewing arrangements between calibration and actual testing are essential to minimize color-temperature interpretation errors.

1.3.5 Infrared Thermography

Infrared thermography (IRT) for non-destructive evaluation (NDE) is aimed at the discovery of subsurface features, such as subsurface thermal properties, presence of surface anomalies/defects etc. The relevant temperature difference also observed and record on the surface with an infrared (IR) camera, illustrates the general concepts. IRT is deployed along two schemes, passive and active. The passive scheme tests materials and structures which are naturally at different (often higher) temperatures than ambient. While in the case of the active scheme, an external stimulus is necessary to induce relevant thermal contrasts, which are not available otherwise specimen at uniform temperature prior to testing an infrared camera senses infrared radiation. The response time of this IRT has been proven to be in the range of microseconds. It is important to note that this strongly depends on the dynamic capabilities of the electronic equipment (amplifier, A/D conversion, etc.) of the measuring line which usually limits the achievable response time.

1.4 Nanoparticles

Nano objects which are nano scales in all three dimensions are called nanoparticles. A nanoparticle (tiny) compares to the size of a soccer ball roughly like a soccer ball compares to the size of the planet Earth. Long before the specific industrial production of nanoparticles, people made and even used such tiny particles. In one of its most important steps, the development of classical photographs is based on the formation of nanoparticles. Slash-and-burn techniques and transport give rise to soot nanoparticles. These are not exclusively man made but also occur in nature. For instance, forest fires and the recurring fires of the savannah every year emit soot nanoparticles much like manmade combustion processes. Nanoparticles may exhibit a

variety of shapes far from uniform. However, they always have very large surfaces in relation to their masses and mostly consist of a relatively small number of atoms or molecules, which gives rise to so-called quantum effects. Their properties therefore clearly differ from those of a material of the same chemical composition which is not nano scale. Gold nanoparticles for instance have a reddish gleam nano ceramics are flexible like foils, all of which properties allow them to be used for completely new applications. Nano materials are being used in many ways from special areas in medicine to everyday products such as skin lotions and wall paint. The classical nano materials long produced in large quantities include the industrial type of soot referred to as “carbon black.” They are found in car tires which increase their abrasion resistance, adhesion and elasticity. Carbon black is also a common black pigment used in inks, paints, polymers and many other compounds.

Nano materials are used in large quantities in synthetic silica or chemically silicon dioxide. When used as fillers they reinforce silicone rubber and thicken printing inks and toothpastes. Powder suspensions made of silicon dioxide, aluminum oxide and cerium oxide nano particles are used in the electronics industry for cleaning and polishing silicon wafers, the substrates of computer chips or solar cells. Nano particles of titanium dioxide and zinc oxide act as effective UV filters in sun creams and textiles protecting against the sun. Paints and dyes also lipsticks and other cosmetic products contain nano materials as pigments producing sparkling and coloring effects. Magnetic fluids so called ferro fluids contain iron oxide nano particles. They are used for instance to cool loud speaker boxes and act as liquid sealants. Also organic materials are being used in which inorganic nano particles are firmly embedded. These composites apply one of nature’s basic principles. Fine structures on the order of a few nanometers in which inorganic minerals combine with organic cement are the reason for the

extraordinary stability of bones, tooth enamel and mother of pearl. When used as binders these composites improve the quality of varnishes, paints and plastering materials. Nano materials also play an important role also in power technology for instance in producing energy storage devices and in the development of improved solar cells. The applications and possibilities listed here indicate that people can come into direct contact with these new materials. Consequently, nano materials must be examined for potential effects on health as a matter of precaution and their possible environmental impacts must be studied. In the nano care project, scientists are focusing especially on aspects of health by examining possible exposures at the workplace and conducting a variety of biological tests in order to exclude if possible any negative influences on health (Iijima et al. 1991, Tsai et al. 2005, Geim et al. 2007, Stampfer et al. 2008 and Li et al. 2008).

1.5 Nanofluids

Nanofluids are one of the potential technologies for heat transfer in future. The stable suspensions of nano particles in liquids are called nanofluids. These fluids are found to have very stable suspensions without substantial sedimentation for a long time. They are found to eliminate most of the problems arising with slurries like sedimentation clogging of small channels, erosion, excessive pressure drop etc. Conventional heat transfer fluids including oil, water and ethylene glycol mixture are poor heat transfer fluids, since the thermal conductivity of these fluids play important role on the heat transfer coefficient between the heat transfer medium and the heat transfer surface. Therefore numerous methods have been taken to improve the thermal conductivity of these fluids by suspending nano/micro or larger sized particle materials in liquids. The solid nanoparticles with typical length scales of (~1-100 nm) with high thermal conductivity are suspended in the base fluid (low thermal conductivity) have been shown to enhance effective thermal conductivity and the convective heat transfer coefficient of the base

fluid. Moreover, the heat transfer capabilities of nanofluids are much enhanced as compared to base fluids. This makes them suitable for use in cooling of electronic equipments, lasers, fuel-cells, car radiators etc. The enhancement in thermal conductivity of nanofluids is unusually high and cannot be predicted by any of the conventional multiphase conductivity models. CNT nanofluids are found to be most effective in this regard, giving two orders of magnitude higher thermal conductivity enhancement compared to the usual slurries. The thermal conductivity of carbon nanotubes is very high (~ 2000 W/mK) and secondly the nanotubes have a very high aspect ratio (~ 2000) as shown in Fig. 1.5 (Hwang et al. 2006, Schniepp et al. 2006, Westervelt et al. 2008 and Peres et al. 2009).

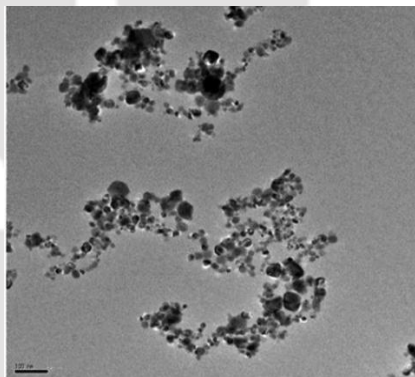


Fig. 1.5: SEM diagram of the nanofluids (Hwang et al. 2006)

1.6 Objectives of the Present Investigation

The measurement of transient heat transfer rates is very important in the design of internal combustion engine, gun barrels and aerodynamics vehicles in high speed flow environments. In these cases, the measurement technique for accurate prediction of heat fluxes must suit for transient conditions and should have a fast response time to trace variations caused by rapidly changing flow conditions. In most surface heat transfer mapping, very fast response sensors are used for dynamic temperature measurements in the flow. With respect to high speed flow environment, the response time of the temperature sensors become more crucial because the

experimental time-scale of measurement is very small (~ milliseconds or less). The transient temperature measurement is usually performed by mounting the temperature sensors, embedded inside the heated material. The surface heat fluxes are then estimated from the temperature history, analytically/numerically by one dimensional heat transfers modelling.

Thin film gauges and coaxial thermocouples are most cost effective resistance temperature detectors for transient temperature measurements because the response time falls in the range of microseconds (Vidal 1956). Thin film heat transfer gauges are made out of temperature sensitive materials (platinum, nickel etc.) and deposited on an insulated substrate material (pyrex, Macor etc.). These gauges are passive sensors and powered by a constant current source. In general, these gauges are suitable for applications where the surface heat fluxes are relatively low, particularly in the transient static temperature measurement. In the stagnation regions, where a large value of surface heat flux is expected, the metal film deposition on the substrate material becomes prone for wear and tear with repeated measurements. Moreover, platinum and nickels are generally precious materials and many a times, it is difficult to get them locally. At the same time, the deposition of metallic film to achieve a desired resistance on the substrate material needs specialized techniques such as sputtering.

Thermocouples are considered to be the most effective method for routine measurement of temperatures. The junction of the thermocouple is formed by two different material wires and a voltage is generated corresponding to the temperature change (Seebeck effect). In contrast to thin film gauges, they are active sensors and do not need any external power sources. In particular, the co-axial thermocouples are special class of temperature sensors that are useful for measurement transient temperatures in short-duration time scale. Moreover, they have high response times (~100 μ s) and more robust for high heat flux measurements. At the same time, its

fabrication does not need special techniques and becomes cost effective compared to the thin film gauges. The coaxial thermocouples are generally fabricated by one metallic element swaged over the second element with 1 μ m thick insulating material in between them. Here, a surface junction is formed by grinding the front surface that provides micro-scratches leading to small scale plastic deformation. Thus, it offers distinct advantages over the conventional heat transfer gauges and the fast-response characteristic ($\sim 100\mu$ s) makes its suitability in the short-duration measurement studies. In these measurements, there is a sudden rise in the heating load (such as step/impulse) on the test surface and subsequently, the heat flux from transient temperatures is obtained by one dimensional heat conduction modelling with semi-infinite assumptions. Many a times, the calibration methodologies seem to be unnoticed, which include uncertainties in measurement of temperature and subsequent determination of surface heat flux. However, they can be performed in the laboratory by performing simple experiments under heating loads. In this back drop, a research work has been initiated to explore the possibility of calibrating the heat transfer gauges under heating loads. In summary, the main objectives of the present investigation reported in the thesis are as follows:

- To Design and Fabrication of Heat Transfer Gauges
 - Platinum based Thin Film Gauges
 - Platinum/CNT based Thin Film Gauges and
 - K-type Coaxial Thermocouples
- To Develop and Perform Static Calibration of Heat Transfer Gauges
 - Experimental set up for oil-bath calibration experiment
 - Measurement of thermal coefficient of resistance (TCR)
 - Sensitivity analysis and comparison of gauges

- To Develop and Perform Dynamic Calibration of Heat Transfer Gauges
 - Radiation and conduction based experimental analysis
 - Theoretical and analytical study of heat transfer modeling
 - Finite element simulation of heat transfer gauges
 - Recovery of transient temperatures and comparison with experiments
- To Apply the Developed Heat Transfer Gauges in Stagnation Point Heat Flux Measurements
 - Fabrication of an experimental setup
 - Measurement of transient temperatures with heat transfer gauges
 - Theoretical and analytical predictions of surface heat fluxes
 - Computational analysis and comparison with experiments

1.7 Thesis Organization

The first chapter of this thesis set the background for the work where the transient heat fluxes and its measurement devices are introduced. The selection of heat fluxes measuring devices from various categories and their importance of the use in the transient heat fluxes measurement are emphasized. **Chapter 2** provides background concerning the heat fluxes measurement techniques and different types of nano-materials or nano-fluids. The work carried out by previous researchers regarding the effects of these heat transfer sensors performance, calibration technique and heat fluxes measurement techniques are reviewed. The performance of the heat transfer sensors relies more heavily upon the thermal properties of the gauge and substrate materials. The use of nano-materials in different devices is promoted by several researchers. The importance of nano-material analysis for present work is also briefed. **Chapter 3** describes the details of fabrication techniques of three types of heat transfer gauges. The thin film sensors are

prepared by depositing a film of high conducting and very sensitive platinum gauge material over the insulating surface of low conducting Pyrex material. The modified design and fabrication details of Platinum/CNT based sensors are also discussed in this section. The K-type coaxial thermocouples are also fabricated in the laboratory by chromel element disposed symmetrically and coaxially into a hollow machined cylinder of the alumel element. The static calibration technique of the handmade heat transfer gauges is discussed in **Chapters 4**. An oil bath based experimental setup has been prepared for static calibration and is used to check the variation of resistance with temperature during heating and cooling process. The thermal coefficient of resistance and sensitivity of each sensor are then calculated by using variation between changes in voltage with change in temperature. **Chapter 5** presents the dynamic calibration of the heat transfer gauges by the radiation and conduction based experimental setups. Step heating loads are applied on the heat transfer gauges by using a laser light for radiation experiments and constant heat fluxes based heater with known input wattage is used for conduction experiments. Transient temperature data are recorded under various known heating load conditions and the experimental results are compared from numerical and analytical analysis. The measured transient temperature histories are used to calculate output heat transfer and then compared with input wattage. In order to justify the usages of these heat transfer gauges, an experimental setup is designed where the gauges are exposed to high speed flows. **Chapter 6** presents the stagnation point based heat flux analysis corresponding to a sonic flow. The numerical technique (CFD-Fluent) is used to measure stagnation point heat fluxes and then compared with experimental results measured by the handmade sensors. Finally, concluding remarks/findings of the present investigation are highlighted in **Chapter 7**. Also, some future scopes of research and developments have been suggested in this chapter.

Chapter - 2

Literature Review

The resistance temperature detectors are the fundamental sensors to measure the transient surface temperatures by mounting them on the heated material surface. With respect to short duration measurements (~ few milliseconds), the sensors must have very high response time and at the same time, they should be capable of recording the temperatures from low to high values of heat fluxes. In other words, the thermal properties of the sensing element should resemble that of a pure metal. With recent advances in nano-technology, it is possible to enhance the thermal properties by mixing nano-materials into the sensing materials. The nano-materials have shown improvement in thermal conductivity and heat transfer considerably. Carbon nano tubes (CNT) are new form of materials and are found to be most effective nano materials because of their unique thermal conductivity, chemical stability and excellent electrical conductivity. In general, conventional heat transfer gauges use costly metals such as platinum/nickel as the sensing element for which the response time is in the order of $1\mu\text{s}$. Addition of CNTs in powder form and re-fabricating the gauge will enhance the thermal characteristics without changing the response time and can reduce the cost to some extent. Another technology is the use of cost effective surface junction coaxial thermocouples as transient measurement devices having response time in the order of $100\mu\text{s}$. Moreover, all these gauges can be fabricated in house and calibrated using simple laboratory devices. In all subsequent chapters, these techniques are discussed in details. This particular chapter deals with summary of the research investigations in the areas of heat transfer gauges and their application. Also, review discussions on some nano-fluid concepts for improving thermal properties of these sensors are highlighted.

2.1 Literature Review on Heat Transfer Gauges

Charles et al. (1984) has developed a transducer consisting of a classical thermocouple made out of two thin wires (W5Re and W26Re) embedded in fused alumina. The electrical contact at the hot junction is provided by a thin film of molybdenum. The measured response time (1ms or less) obtained under dynamic conditions of temperature and pressure (explosion) is in agreement with the values calculated by a computer simulation. Because of its structure, the tip of this transducer can withstand temperatures of up to 1900°C and pressure of several thousand bars mounted on an apparatus. At high temperatures, especially above 1000°C, the best measurement conditions prevail when the tip of transducer has an emissivity close to that of the surface. It is used to determine thermal response inside autoclaves during reactions, in the cylinders of internal combustion motors, in jet nozzles or in the combustion chamber of ballistic missiles. Also, it is shown that transducer response time can be improved with appropriate supplement of thin layer coatings.

George et al. (1991) has discussed the importance of frequency response considerations in the use of thin film gauges for unsteady heat transfer measurements in transient facilities. They proposed different methods of evaluation. A departure frequency response function is introduced and illustrated through an analog circuit. The *Fresnel integral temperature* is introduced and further used to evaluate the numerical algorithms. This temperature possesses the essential features of the film temperature in transient facilities. Finally, evaluation criteria are proposed for the use of finite-difference algorithms for the calculation of the unsteady heat flux from a sampled temperature signal. The removal of Fourier components by the finite frequency response of analog Q-meters is shown to have a significant effect on the inferred heat fluxes. Similarly, the sampling rate and choice of computational algorithm were shown to introduce

similar problems for the numerical reconstruction of the unsteady heat transfer from the digitally sampled film temperature. The digital methods have the advantage of using less hardware and can easily include the effects of the temperature dependent thermal properties of the substrate materials.

Jessen and Snig (1991) have developed a new method for the production of thin film heat flux gauges. The main advantages are the rigid construction of the sensors, the uncomplicated manufacturing method and the convenient contact of the film. Furthermore, the sensors are reusable. In case a sensor is damaged, it only has to be equipped with a new film, or if the surface is damaged, then it can be polished again. The calibration of these thin film gauges have been carried out successfully. Notably, the pulse calibration has demonstrated remarkable repeatability and accuracy. Several sensors are in use in the Aachen shock tunnel with satisfactory results. To check the durability, a sensor has been repeatedly exposed to the stagnation point of a sphere without serious damage or remarkable change in the values of the calibration.

At NASA Lewis Research center, **Lei et al. (1998)** have developed an advanced thin film sensor techniques that can provide accurate surface strain and temperature measurements. These sensors are sputter deposited directly onto the test articles and are only of few micrometers thick. The surface of the test article is not structurally altered and there is minimal disturbance of the gas flow over the surface. The strain gauges are palladium-13% chromium based and the thermocouples are platinum-13% rhodium versus platinum. The fabrication techniques of these thin film sensors were made in a class 1000 clean room at the NASA Lewis Research Center. Their demonstration on a variety of engine materials, including super alloys, ceramics and advanced ceramic matrix composites in several hostile, high temperature test environments is

discussed. Measurement techniques for propulsion systems are advanced through the development of thin film thermocouples and strain gauges. These thin film sensors have the advantage of providing minimally intrusive measurements. Thin film thermocouples made of Pt13Rh/Pt, have proven to be applicable to a range of materials and applications, such as super alloys, ceramics, ceramic composites and inter metallica. Data have been obtained in furnace testing under high heat flux conditions and in harsh engine environments. Thin film strain gauges based on a newly developed alloy have been developed for both dynamic and static strain applications in the temperature range from room temperature to 1100°C. The measurements from these thin film sensors provide minimally intrusive characterization of advanced materials (such as ceramics and composites) and structures (such as components for Space Shuttle main engine, high-speed civil transport and general aviation aircraft) in hostile, high temperature environments and for validation of design codes.

Wilson and Chana (2001) has developed deposition is on ICE advanced experimental technique for heat transfer measurement used for gas turbine engine research using platinum thin film resistance thermometers. Heat transfer rate measurements have been successfully obtained on the piston surface and cylinder head exposed to the combustion gases on a single cylinder engine. The thin film gauge system has a frequency response of around 100 kHz and hence can track the heat transfer rate changes on the piston surface and cylinder head adequately. Measurements taken with the engine motored and at low load are presented and discussed. Despite the difficulties of instrument and obtaining heat transfer on the piston of a spark ignition engine, experimental data has been successfully obtained on both the piston and the cylinder head for a number of positions. The investigation has clearly demonstrated the use of thin film gauges for taking heat transfer measurements in a spark ignition engine operated at realistic conditions. The

peak heat transfer levels found on the piston and cylinder head are of the order of 2.5MW/m^2 and varied significantly from cycle to cycle. The cylinder head data has shown many structures that can be clearly identified with the combustion process and the engine cycle.

A new form of surface junction thermocouple sensor has been developed and tested by **Sanderson and Sturtevant (2002)**. The novel feature of the design is the use of a tapered fit between two coaxial thermocouple elements to form a thin film robust junction. The gauge has a response time of the order of $1\mu\text{s}$ and is suitable for measuring large transient heat fluxes in hypervelocity wind tunnels. Asymptotic analysis is used to demonstrate the operating principles and to assess the errors associated with the finite thickness of the surface junction. Spectral deconvolution methods are used to infer a mean square optimal estimate of the surface heat flux from time resolved surface temperature measurements. This improved signal processing method is applicable to transient heat flux gauges of all types. Potential error sources and other systematic errors have been described. Measurements of the heat flux about the fore body of a cylindrical body in a hypervelocity flow demonstrate the functioning of the gauge and are used to obtain statistical estimates of the repeatability of the technique.

Sahoo (2003) has design and measured the heat transfer rates at different locations on the blunt body by using platinum thin film gauges by deposited gauge (platinum) on the ceramic substrate (macor) material inserts which in turn are embedded on the surface of the metallic blunt cone model. Simultaneous measurement of aerodynamic forces and surface heating rates are carried out in hypersonic shock tunnel at Mach 5.75 with different stagnation enthalpies for various angles of attack. The experimentally measured surface heat transfer results are expressed in terms of normalized heat transfer rates, Stanton numbers and correlated Stanton number. From the heat transfer measurements at 0° angle of attack, it is concluded that maximum heating rates

occurs at stagnation point and corner heating is about 20-30% of the stagnation point heat transfer rates. At angle of attack of 12° , the corner heating forms a considerable fraction (around 70%) of the maximum heat measured on the cone surface. The effects become severe at higher enthalpies.

Brohez et al. (2004) have developed bare bead thermocouples for measuring temperature fields in compartment fires. It is well known that temperature readings using such a device can be significantly affected by radiation errors, the apparent thermocouple junction temperature being thus different from the true gas temperature. However, a probe consisting of two thermocouples of unequal diameters but made of the same material can be used for estimating the gas temperature in a fire environment. Using a steady state heat transfer model applicable to a bare-bead thermocouple, a very simple rule is proposed for the estimation of radiation errors when temperatures are measured by use of two thermocouples of different diameters. Radiation errors obtained from this simple rule are compared and discussed with experimental results involving a compartment fire with pyridine as the fuel.

Talib et al. (2005) have developed one numerical analysis on conduction heat transfer through a custom built thin film gauge (TFG). The authors fabricated a custom built heat transfer gauge to measure the heat flux from ISO2685 fire certification burner under isothermal wall conditions. During the calibration of TFG using a hot air gun, the heat flux from the hot air gun was not uniform. There was a high heat flux level directly underneath the hot plum. In order to investigate the effect of the non uniform distribution of the heat flux, the author conducted a two dimensional numerical analysis to confirm that one dimensional conduction conditions prevailed throughout the temperature sensing section of the TFG. The numerical results were also compared directly to the temperature readings from the two thermocouples placed under the

enameled disc. The contribution of lateral conduction on the uncertainty of the TFG is considered small.

Mohammed et al. (2007) proposed transient response of erodible surface thermocouples and numerically assessed its performance with two dimensional finite element analyses. Four types of base metal erodible surface thermocouples have been examined in this study; K-type (alumel/chromel), E-type (chromel/constantan), T-type (copper/constantan) and J-type (iron/constantan) each of 50mm thickness. The practical importance of these types of thermocouples is to be used in internal combustion engine studies and aerodynamics experiments. The step heat flux was applied at the surface of the thermocouple model. The heat flux from the measurements of the surface temperature can be commonly identified by assuming that the heat transfers within these devices as one dimensional. The surface temperature rises at different positions along the thermocouple are presented. The normalized surface temperature histories at the center of the thermocouple for different types at different response time are also depicted. The thermocouple response to different heat flux variations were considered by using a square heat flux with 2ms width, a sinusoidal surface heat flux variation width 10ms period and repeated heat flux variation with 2ms width. The results demonstrate that the two dimensional transient heat conduction effects have a significant influence on the surface temperature history measurements made with these devices. It was observed that the surface temperature history and the transient response for thermocouple E-type are higher than that for other types due to the thermal properties of this thermocouple. It was concluded that the thermal properties of the surrounding material do have an impact, but the properties of the thermocouple and the insulation materials also make an important contribution to the net response.

Mohammed et al. (2008) have shown low cost K-type (chromel and alumel) coaxial surface junction thermocouples (CSJT) that has been fabricated in house. They were calibrated to measure the transient surface temperature rise within a UNITEN's shock tube facility. The authors also discussed and explained the design and fabrication technique of the CSJT and the difficulties that have occurred during the fabrication process. The micro structural analysis and the chemical characterization of these types of thermocouples have also been carried out to verify the surface morphology and to qualitatively evaluate the CSJT material composition. The preliminary testing was performed to demonstrate the performance of this thermocouple to be used to measure the surface temperature and heat transfer rates under transient conditions. The preliminary results from the shock tube tests have shown that thermocouples have a time response on the order of microseconds and found to be suitable for making heat transfer measurement in highly transient conditions. It was concluded that the current construction technique produced gauges that were reliable, reproducible, rugged and inexpensive.

Saravanan et al. (2009) used technique for gauge fabrication by depositing a thin metal film (typically platinum) on a glass or ceramic substrate. Then the surface temperature is sensed and measured through the temperature dependence of the resistance of the metal film. After gauge fabrication, the experiments are carried out with air as the test gas to obtain the surface convective heating rate on a missile shaped body flying at hypersonic speeds in a shock tunnel. The effect of fins on the surface heating rates of missile frustum is also investigated. The tests are performed in a hypersonic shock tunnel. The experiments are conducted at flow Mach number of 5.75 and 8 with an effective test time of 1ms. The measured stagnation point heat transfer data compares well with the theoretical value estimated using Fay and Riddell expression. The measured heat transfer rate with fin configuration is slightly higher than that of

model without fin. The normalized values of experimentally measured heat transfer rate and Stanton number compare well with the numerically estimated results.

Marr et al. (2010) have developed a fast response thermocouple for measuring surface temperatures of aluminum components in internal combustion engine combustion chambers. The key features of the design are the use of the aluminum substrate as one of the thermocouple metals and the use of a thick copper layer as the hot junction at the surface. The copper equalizes the hot junction temperature with the surrounding aluminum to correct for the differences in thermal properties between the two materials. Finite element analysis determined the optimum thickness of the copper layer to be between 100 μ s to 125 μ s. Under typical spark ignition engine heat flux conditions, the thermocouple was capable of measuring the average surface temperatures within 0.19°C and the magnitude of temperature swings was within 6% of true values. Experimental results displayed the same trends as the finite element analysis at measuring average temperatures and temperature swings, thus check the performance of thermocouple.

Menezes and Bhat (2010) have designed, fabricated, calibrated and tested a chromel/constantan based coaxial surface junction thermocouple to measure the transient temperature history on the surface of a body in a hypersonic free stream of Mach 8 in a shock tunnel. The experimental data obtained from the thermocouple compare well with the data obtained through analytical and numerical procedures for the same application. The coaxial thermocouple with a diameter of 3.25mm was flush mounted in the surface of a hemisphere of 25mm diameter. The hypersonic free stream was of a very low temperature and density, and had a flow time of about a millisecond. Preliminary test results indicate that the thermocouple is quite sensitive to low temperature rarefied free streams and also has a response time of a few microseconds to meet the

requirements of short duration transient measurements. The sensor developed is accurate, robust, reproducible and highly inexpensive.

Mohammed et al. (2010-a) has presented an experimental method for determining the effusivity values of different scratched coaxial temperature sensors. These sensors have a response time in the order of microseconds ($50\mu\text{s}$) with a rise time of less than $0.3\mu\text{s}$. Two types of scratch were made using abrasive papers with different grit sizes and scalpel blades with different thicknesses to form the sensor junctions. The effect of the scratch technique on the sensor's effusivity is also investigated. The sensors were tested and calibrated in the test section of a shock-tube facility at different operating conditions (**Mohammed et al. 2010-b**). It was observed that the effusivity of a particular sensor depends on the Mach number, scratch technique, scratch direction, junction location as well as on the enthalpy condition. It was also noticed that a scratched sensor using the scalpel blade technique does not require an individual calibration. However, for a sensor scratched using the abrasive paper technique, a calibration for each sensor is likely to be required. The present results have provided useful and practical data of the effusivity values for different scratched temperature sensors. These data are beneficial to experimentalists in the field, and can be used for accurate transient heat transfer rate measurements.

Mohammed et al. (2011-a) presented an experimental technique to estimate the appropriate thermal product values of rugged and fast response temperature probes (TPs) for hypersonic aerodynamic experiments. Two types of scratches were used mainly abrasive papers with different grit sizes and scalpel blades with different thicknesses to form the probe junction. The effect of the scratch technique on the probe's thermal product is investigated. The probes are tested and calibrated in the test section and in the end wall of shock tube facility. It is observed that the thermal product of a particular TP depends on the Mach number, junction scratch

technique and junction location as well as on the enthalpy conditions. It is noted that depending on the scratch technique some of the temperature probes do not require individual calibration.

Mohammed et al. (2011-b) have discussed the effect of different scratch techniques of abrasive papers and scalpel blades used to form the junctions of temperature sensors. A dynamic calibration procedure of scratched sensors in a shock tube facility allows easy evaluation of their thermal product value. For a particular sensor, the thermal product is found to be dependent on the flow Mach number, junction scratch technique, junction location and also on the enthalpy conditions. It was shown that different scratch techniques normally results in different thermal product values of sensors. The experimental procedure used in the present study has yielded practical data on characteristics of scratched temperature sensors, these data can be used in accurate measurement of transient heat transfer under hypersonic flow conditions.

Mohammed et al. (2011-c) proposed an experimental dynamic calibration technique of reliable, rugged, low-cost and fast response coaxial temperature probes. These probes were successfully designed and fabricated in-house, in conjunction with its signal processing circuit, which can be used for transient heat transfer measurements in a hypersonic testing facility. These probes have a response time less than $50\mu\text{s}$ with a rise time less than $0.3\mu\text{s}$. Two types of scratches were used, mainly abrasive papers with different grit sizes and scalpel blades with different thicknesses to form the probe junction. The effect of the scratch technique on the probe's thermal product is investigated. The probes were tested and calibrated in the test section and end wall of the UNITEN shock tube facility at different axial and radial locations. The effects of placing the coaxial temperature probe at different axial and radial distances, different working fluids and different Mach numbers on the transient surface temperature rise were examined. It was observed from the dynamic calibration results that the thermal product of a particular coaxial

temperature probe depends on Mach number, junction scratch technique and junction location as well as on the enthalpy conditions. It was also noticed that the calibrated coaxial temperature probe using the scalpel blade technique with a particular blade size gives consistent thermal product values. Thus, it does not require an individual calibration. However, for a coaxial temperature probe whose junction was created using the abrasive paper technique with different grit sizes a calibration for each coaxial temperature probe is likely to be needed.

2.2 Literature Review on Transient Heat Transfer Measurement Techniques

Beck (1967) has determined the surface heat flux from the transient temperature history measured at an interior position in a heat conducting solid possessing constant thermal properties. These methods involve the numerical inversion of a convolution integral. Each of the new methods employs a least squares procedure. A comparison is given for the simplest formulation of the new methods with an older numerical inversion procedure. In this comparison it is shown that the new method is stable with time steps as small as one sixth of the minimum allowable time step and analyses of the stability are given for several formulations with more desirable characteristics.

Mehta et al. (1988) has investigated the influence of normal and lateral conduction on the temperature distribution and heat transfer coefficient on the surface of a typical sounding rocket. A two dimensional heat conduction equation with a time dependent aerodynamic heating condition at one surface and a radiation boundary condition at the other end is solved using finite element method. Unsteady heating of a thin skinned body subjected to an aerodynamic heating rate has a wide practical interest in high speed free flight and in the thin skin technique. They include normal and lateral heat conduction and heat loss into thermocouple lead wires. The measured thermocouple temperature history on the inner surface of the thin skin is customarily

employed to estimate heat transfer coefficient while neglecting normal and lateral heat conduction terms.

Taler (1996-a) proposed a mathematical procedure of transient methods for measuring surface heat transfer rates. The heat flux gauges are modeled with semi-infinite concepts, thin film and thick wall gauges. The aim of this work is to present a method for simple and accurate determination of the time varying heat transfer rates from the measured temperature history. The temperature measurements are converted into local instantaneous heat transfer fluxes by solving the heat conduction problem for the gauge. The effect of the inaccuracies in the measurement of the temperature was eliminated by cubic spline smoothing or digital filtering of the raw temperature data prior to using it in the inverse heat conduction analysis. General case closed form equations for instantaneous surface heat flux or heat transfer coefficients are developed. The heat flux at the location of the temperature sensor is determined from the solution of one dimensional heat conduction using Duhamel's theorem. Global and local spline approximations are used to smooth the measured interior temperature time curves.

Taler (1996-b) has developed a semi numerical method for solving the inverse heat conduction problems in homogeneous and composite bodies. The presented solution does not require both the initial temperature distribution in the body and the whole temperature time history at the temperature sensor locations. It is an accurate and simple technique which is capable of treating linear inverse heat conduction problems with data containing random errors. The presented approach utilizes past and future time data while requiring no iteration. In contrary to most previous works on inverse heat conduction problems the method requires no information about initial temperature distribution in the solid. The surface heat flux at a specific time can be directly calculated from the measured transient temperature inside a solid without step by step

computation in the time domain. It is not necessary to compute all nodal temperatures at each time step to calculate the surface heat flux. To obtain results of very good accuracy, the space domain may be divided only in three or four control volumes. Sample calculations confirmed that this approach produces stable and accurate results for both exact and noisy data.

Chen et al. (2001) have developed a hybrid numerical algorithm of the Laplace transform technique and finite difference method with a sequential in time concept. The least squares scheme is proposed to predict the unknown surface temperature in two dimensional inverse heat conduction problems. In their study, the expression of the surface temperature is unknown a priori. The whole time domain is divided into several analysis sub time intervals and then the surface temperature in each analysis interval is estimated. In order to enhance the accuracy and efficiency of the present method, a good comparison between the present estimations and previous results is demonstrated. Results show that good estimations on the surface temperature can be obtained from the knowledge of the transient temperature recordings only at a few selected locations even for the case with measurement errors. It is worth mentioning that the unknown surface temperature can be accurately estimated even though the heat transfer gauges or thermocouples are located far from the estimated surface. Due to the application of Laplace transform technique, the unknown surface temperature distribution can be estimated at a specific time.

Masanori et al. (2003) have developed an analytical method for two dimensional inverse heat conduction problems by using the Laplace transform technique. The inverse solutions are obtained under two simple boundary conditions in a finite rectangular body with one and two unknowns, respectively. The method first approximates the temperature changes measured in the body with a half polynomial power series of time and Fourier series of Eigen function. The

expressions for the surface temperature and heat flux are explicitly obtained in a form of power series of time and Fourier series. The verifications for two representative testing cases have shown that the predicted surface temperature distribution is in good agreement with the prescribed surface condition as well as the surface heat flux. A procedure to solve Inverse Heat Conduction Problems (IHPC) is to derive surface heat flux and temperature from temperature changes inside a solid. This method is proved to be very powerful and useful when a direct measurement of surface heat flux and temperature is difficult, such as those in space vehicle atmosphere re-entry, during accidents involving coolant breaks in the plasma facing components and in the quenching of a high temperature surface. The IHCP has been numerically treated and extended to multiple dimensions with the help of the development of computer technologies related to software and hardware and the improvement of computer capability.

Woodfield et al. (2006) have developed two improvements to practical implementation for the solution of two dimensional inverse heat conduction problems. The first concept is useful for experimental data with strong or irregular fluctuations in time. The second procedure improves the spatial resolution for problems where the source of the surface heat flux distribution is moving along the surface. The method is tested against analytical solutions and data from quench cooling experiments. Both procedures are found to enhance the quality of the inverse solution results. Two innovations for application of the two dimensional Monde method to experimental data were presented. The first represented an improvement for applying the procedure to data with strong or irregular fluctuations in time. The second is most useful for circumstances where the source of the surface heat flux is moving in the spatial direction. This circumstance can occur in quenching experiments with a moving wetting front. It is also demonstrated that the spatial resolution for the surface heat flux estimate is limited by the sensor spacing, the depth beneath

the surface and the accuracy of the sensor. Finally, the authors are pleased to make available openly the software developed for implementing the present inverse solution.

The time dependent boundary heat flux in two dimensional heat conduction domains with heated and insulated walls was developed by **Ijaz et al. (2007)**. The estimation of the algorithm requires only the temperatures measured at the insulated walls. In addition, the estimator also predicts the bias in the measurements. In modeling the system, it is assumed that the input flux and bias sequence dynamics can be modeled by a semi Markov process. By incorporating the semi markovian concept into a Bayesian estimation technique, the estimator consists of a bank of parallel, adaptively weighted, Kalman filters. Computer simulation results reveal that the proposed adaptive estimator has improved estimation performance even for step changing heat flux and measurement bias.

Kawale and Sahoo (2008) have discussed the transient temperature data from nickel thin film heat transfer gauges analyzed by using one dimensional semi infinite heat conduction model to measure surface heating rates. First of all, the one dimensional semi-infinite heat conduction model has been used successfully to infer the surface heating rates from the temperature history. The main purpose of this work is to investigate the influence of normal conduction on the temperature distribution at the surface as well as along the depth of the substrate. In order to check the presence of lateral conduction, finite element analysis was carried out. Results show that lateral conduction is significant for larger time scales.

Rainieri et al. (2008) proposed an experimental analysis and a data processing procedure, aimed to characterize the cooled micro bolometric infrared camera. The instrument performance test is addressed to the application of infrared thermography for the parameter estimation problem

based on the solution of the inverse heat conduction problem. With this regard, a new picture of merit which enables estimation of the local noise level in the thermal image has been suggested. This parameter may be used to characterize the performance of IR and also of other thermographic devices for applications common to a wide category of heat transfer measurements in which the spatial first or second derivatives of a thermal two dimensional signal are needed. The instrument has been compared in terms of local noise level to an IR camera based on the cooled photon detector array technology. The characterization of an infrared camera based on the uncooled micro bolometer detector technology has been performed in the temperature range 30°C to 80°C with regards to its application to the solution of the two dimensional inverse heat conduction problems. The uniformity and the stability of the sensors response have been quantified together with the overall and local noise level present in the thermal image. Besides, the local noise level, a new figure of merit, named LNL, capable of estimating the performance of the instrument in the reconstruction of the Laplacian of the temperature distribution has been suggested. This parameter may be used to characterize the performance of IR and also of other thermographic devices for applications common to a wide category of heat transfer measurements in which the spatial first or second derivatives of a thermal two dimensional signal are needed. Besides, the dimensionless expression revealed to be useful in the characterization of given sensor in terms of the relative effect due to local discontinuities and random noise in the reconstruction of the signal's second derivative. The analysis has been completed with the comparison of the instrument performance with the behavior of a cooled photon detector. The results allow concluding that by following an optimal methodology in the acquisition and processing of the thermal images the micro bolometric IR camera under test shows in the temperature range 30°C to 80°C and in standard temperature operating conditions, a performance

similar to that of a cooled photon detector IR camera with regards to the particular application field above address.

A sequential method is proposed by **Yang (2009)** to estimate boundary condition of the two dimensional hyperbolic heat conduction problems. An inverse solution is deduced from a finite difference method, the concept of the future time and a modified Newton Raphson method. The undetermined boundary condition at each time step is denoted as an unknown variable in a set of non linear equations, which are formulated from the measured temperature and the calculated temperature. Then, an iterative process is used to solve the set of equations. No selected function is needed to represent the undetermined function in advance. The example problem is used to demonstrate the characteristics of the proposed method. In the example, a well known problem is used to demonstrate the validity of the proposed direct method and then the inverse solutions are evaluated. In the second example, the larger value of the relaxation time is implemented in the direct solutions and the inverse solutions. The close agreement between the exact values and the estimated results is made to confirm the validity and accuracy of the proposed method. The results show that the proposed method is an accurate and stable method to determine the boundary conditions in the two dimensional inverse hyperbolic heat conduction problems. A sequential method has been introduced for determining the boundary condition in the two dimensional inverse hyperbolic conduction problems. The direct solution at each time step is computed by a finite difference method within a stable interval and the inverse solution at each time step is solved by a modified Newton Raphson method. The inverse method does not adopt the non linear least squares error to formulate the inverse problem, but it employed a direct comparison of the measured temperature and calculated temperature. Special features about this method are that no preselected functional form for the unknown function is necessary and no non

linear least squares are needed in the algorithm. An example has been illustrated based on the proposed method. The results show that the proposed method is able to find the direct and inverse solution.

Sahoo and Peetala (2010) proposed a one dimensional heat conduction model to infer transient surface heat flux from the temperature history. The experimental temperature data is obtained from the nickel film sensor for a supersonic flight test. Curve fitting techniques are used to recover the actual experimental signal and the comparison shows a very good agreement. The temperature data obtained from various techniques are used in one dimensional heat conduction modeling and transient surface heat fluxes are predicted. It is seen that during a small experimental time scale piecewise linear fitting of temperature data predicts surface heat flux values with reasonable accuracy and it also reduces the computational time. However for a longer duration the third order cubic spline method can give better approximation because it reproduces the experimental data points more closely compared with polynomial fitting of temperature data.

Sahoo and Peetala (2011) have discussed convective surface heat transfer measurement technique for aerodynamic problems. In most of the cases, the flow is unsteady which results in temperature variation in the body. The surface heating rates are predicted from the measured temperature histories by suitable heat transfer modeling. In this work, the temperature history obtained from a nickel film sensor during a flight test is considered to study the effect of sensor thickness on surface heat flux measurements during the flight measurement. Inverse methods using analytical solutions as well as control volume approximations are used to infer the surface heat flux. The experimental temperature data are discretized using cubic spline method to obtain the closed form solution which is used for inverse analysis. The results are compared with that of

standard bench mark results with thin film gauge analysis based on semi infinite one dimensional medium. No significant change in surface heat flux is observed between inverse and thin film analysis. However, when the thickness of nickel film is increased by 100 times during numerical simulation of inverse method, it is seen that peak surface heat flux increases by 20%.

2.3 Literature Review on Nanomaterials and Nanofluids

Tsung et al. (2005) have developed a submerged arc nano synthesis system for preparing copper based nanofluids with different morphologies and using various dielectric liquids. Pure copper is selected as the electrode as well as the work piece material. Copper is heated and vaporized by arc sparking between two electrodes immersed in dielectric liquids. The copper aerosol can be condensed to form nanoparticles immediately by the cooling media (dielectric liquids). The nanoparticles then dissolve in the dielectric liquids which become metal nanofluids. Various morphological copper based nanoparticles can be synthesized using different dielectric liquids. The effects of experimental parameters and dielectric liquids on the characteristics of final products have been investigated. The possible formation mechanism of copper based nanoparticles with the faster growing faces is suggested.

Hwang et al. (2006) have discussed nanofluid as a new kind of engineering material consisting of nanometer sized particles dispersed in base fluid. In this study, various nanoparticles, such as multi walled carbon nano tube (MWCNT), fullerene, copper oxide and silicon dioxide have been used to produce nanofluids for enhancing thermal conductivity and lubricity. As base fluids, diluted water, ethylene glycol and oil have been used. In order to investigate the thermo physical properties of nanofluids, thermal conductivity has been measured. The experimental results of thermal conductivity of nanofluids are compared with the modeling results. The stability of nanofluid has been estimated with ultra violet (UV) pectro-photometer. Thermal conductivity of

nanofluid has been increased with increasing volume fraction of nanoparticle except for water based fullerene nanofluid because it has lower thermal conductivity (0.4W/mK) than that of base fluid. Stability of nanofluid gets influenced by the characteristics between base fluid and suspended nanoparticles. Various nanofluids have been prepared and their stability has been estimated by UV spectrum analysis. Stability of nanofluid is strongly affected by the characteristics of the suspended particle and base fluids such as the particle morphology, the chemical structure of the particles and base fluid. Moreover, addition of surfactant can improve the stability of the suspensions. Thermal conductivities have been measured by the transient hot wire method. Conclusively, thermal conductivity enhancement depends on the volume fraction of the suspended particles, thermal conductivities of the particles and base fluids. Also the experimental results of the thermal conductivity of MWCNT nanofluids have been validated with the calculated results.

Yang et al. (2007) has prepared novel nano silver coated multi walled carbon nano tube composites, used them to fabricate a modified electrode and to determine traces of thiocyanate for the first time. The characterization of nano silver coated multi walled carbon nano tubes was revealed through SEM (Scanning Electron Microscope) and XRD (X-Ray Diffraction) methods. The electro chemical behavior of the modified electrode with thiocyanate was investigated by cyclic voltammeter. It is found that the anodic peak current decreased with the addition of trace thiocyanate. So the electrode developed was used to determine the trace of thiocyanate and limit of deletion was obtained. Actual samples, such as saliva and urine of smoker and non smoker were analyzed by the proposed method and satisfactory results have been obtained. The constructed electrode showed excellent reproducibility and stability. This method provides a new way to construct modified electrode for biological and environmental analysis.

Alexander et al. (2008) discussed a graphene material discovered from carbon that consists of only one plain layer of atoms arranged in honeycomb lattice exhibiting a number of intriguing properties. The unusual energy dispersion relation, the low lying electrons in single layer graphene behave like mass less relativistic. Dirac fermions, gives rise to unique phenomena such as quantum spin Hall Effect, enhanced Coulomb interaction, suppression of the weak localization and deviation from the adiabatic born oppenheimer approximation. Its extraordinary high room temperature carrier mobility, conductance quantization possibilities of inducing a band gap through the lateral quantum confinement and prospects for epitaxial growth make graphene a promising material for future electronic circuits. Despite theoretical suggestions that graphene may also have unusually high thermal conductivity. This work was the first experimental investigation of thermal conduction in a suspended single-layer graphene performed with the help of con focal micro-Raman spectroscopy. The room temperature values of the thermal conductivity of up to 5300W/mK, were extracted for a single layer graphene from the dependence of the Raman peak frequency on the excitation laser power. The extremely high values of the thermal conductivity suggest that graphene can outperform carbon nano tubes (CNTs) in heat conduction. The superb thermally conducting property of graphene is beneficial for the proposed electronic applications and establishes an excellent material for thermal management. The discovered outstanding thermal properties of graphene provide an extra motivation for integration with the nanometer scale silicon complementary metal oxide semiconductor technology. Furthermore, it increases the range of graphene applications as the thermal management material in optoelectronics, photonics and bioengineering.

Malongo et al. (2008) has developed a silver based solid carbon paste electrode for use as a detector in ion chromatography (IC) for the sensitive determination of iodide in real samples.

Micro and nanoparticles of silver were investigated for the fabrication of different electrodes. The iodide assay was based on IC with amperometric detection (IC-AD) at a silver composite electrode polarized. Free iodide and organic iodide compounds were studied. The detection process was characterized by studying the redox behavior of iodide ions at both silver and silver composite electrodes by cyclic voltammetry (CV). The presence of iodide ions in solution was found to considerably facilitate metallic silver oxidation with response currents directly related to iodide concentration. The calibration curve at the selected silver carbon paste electrode was linear in this concentration range. The relative standard deviation for successive injections was below 3% for all iodide standard solutions investigated. The IC-AD method was successfully applied to the determination of iodide in complex real samples such as table salts, sea products and iodide bound drug compounds. With the developed IC-AD methodology, the detector can be operated for weeks without surface cleaning or renewing and the sample treatments do not require tedious cleaning or extraction procedures. Linear responses within a broad dynamic range and detection and quantification limits down have been achieved.

Acharya et al. (2009) has demonstrated a facile route to decorate the surface of networked single walled carbon nano tubes (SWNTs) with silver nano particles (Ag-NPs). The method is based on utilization of either spherical poly (styrene-*b*-4vinylpyridine) (PS-*b*-P4VP) or cylindrical poly (styrene-*b*-acrylic acid) (PS-*b*-PAA) copolymer micelles capable of stabilizing nano tubes in solution and subsequently forming a thin and uniform block copolymer/SWNTs composite film upon spin coating. The selective doping of silver acetate into either P4VP or PAA domains in a thin composite film followed by thermal treatment result in the formation of Ag-NPs in the cores of micelles. Further, heat treatment at 500°C sufficiently high for degrading both block copolymers allows these to fabricate a thin SWNTs network in which Ag-NPs are

efficiently deposited on the surface of nano tubes. A sharp surface plasmon absorption band around 400nm of the networked SWNTs with Ag-NPs confirms the presence of Ag-NPs with narrow distribution in their size. The networked SWNTs/metal NPs are potentially useful for chemical sensors, conducting networks and 2D templates for vertical metal/semiconductor nano wires.

Rochefort et al. (2009) has performed calculations on the interaction of graphene with benzyl mercaptan and on the role of the mercaptan in the adhesion of platinum nano particles. The calculations indicate that these particles adhere more strongly to defect free graphene than does benzyl mercaptan, which is essentially physisorbed. The role of the physisorbed mercaptan is to offer an abundance of SH sites, to which the platinum bonding energy is greater than to graphene. This would lead to a higher deposition density of nano particles, which are decorated with chemisorbed mercaptan. The presence of benzyl mercaptan on the surfaces of platinum particles should also contribute to hindering the metallic phase coalescence.

An extensive review of heat transfer enhancement using nanofluids and their relative advantages over conventional heat transfer fluids have been discussed by **Sadik and Anchasa (2009)**. Over a decade ago, researchers focused on measuring and modeling the effective thermal conductivity and viscosity of nanofluids. Recently, important theoretical and experimental research works on convective heat transfer appeared in the open literatures on the enhancement of heat transfer using suspensions of nano metered sized solid particle materials metallic or nonmetallic in base heat transfer fluids. Further, theoretical modeling and experimental works on the effective thermal conductivity and apparent diffusivity are needed to demonstrate the full potential of nanofluids for enhancement of forced convection. The understanding of the fundamentals of heat

transfer and wall friction is prime importance for developing nanofluids for a wide range of heat transfer applications.

Tsai et al. (2009) have presented an effective procedure for the preparation of Ag/MWCNT Nafion nano composite which exhibited sensitive SERS ability. The resulting Ag/MWCNT Nafion nano composite was characterized by scanning electron microscopy and energy dispersive X-ray spectroscopy. The silver nanoparticles can be decorated in the MWCNT Nafion by an electro deposition method. The enhancement of the in situ determination of R6G in aqueous solution can be achieved by using this methodology under optimum conditions. The advantage of the preparation of Ag/MWCNT nafion composite over most forms of SERS active substrates is procedural simplicity. The present methodology demonstrates that the nano composite film composed of Ag/MWCNT and Nafion has potential for optical chemical sensor applications.

Xie and Chen (2009) have prepared homogeneous and stable nanofluids by suspending well dispersible multi walled carbon nano tubes (CNT) into ethylene glycol base fluid. CNT nanofluids have enhanced thermal conductivity and the enhancement ratios increase with the nano tubes loading and the temperature. Thermal conductivity enhancement was adjusted by ball milling and cutting the treated CNT suspended in the nanofluids to relatively straight CNT with an appropriate length distribution. The addition of CNT into a fluid leads to substantial enhancement of the thermal conductivity with the enhancement ratios increasing with the nano tube loading and the temperature. Mechanical ball milling with chemical treatment is an effective means to obtain relatively straight CNT with an appropriate length distribution which enables optimized thermal conductivity enhancement in CNT nanofluids. The experiments demonstrate that the collective effects involving straightness ratio, aspect ratio and aggregation play a key

role in the thermal conductivity of CNT nanofluids. The researcher also focuses on the qualitative interpretation according to the experimental results and more detailed quantitative clarification of the effect of every specified factor. This study suggests that the thermal characteristics of nanofluids might be manipulated by means of controlling the morphology of the inclusions which also provide a promising way to conduct investigation on the mechanism of heat transfer in nanofluids.

Muthamilselvan et al. (2010) have discussed a numerical study to investigate the transport mechanism of mixed convection in a lid driven enclosure filled with nanofluids. The two vertical walls of the enclosure are insulated while the horizontal walls are kept at constant temperatures with the top surface moving at a constant speed. The numerical approach is based on the finite volume technique with a staggered grid arrangement. The SIMPLE algorithm is used for handling the pressure velocity coupling. Numerical solutions are obtained for a wide range of parameters and copper water nanofluid. The streamlines isothermal plots and the variation of the average Nusselt number at the hot wall are also presented. It is found that both the aspect ratio and solid volume fraction affect the fluid flow and heat transfer in the enclosure. Also the variation of the average Nusselt number is linear with solid volume fraction.

Xie et al. (2010) prepared stable ethylene glycol based copper nanofluids using polyvinyl pyrrolidone as dispersant, which was vital for the long term stability of nanofluids. The substantial thermal conductivity enhancements were seen for the nanofluids. For ethylene glycol based copper nanofluids with 0.5% volume at 50°C, the enhancement ratio was up to 46%. The thermal conductivities depended strongly on the temperature of fluid and the enhancement ratios increased along with the increasing temperatures. Brownian motions of copper nanoparticles played the key role in determining the effects of the temperature on thermal conductivity

enhancement of nanofluids. The measured apparent thermal conductivity showed the time dependent characteristic within 15min. It indicated that the measurement should be made after 15min at least to obtain the true thermal conductivities of ethylene glycol based copper nanofluids.

Duong et al. (2010) has developed platinum nano particles (Pt/NPs), grown directly on multiwall carbon nanotubes (MWNTs) using a wet chemical reduction process. Gases permeable Pt supported MWNT (Pt/MWNT) electrodes were then formed on micro porous PTFE membranes through the vacuum filtration of a Pt/MWNT solution. The potential use of these electrodes in amperometric hydrogen sensor applications was assessed. Various material analysis methods such as SEM, TEM and XRD were employed in order to characterize the morphologies and microstructures of the Pt/MWNT nano composites. The electrodes exhibited a nano porous interwoven surface morphology as a result of Pt agglomerates attached to the MWNTs. From the XRD and TEM measurements individual polygonal, Pt/NPs were confirmed to have polycrystalline face centered cubic (FCC) structures and very small particle sizes of 2nm to 7nm. The electrode fabrication process was sequentially optimized by adjusting the MWNT content, H_2PtCl_6 concentration, $NaBH_4$ concentration and the drying temperature. At optimized conditions, the Pt/MWNT electrode displayed a high sensitivity greater than 200mA/ppm. It has a fairly good selectivity to interfere CO species and has an excellent linear response over the wide concentration range of 5ppm to 1000ppm. Furthermore, the performances of the electrodes were found to be better than those of binary supported MWNT systems.

Xin et al. (2011) discussed a simple way to synthesize well dispersed platinum (Pt) and graphene (G) catalysts using graphene oxide as a precursor. The introduction of lyophilization offered a facile and efficient approach to produce well soluble graphene and heat treatment was employed

to improve the performance of Pt/G catalysts. Electrochemical experiments toward methanol oxidation indicated that Pt/G had higher catalytic activity than that of Pt/C and the stability of Pt/G was better than Pt/C catalysts. Pt/G after heat treatment at 300°C performed higher intrinsic activity and stability for methanol oxidation, which may be attributed to four effects induced by heat treatment: (i) the enhancement of interaction between Pt and graphene; (ii) additional Pt active sites exposed by the rolling of graphene sheets; (iii) decompose of partially surface functional groups resulting to less defects on graphene for stability improvement; (iv) Pt surface morphology from amorphous to more ordered states introducing more active catalytic sites. The SEM and TEM results also showed that graphene was in favor of improving the distribution of Pt particles. It indicates that graphene is a promising supporting material to modify catalytic properties of Pt for fuel cell catalysts.

Chapter - 3

Design and Fabrication of Heat Transfer Gauges

Thin film gauges and coaxial thermocouples are most cost effective resistance temperature detector (RTD) thermal sensors for dynamic temperature measurements mainly because of very fast response time (milliseconds or less). The thin film gauges have a sensing element mounted on an insulated substrate. Typically, the sensing element is a metal with high values of thermal conductivity (platinum/nickel/gold). Since, the gauges are intended to measure surface heat flux, it is essential that there should not be any heat conduction in the substrate. So, the material of the substrate must be an insulator with a very low value of thermal conductivity. While preparing the film, if adequate resistance is not maintained, then there is a chance of self heating. So, it is an art and needs expertise to prepare these handmade thin films gauges. In order to enhance the thermal properties of platinum, if some suitable proportions of nanomaterials are mixed, then gauges can be re-fabricated with improved value of sensitivity. The CNTs are the most effective nanomaterials with high value of thermal conductivity and very high aspect ratio. A surface junction coaxial thermocouple is also a fast response sensor that can be considered for short duration applications. Here, the sensing area is a surface not as junction point as in the case of conventional thermocouple. All these thermal sensors need an insulating substrate of certain minimum thickness such that the substrate behaves a semi-infinite medium for the heat flux to penetrate during the experimental time scale of measurement. In this chapter, the fabrication techniques of each of the heat transfer gauges, enhancement of thermal properties of the thermal sensors with CNTs and some design aspects of substrate are discussed in details.

3.1 Introduction

The measurement of heat transfer rates of highly transient surfaces are very important in the design of internal combustion engine, aerodynamics vehicles, gun barrels and high speed flow environments. In such cases, the technique used for accurate heat fluxes measurement should suit transient conditions and must have a fast enough response time to trace variations caused by rapidly changing flow conditions. In most surface heat transfer mapping, very fast response sensors are used for dynamic temperature measurements in the flow. With respect to high speed flow environment, the response time of the temperature sensors become more crucial because the experimental time scale of measurement is very small (~ milliseconds or less). Thin film gauges and coaxial thermocouples are suitable for measuring highly transient surface temperatures because the response time of these sensors are in the range of microseconds. The transient measurement of temperatures is usually performed by mounting the temperature sensors embedded inside the heated material. The surface heat fluxes are then estimated from the temperature history, analytically/numerically by one dimensional heat transfers modelling. These heat transfer thin film gauges are RTD sensors prepared by deposited high conducting temperature sensitive materials (platinum/nickel/silver) on the insulating surfaces of low conducting material (Pyrex/Macor/Quartz). The thermal conductivity of the thin film gauge material plays an important role in the measurement of highly transient heat transfer rate. High conducting nanomaterials have been extensively researched in recent years. Nanomaterial becomes a new challenge for the heat transfer material because of their higher thermal conductivity and stability than those of the conventional heat transfer material or the suspension of micro sized particles (Iijima et al. 1991, Tsai et al. 2005, Geim et al. 2007, Stampfer et al. 2008 and Li et al. 2008). Since the solid nanoparticles with typical length scales of 1nm to 100nm

with high thermal conductivity are suspended in the base material (low thermal conductivity), have been shown to enhance effective thermal conductivity and the convective heat transfer coefficient on the base material.

Thin film sensors suitability for measuring surface temperatures history in very short duration tests has been well established by (Vidal 1956 and Schultz et al. 1973). Further, the application and development of the traditional TFG are described by several researchers (Doorly and Oldfield 1985, Oldfield et al. 1980, Dunn et al. 1986, Piccini 1999 and Piccini et al. 2000). In recent years, there has been considerable interest in extending the thin film technique for the measurement of fluctuating heat transfer rates in transient experiments, especially for gas turbine applications (Dunn and Holt 1982). Thin film heat transfer gauges are made out of temperature sensitive materials and deposited on an insulated substrate material. Normally, these thin film gauges have a highly sensing gauge material (Platinum/Nickel/Silver) mounted on insulating substrate (Pyrex/Macor/Quartz). Platinum is in the form of paste that can be used to fabricate a thin film on the substrate material surface. Also, it has extremely sensitive resistance that varies linearly with temperature (Benedict 1984). Most of the literatures do highlight the importance of thin film gauges for prediction of transient heat flux measurement. However, when it is desired to have measurement of small order of magnitude of heat flux ($\sim 1 \text{ W/m}^2$), the accuracy becomes an issue. It is mainly because of the limitations in thermal properties of gauge material and its sensitivity. With recent advances in nano technology, it is possible to enhance the thermal properties by mixing nanomaterials into the gauge material (Platinum/Nickel/Silver). Recently, there has been interest in using nanomaterials as additives to modify heat transfer materials to improve their performance (Lee and Choi 1996). Dispersion or suspension of nanomaterials of high thermal conductivities into base materials gives rise to higher thermal conductivity of the

mixtures (Wang et al. 1999), thereby increasing the heat transfer coefficient. CNTs are a new form of materials are found to be most effective nanomaterials because of their unique thermal conductivity (3000W/mK), chemical stability, excellent electrical conductivity, high surface area and strong mechanical strength associated with high aspect ratio (Iijima 1991, Tsai et al. 2005, Schniepp et al. 2006, Geim and Novoselov 2007, Stampfer et al. 2008, Li et al. 2008, Westervelt 2008 and Peres et al. 2009). Because of the high thermal conductivity and large aspect ratios, the nanomaterials are expected to improve the thermal property when mixed with base fluid. CNT based electrodes are prepared by mechanical abrasion onto graphite surface as paste (Rubiane and Rivas 2005) and in the form of composite (Pumera et al. 2006). The electrodes modified with the mixture of (platinum chemicals and CNT) have recently received much interest for the purpose of designing thermal sensors (Shan et al. 2009, Kou et al. 2009, Duong et al. 2010 and Belinda et al. 2010). Noble nanoparticles such as platinum exhibit electro catalytic behaviour to hydrogen peroxide and have been widely used for sensing applications (Chu et al. 2007 and Qu et al. 2007). It will be attractive to prepare nanoparticle functionalized means platinum nanoparticles nanocomposite because such a functionalized may generate synergy on electro catalytic activity and thus enhance the sensitivity of the biosensors. However, severe aggregation always takes place in the as prepared CNTs because of the non-reactive surfaces, intrinsic Vander Waal forces and very large specific surface areas and aspect ratios (Park et al. 2002).

In coaxial thermocouples, two dissimilar metals are joined together to form a junction and when exposed to a temperature gradient, a corresponding voltage is generated (Seebeck effect). The coaxial thermocouples are generally fabricated by one thermocouple element is swaged over the second element with an insulating material in between with a typical thickness of about a few micrometers. The thermocouple junction is simply formed by grinding its front

surface with sandpaper. The micro-scratches generated by this process form the active junction of the thermocouple and it represents a very small amount of active mass resulting in a short response time. The voltage difference generated can then be measured and related to the corresponding temperature gradient with respect to a known reference temperature. The coaxial thermocouple design has originally been proposed by (Bendersky 1953), which is made of a small wire coated with a thin layer of aluminum oxide insulation. Various types of surface temperature sensors are, eroding surface thermocouples on cast iron substrates, spot-welded surface thermocouples on iron, brass and stainless steel substrates, vacuum deposited thermocouples and platinum thin film resistance thermometers (Gatowski et al. 1989). The surface junction thermocouples have been formed by using scratches from abrasive paper or scalpel, this causes a small scale plastic deformation of the thermocouple materials and bridges the insulation gap, forming a fine junction which gives a response time of the order of microseconds (Mohammed et al. 2008). Tapered conical inner electrodes can also provide a reliable insulation and allows sufficiently thin sensing junctions for a fast response time (Davis 1999). There are several methods of making a K-type coaxial thermocouple that are described in the literatures. Over five decades ago, Kovacs and Mesler (1964) devised an electro less nickel plating and deposition of camphor black onto the Chromel strip to prepare a thermocouple. Buttsworth (2001) prepared a thermocouple by placing a Chromel wire inside a hole of alumel annulus and baking the assembly in furnace so that an oxidation layer would build along the length. Another method was proposed by Mudford and Gai (1992) where a chromel wire is disposed into a hollow alumel cylinder and the two thermo elements were separated by a thin film of araldite as insulation. The data reduction techniques and the theory of one dimensional, unsteady heat conduction into a semi-infinite medium were also reported (Cook and Felderman

1966, Schultz and Jones 1973, Sundqvist 1992, Menezes and Bhat 2010). The analysis was based on the non-dimensional thermal penetration depth, the variation of material properties like thermal diffusivity, thermal conductivity for alloys like chromel, alumel and constantan within the temperature ranges.

The coaxial thermocouples are less sensitive than thin film sensors but are more robust for use in harsh environment while the thin film sensors provide very fast response and accurate measurement of the surface heat fluxes (Sanderson and Sturtevant 2002, Michael et al. 2010). In certain harsh flow conditions, the thin metallic film (in case of evaporated or sputtered thin film gauges) may be destroyed by the impact of small particles carried by the flow or due to high heat fluxes which cause too high thermal stresses in the film resulting in its destruction. Therefore, for determining relatively low heat fluxes in clean environmental conditions, thin film gauges are recommended whereas for high heat fluxes in harsh conditions thermocouples represent the better choice (Olivier and Gronig 1995).

The different types of thin film gauges and coaxial thermocouples are well established in engineering and scientific application. So, in this work an attempt has been made here to fabricate two types of thin film gauges and one type of coaxial thermocouple in the laboratory. The thin film gauges are fabricated by depositing the paste of (platinum and platinum/nanomaterials) based over the substrate material (pyrex) surface. The K-type coaxial thermocouples are also fabricated by one metallic element swaged over the second element with 1 μ m thick insulating (Teflon) material in between them. Here, a surface junction is formed by grinding the front surface that provides micro-scratches leading to small scale plastic deformation. The micro-scratches generated by this process form the active junction or sensing area of the coaxial thermocouple and it represents a very small amount of active mass resulting

in a short response time. The voltage difference or change in temperature generated can then be measured and related to the corresponding temperature gradient with respect to a known reference temperature.

3.2 Design and Fabrication of Heat Transfer Gauges

3.2.1 Platinum Thin Film Gauges

These thin film gauges are prepared with the help of metallic platinum ink mounted on insulating substrate materials. The type of substrate materials can be Pyrex/Macor or any other ceramic glass having good insulation properties. It ensures the validity of the semi-infinite slab assumption where heat does not penetrate into the substrate during the measurement time scale. Pyrex or Macor materials are the ideal substrate material because it has a low thermal conductivity and they can be heated up to 1000°C without significant geometric deformation. It should also be noted that this material may be machined easily so that gauges may be placed on complex geometrical shapes. Although substrate materials are available in different shapes, a small cylindrical shape is suitable and convenient for constructing rapid response RTD to be used in transient facilities. During the preparation of the gauge, the thickness of the film is maintained to be very small (0.1 μ m - 1.0 μ m) that the temperature on the surface of the substrate is same as that of film. So, the solid rods of pyrex material with 10mm long and 6mm diameter are used (Fig. A1: Appendix - I). For the gauge material to sit properly on the substrate materials, the surface is polished to remove sharp irregularities and to maintain sufficient smoothness. It is achieved through hand polishing the surface with grain silicon carbide sandpaper (wet and/or dry). The smoothing is also done with grain sandpapers by mounting the substrate on a rapidly rotating flat disk. It is performed for several minutes until the substrate material surface appeared visibly polished. Sufficient care is taken to ensure that the substrate

surface remain flat and level during polishing. The edge of the cylinder is slightly chamfered using grain sandpaper with the RTD mounted in a rapidly rotating drill. Rounding of the edges is required to avoid wrapping the lead connections around sharp corners, which would result in poor electrical contact. In order to complete the smoothing process, a crocus cloth is used with the rotating flat disk. After the surface is adequately polished and the substrate piece is washed with water, it is then placed under heating lamp to dry. The drying process is very important since geometric discontinuities in the substrate material such as cracks or cavities may produce faulty sensors. Therefore, the surface of the substrate material is examined using a metallographic microscope before the gauge material being applied. In this, the platinum ink with 99% purity (Fig. A2: Appendix - I) is used to prepare the film.

Commercially, the platinum films are formed on insulating substrates by using preparations of metalloids organics (Benedict 1984). These are solutions of metal compounds in organic solvents. The liquid contains fine metallic particles in suspension and chemical agents that attack the surface of the substrate to provide a highly adherent film. Before depositing them on the substrate material, the liquid bright platinum solution is mixed with thinner. The relative concentration of the platinum and thinner is also important because the final resistance of the gauge depends strongly on the amount of platinum deposited on the surface. Further, poor adhesion may arise due to thick liquid and importance of thinner is felt. After mixing appropriate be more specific quantity of thinner, the liquid becomes thin enough to be applied on the polished surface using a needle. During the present investigation, it is found that a mixture of three parts thinner and one part of liquid bright platinum applied using a small brush with fine hairs produces the best films. The platinum is deposited on the surface of the substrate using the needle in a single stroke such that uniform film thickness is ensured. Immediately after the

platinum is applied, the gauge is dried by a high power lamp for about 10-20mins. Drying is performed in a clean environment to avoid the collection of dust or other impurities on the gauge surface. The gauge is baked further at high temperature (~ 120°C) in a temperature controlled electric furnace to remove the carriers and subsequently brought to room temperature. After pre-baking, the substrate is supported on steel base and inserted into an electric furnace (Fig. A3: Appendix - I). The temperature in the furnace is gradually increased to 650°C by keeping the gauge inside the furnace which is achieved in an hour. After this temperature is achieved, the gauge experiences constant temperature (650°C) for about 30mins. During firing, it is necessary that the rate of increase needs to be gradual so that blistering or boiling of the film does not occur. A number of changes occur in the film during the firing operation and understanding these changes can help to achieve satisfactory films. The gradual thermal decomposition and combustion of metalloids organic molecules leaves the metal components free to form the film. Also, during firing, the base metal additions are oxidized. These base metals form a glass which acts as the interface bond between the substrate and the platinum. As temperatures are further increased, the development of this interface bond becomes optimum. The exact peak temperature is determined by both the requirements of the platinum bond as well as the limitations of thermal deformation of the substrate material. After baking, the thin film gauges are cooled slowly to natural room temperature in the furnace in order to avoid cracking inside the platinum, substrate and interface between the materials. These cracks may cause the film resistance to increase with time due to stress relief. After the preparation of the gauge, it is desired to have necessary electrical connections at the bottom of the substrate. So, further thin films have to be prepared using some metalloids organic materials, which can maintain appropriate contact between the platinum gauges and connecting wires.

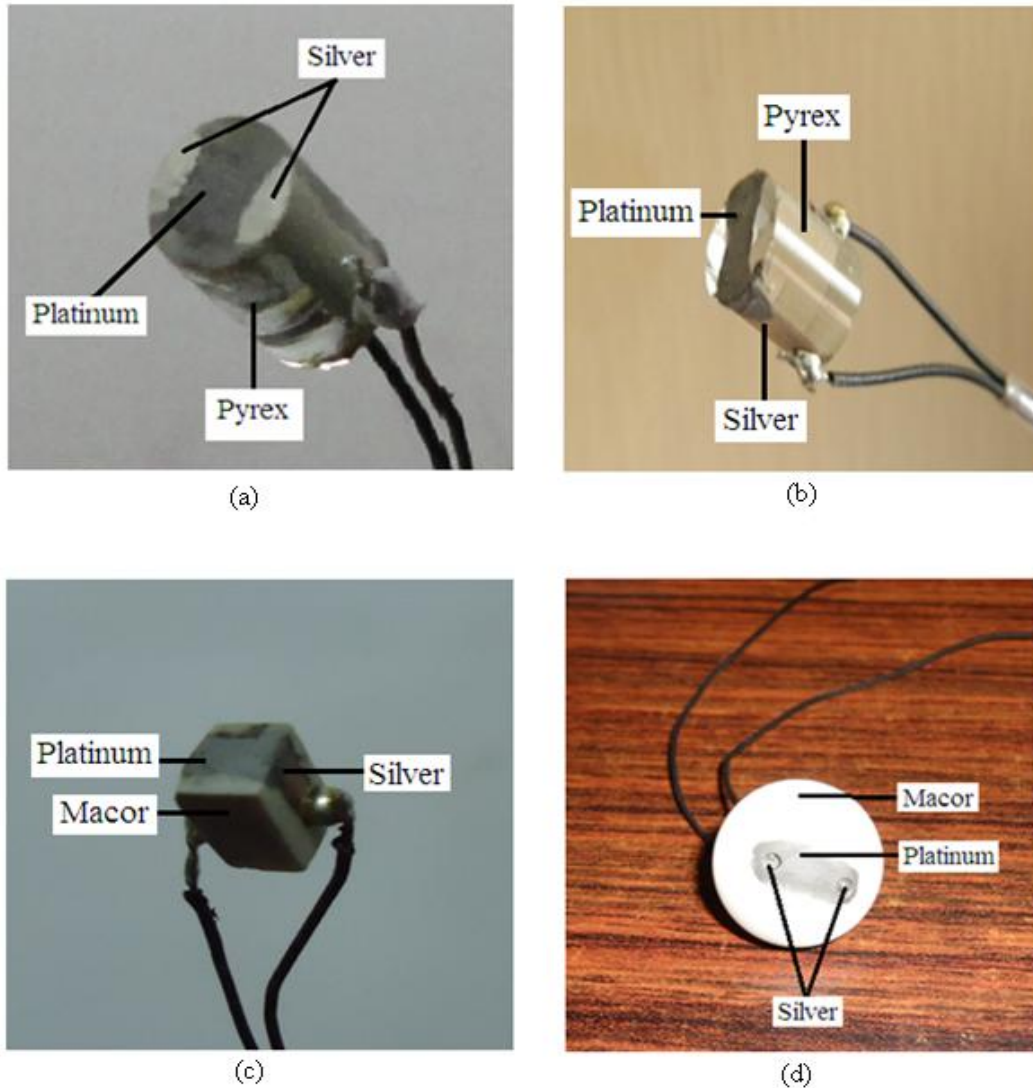


Fig. 3.1: Platinum thin film heat transfer gauges or thermal sensors when Pyrex or Macor as a substrate material

Gold/silver are some of the appropriate metals to achieve suitable electric contacts because they have the baking temperatures in the same range as that of platinum. Here, a silver paste is used as a film on both sides of platinum sensors for the purpose of electrical connections (Fig. A2: Appendix - I). Thin silver films are applied by hand painting on both sides using a needle on the polished surface of the substrate material. After painting, the films are dried at 350°C in the same furnace to allow the evaporation of the chemicals used as binders in the

preparation of the ink. When silver film becomes completely dry, the gauge becomes ready for electrical connections. An insulated lead wire with an outer diameter of 0.3mm is used for making the connections. The wires are attached to the silver film using soldering operations. Insulation tapes (Teflon) is then used to increase the structural stability of the wire leads. The photographs of few such platinum thin film gauge prepared in the laboratory with above procedure are shown in Figs. 3.1(a-d).

3.2.2 Platinum-CNT Thin Film Gauges

The application of carbon nano tubes (CNT) in the heat transfer research area was first demonstrated by Ijima (1991). At present, CNT is the thinnest tube that a human can prepare. It has advantages in lightweight, high strength, high toughness, flexibility, high surface area, high thermal conductivity, good electric conductivity and chemical stability. CNT can be applied to manufacture smaller transistors or electronic devices. Since, it has high toughness; it can be made into high strength composite with other materials. Besides, CNT has both conductor and semiconductor properties. Therefore, for electronic circuit, the semiconductor property of CNT enables its application to field emission transistor gate electrode, which has 100-times higher electric conductivity than silicon semiconductor. The conductor property makes CNTs to have similar thermal conductivity as compared to diamond and superior current carrying capacity to copper and gold.

Platinum materials are commonly used metals to prepare thin film sensors because of their high reactivity and chemical inertness. In order to fully utilize the catalytic activity of platinum, it is critical to anchor the platinum strongly on the supporting material and to prepare platinum based working sensors with a large surface area on which electrochemical reactions can take place. Carbon nanomaterials such as carbon black, carbon nano fibers and CNTs are widely

used as a supporting matrix. Considering the excellent electro catalytic characteristics of platinum and CNT materials, the supported nano composites would be an ideal material for thin film sensors. In this work, purified form of CNTs with a spherical nanostructures are used (Fig. A4: Appendix - I). These spherical carbon molecules have unusual properties and can be activated so as to generate functional groups such as COOH, OH and CO for better adhesion of the platinum to the CNT surface.

The procedure for preparation of platinum-CNT thin film gauge involves the mixing of suitable quantity of platinum (by mass) with CNT with adequate amount of thinner (Fig. A5: Appendix - I). The CNTs mixed with platinum by a mass fraction ($\beta = 5\%$) are placed in the beaker and further in a tip-sonicator (Fig. A6: Appendix - I). The solution is then continuously stirred for 45min under ultrasonic vibration. Thus, the ultrasonic power is converted into high frequency mechanical vibrations, that intensifies the probe focused at the tip where the atomization takes place. Mixing takes place uniformly with the probes by holding the jack with adjustable elevation. Booster are generally used to connect the converter and the probe acts as a mechanical amplifier that increase the amplitude of vibration at the probe tip. Generally, the probes are one-half wavelength long tools that act as mechanical transformers to increase the amplitude of vibration generated by the converter. In the tip sonicator, VCX digitally displays the actual amount of energy that being delivered to the probe and terminates the ultrasonics waves when the desired amount of energy is dispensed. In mixing process even though ultrasonic vibrations are above the human audible range, ultrasonic processing produces a high pitched noise in the form of harmonics which emanate from the vessel walls and the fluid surface. Therefore, an enclosure is used in this process which is a white laminated with its interior as

white waterproof polyethylene noise abating material. The access door permits observation during treatment and protects the operator against accidental splashing.

After mixing of platinum chemical with CNT material, the mixtures are deposited on the highly polished substrate (Pyrex) material surface. This platinum/CNT mixture is necessarily the liquid containing fine platinum particles in suspension of chemical agents which attack the surface of the substrate material surface to provide highly adherent film. The drying of these mixtures is also done by evaporation of these chemical binders at temperatures around 200°C in the temperature controlled oven. These platinum/CNT films are then naturally cooled to the atmospheric room temperature. Since this film does not make appropriate contact with connecting wires, a thin film of silver paste is applied on either sides of the substrate material surface. When silver film becomes completely dry, the gauge becomes ready for electrical connections, to achieve necessary electrical connections in the same procedure as discussed in Section 3.2.1. The platinum/CNT based thin film heat transfer sensor design and prepared using this procedure is shown in Fig. 3.2.

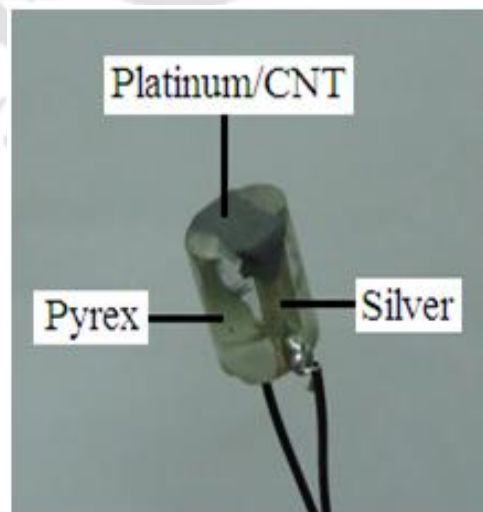


Fig. 3.2: Photograph of a platinum/CNT thin film heat transfer gauge

3.2.3 Fabrication of K-type Coaxial Thermocouple Sensor

Thermocouples have been widely used techniques for many years as accurate temperature measurement sensor in internal combustion engine cylinder walls (Alkidas 1985), aerodynamics facilities (Jessen 1991), gun barrels (Chen 1995) and in boiling experiments (Lee 1985). Thermocouples offer advantages of being capable of operating over a large temperature range and are low in cost. The most important factor that determines the performance of the thermocouples (such as accuracy, response time and repeatability) is the quality of the junction. In conventional thermocouples, two dissimilar metals are connected together to form a junction. Depending on the type of materials used and temperature range of applications, they are classified as K or E or T-type thermocouples (Chung and Brill 1993) and are best suited for steady state temperature measurements. In contrast, a coaxial thermocouple has a unique design in which one thermocouple material is swaged over the second element with an electrical insulation between them. The surface junction is formed by grinding the front surface, thus micro-scratches are generated by this mechanism, which makes it suitable to respond in short duration time scale. Being coaxial, they can be easily fitted to any types of surfaces for accurate measurement of rapidly varying temperatures.

The K-type coaxial thermocouple is prepared with chromel and alumel wires of diameters 0.9mm and 3.25mm, respectively (Fig A7: Appendix - I). Since, the diameters of the wires are very small, it needs precision work during the fabrication process. Before assembling the two wires to form the junction, appropriate length of each wire (about 10mm) is prepared, so as to keep the overall size of the sensor as small as possible. An insulating material (Teflon) is used to tightly fix over the chromel wire, so as to avoid electric contact between two thermocouple materials. A hole of 1mm diameter, is drilled into the alumel wire in which the insulated chromel

wire is inserted and tightly fitted. Thus, the chromel wire forms the inner element while alumel wire forms the outer tube element with an insulated coating in between the wires. The surface junction is formed at the flush end, by using grinding process and subsequently scratching the surface in the order of 10-15 μ m. It creates a plastic deformation of one metal over the other by bridging the insulating material between chromel and alumel elements, thus forms a microscopic junction on the surface with very low thermal mass and inertia (Sundqvist 1992 and Mohammed et al. 2008). The connecting leads are then soldered to each of the thermocouple wires and it is then ready for mounting on the brass model to have proper stability this coaxial sensor. A small acrylic piece is used as thermal insulation of this sensor with the brass and the photograph is shown in Fig. 3.3.



Fig. 3.3: Photograph of a coaxial thermocouple sensor

3.3 Preliminary Analysis of the Heat Transfer Gauges

3.3.1 Thermal Property Analysis of the Platinum-CNT Mixtures

The high thermal conductivity of nanoparticles suspended in the base fluid which has a low thermal conductivity, remarkably increase thermal conductivity of nanofluids or base materials.

Researchers developed many analytical models to quantify the amount of increase and compared them with experimental results (Tsai et al. 2005). Still, it needs further research to develop a sophisticated theory to predict thermal conductivity of nano fluids or mixtures. But there exists some empirical correlations to calculate effective thermal conductivity of two phase mixtures. In the literature, the thermal conductivity enhancement ratio has been defined as the ratio of thermal conductivity of the nanomaterials (high conducting material) to the thermal conductivity of the low conducting base material (K_{eff} / K_1). Researchers developed their thermal conductivity models based on the Maxwell classical research on conduction through heterogeneous media (Hamilton 1962). The effective thermal conductivity (K_{eff}) for a two phase mixture consisting of a continuous and discontinuous phase is expressed in the following from;

$$K_{eff} = \frac{2K_2 + K_1 + \beta(K_2 - K_1)}{2K_2 + K_1 - 2\beta(K_2 - K_1)} K_1 \quad (3.1)$$

Where, β is the particle mass fraction of CNT in the platinum material, K_1 and K_2 are the thermal conductivity of the platinum and the CNTs, respectively. Maxwell derived this model based on the assumption that the discontinuous phase is spherical in shape and the thermal conductivity of nanoparticles depend on the thermal conductivity of spherical particles, the base fluid and the particle mass fractions. The thermal diffusivity of the mixtures given in the terms of thermal conductivity, density and specific heat is given below;

$$\alpha_{eff} = \frac{K_{eff}}{(\rho c)_{eff}} = \frac{K_{eff}}{(1-\beta)(\rho c)_1 + \beta(\rho c)_2} \quad (3.2)$$

Here, α_{eff} is effective thermal diffusivity of the mixtures, ρ and c are density and specific heat of the materials, $(\rho c)_1$ and $(\rho c)_2$ are the thermal products of platinum and carbon nano tubes.

The variations of effective thermal conductivity and diffusivity for four different mass fractions

($\beta = 5\%, 15\%, 25\%, 35\%$) are shown in Fig. 3.4 and Fig. 3.5. The results showed that all the models predict increasing effective thermal conductivity and effective thermal diffusivity for increase of particle mass fraction of carbon nano materials in the platinum base material.

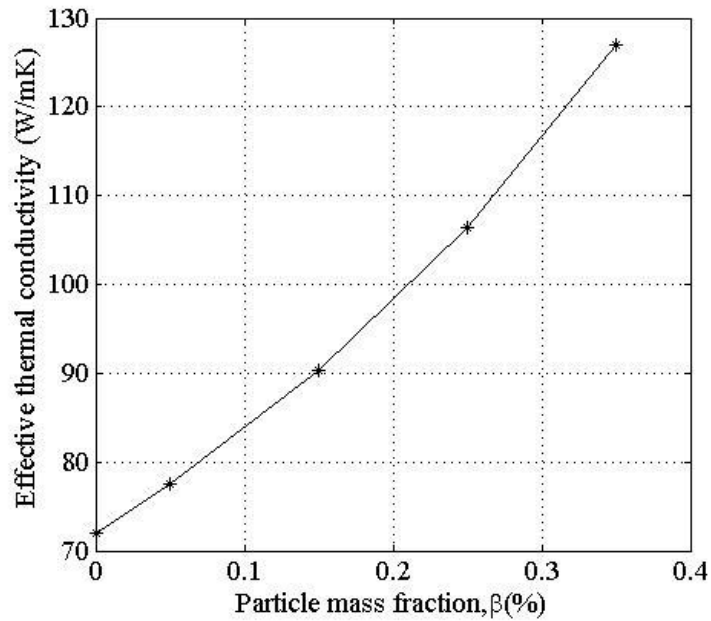


Fig. 3.4: Variation of effective thermal conductivity with CNT mass fractions

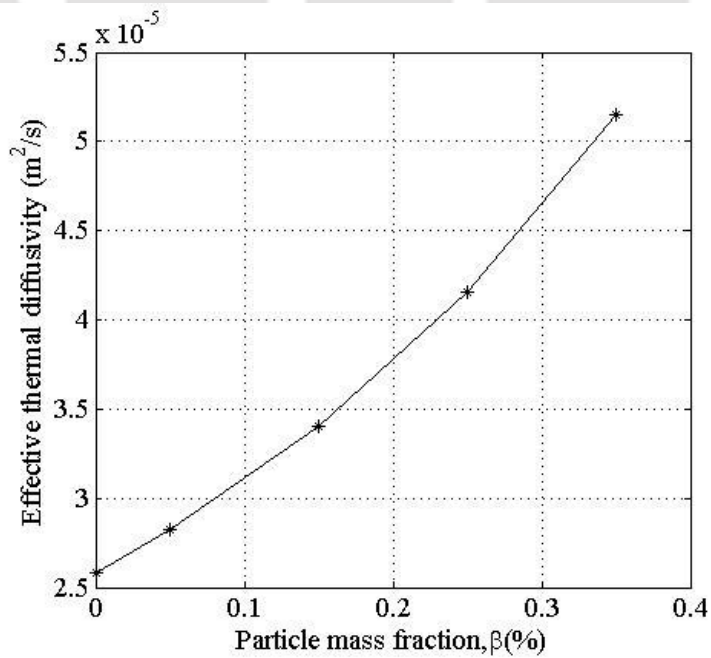


Fig. 3.5: Variation of effective thermal diffusivity with CNT mass fractions

3.3.2 Surface Morphology of the Platinum-CNT sensor

A scanning electron microscope (SEM) is a type of electron microscope that produces images of a sample by scanning it with a focused beam of electrons. The electrons interact with electrons in the sample, producing various signals that can be detected and that contain information about the sample's surface topography and composition. The electron beam is generally scanned in a raster scan pattern, and the beam's position is combined with the detected signal to produce an image. SEM can achieve resolution better than one nanometer. A SEM typically has orders of magnitude better depth of focus than an optical microscope making SEM suitable for studying surface properties. The SEM characterization of CNT formed on the surface and inside of platinum by catalytic process is shown in Fig. 3.6(a-b). The multi graphitic structure of CNT wall is not clearly seen but it is likely that CNT are multilayered. Results obviously show differences between these structures that confirm different mechanism of their growth. The morphology of these structures is very similar to platinum/MWCNT growth by Fe nanoparticles from planar surface as reported in previous studies (Belinda et al. 2010).

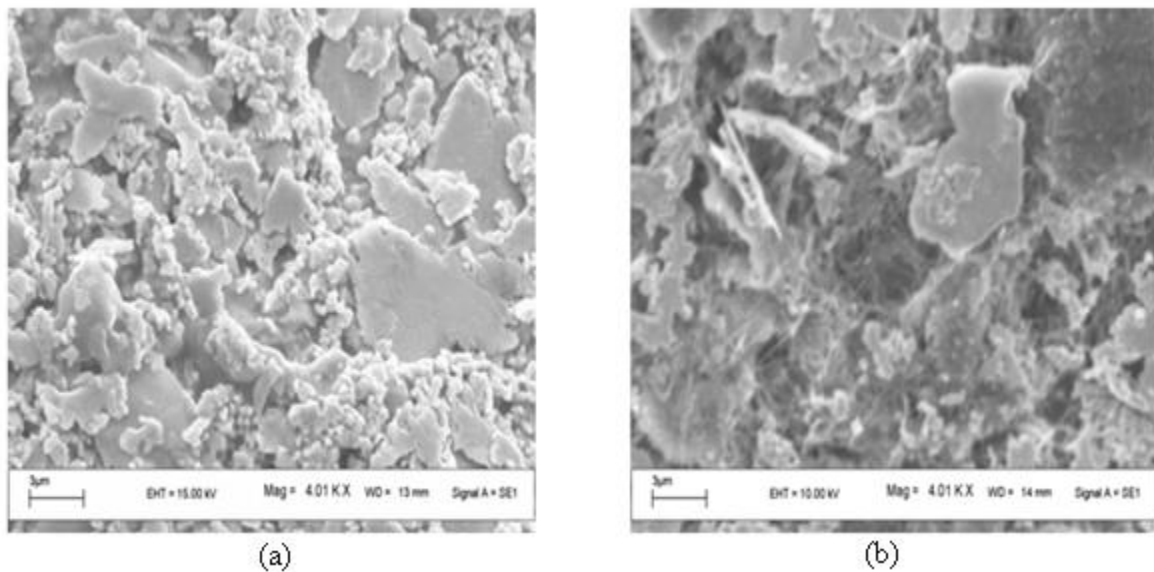


Fig. 3.6: Surface morphology (SEM image) of thin film sensors

3.3.3 Effective Thermal Properties for Sensors

The coaxial thermocouple is intended to capture the time varying surface temperatures and subsequently estimate the surface heat flux. So, there is a need to know the thermo physical properties of the substrate or more precisely the value of the thermal product (β). The effective thermal product is an important parameter because it is used for deducing heat flux from the temperature time history of the sensor. Thermal product is defined as the square root of thermal properties ($\beta = \sqrt{\rho ck}$) of the materials used for gauge fabrication. In case of platinum/platinum-CNT thin film sensors, it is the properties of the backing material (i.e. pyrex or macor). These properties are given in Table - 1 (Appendix - II). For the coaxial thermocouple, it becomes the effective thermal product of the metallic substrate on which the surface junction is formed. Depending on the way the junction is formed, appropriate weighting factors are used to account for the contribution of each metal that holds the junction over it. In the present K-type thermocouple, it is the contributions of both chromel and alumel wires. Usually, the weighting factors for each material are difficult to estimate accurately. However, equal contribution (weighting factor of 0.5) can be assumed for each of the metals by which the junction is formed. So, the effective thermal product of the substrate has been taken as the average of the values for chromel and alumel at ambient temperature for each step heating loads. In the literature, the thermo physical properties selection of coaxial thermocouple (chromel and alumel wires) and correlation equations are developed for the specific heat and thermal conductivity of calculations as a function of temperature (Buttsworth 2001 and Mohammed et al. 2008).

Chromel materials

$$C_{cr} = 0.1786T + 394.3 \quad (3.3)$$

$$K_{cr} = 0.01912T + 12.11 \quad (3.4)$$

Alumel materials

$$C_{al} = 0.07512T + 500.8 \quad (3.5)$$

$$K_{al} = 0.02981T + 18.42 \quad (3.6)$$

Here, the temperature T is expressed in K , the specific heat C is in J / KgK and the thermal conductivity K is in W / mK . Based on the data reported in (Buttsworth 2001), the densities of the chromel and alumel materials are taken to be $8730 \text{ Kg} / m^3$ and $8600 \text{ kg} / m^3$ respectively. The analysis of thermocouple materials and the variation of thermal products with change in temperature are as given in Appendix - III.

3.3.4 Analysis of Heat Transfer Sensors Thickness

The thicknesses (gauge and substrate materials) of heat transfer sensors are very important for heat transfer modeling because thickness plays a crucial role in time scale of measurement and heat penetration into the substrate. In the heat transfer sensors, the thickness of gauge film (sensing area) material is very small for various types of films. Although, there are number of methods are available, the most accurate one is the real time monitoring using optical technique such as a profile meter (Fig. A8: Appendix - I). It consists of a phonograph needle that moves on the surface of the gauge material and its mechanical movement is sensed electromagnetically. Thus, the surface topography of the image is obtained. Sensing the mechanical movement of probes as it traces the topography of a film-substrate step. The step can be made by masking or etching during or after deposition respectively. Diamond probes with conical shaped are commercially available for this purpose. Film thickness for heat transfer thin film gauges are directly read out as the height of the resulting step contour trace as shown in Fig. 3.7(a-b). The average values of measured thickness of the gauge or sensing materials are $1.21\mu\text{m}$ and $1.36\mu\text{m}$

for platinum and platinum/CNT based heat transfer gauges. The thickness of substrate materials are measured by using a vernier caliper (Fig. A8: Appendix - I) and is obtained as 10mm.

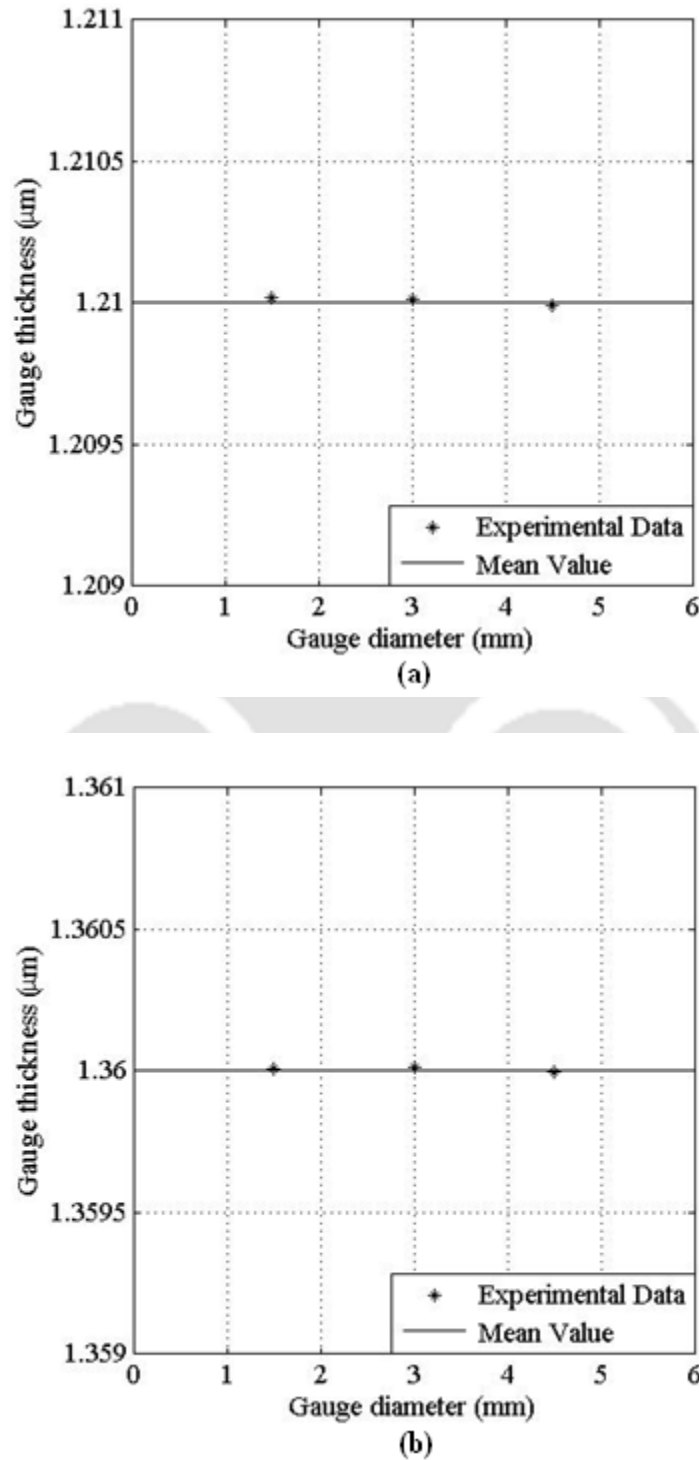


Fig. 3.7: Gauge material thickness of (a) platinum and (b) platinum/CNT sensor

3.4 Surface Temperature Analysis

If accurate heat flux measurements are to be made, then the thin film heat transfer gauges must follow the one dimensional theory and follow the assumption of semi-infinite bodies. In order to achieve this, the substrate materials on which the thin film gauges (sensing areas) are mounted must be thin enough so that heat transfer occurs into the substrate is similar to that into a semi-infinite solid. Furthermore, the films must be placed away from substrate discontinuities at distances equivalent to or greater than those required for a semi-infinite substrate behavior. The minimum thickness required can be obtained by considering the substrate base temperature to surface temperature ratio for the situation shown in Fig. 3.8. For constant heat flux value applied on the sensing (gauge) material, the temperature ratios at the surface and at any depth of substrate material can be obtained (Vidal 1956).

$$\frac{T(x,t)}{T(0,t)} = e^{-\frac{x^2}{4\alpha t}} - \left(\frac{\pi}{\alpha t}\right)^{1/2} \frac{x}{2} \operatorname{erfc}\left(\frac{x}{2(\alpha t)^{1/2}}\right) \quad (3.7)$$

On the surface of the gauge material at $x = 0$,

$$\frac{T(x,t)}{T(0,t)} = e^{-\frac{x^2}{4\alpha t}} \quad (3.8)$$

Where $(\alpha = k / \rho c)$ is the thermal diffusivity of the substrate materials and k , ρ and c are thermal conductivity, density and specific heat of the substrate material, t is experimental time intervals and x is the penetration depth of the substrate materials. Ideally, the temperature at the substrate base should be the same as ambient or room temperature for all testing time. Therefore at the end of a test, the temperature ratio in Eq. (3.7) should be very small. Then, by using Eq. (3.8), the temperature ratio can be plotted as a function of the substrate depth for different time scale of measurement. The results are shown in Fig. 3.9, Fig. 3.10, Fig. 3.11, and Fig. 3.12 with substrate materials as pyrex, macor, chromel and alumel materials. With the present thickness

(10mm) of pyrex and macor substrate materials, the surface temperature ratio drop is very small (~ 1.0%) even the tests are conducted for 10s. In other words, the semi-infinite assumption of heat flux penetration holds good for this case. However, these insulating substrates are actually over 10.0mm thick to have proper mechanical strength while performing actual measurements (Schultz and Jones 1973). It is obvious that substrates which exceed this value are satisfactory for all test durations less than about 10s. Therefore, the semi-infinite assumption is well satisfied for short duration testing. Similar plots are obtained for chromel and alumel materials as substrate materials as shown in Fig. 3.11 and Fig. 3.12. Here, the temperature drop is less than 1%, for any value of junction thickness of 0.004mm when the duration of measurement is 200ms. With increase in time scale of measurement analysis, the surface temperature ratio drops drastically and it is unlikely to have semi-infinite assumption of heat conduction modeling. With the present design of substrate for thin film gauge and coaxial thermocouple sensors, all the subsequent experiments are performed so that time scale of measurement justifies the semi-infinite assumption during heat conduction modeling.

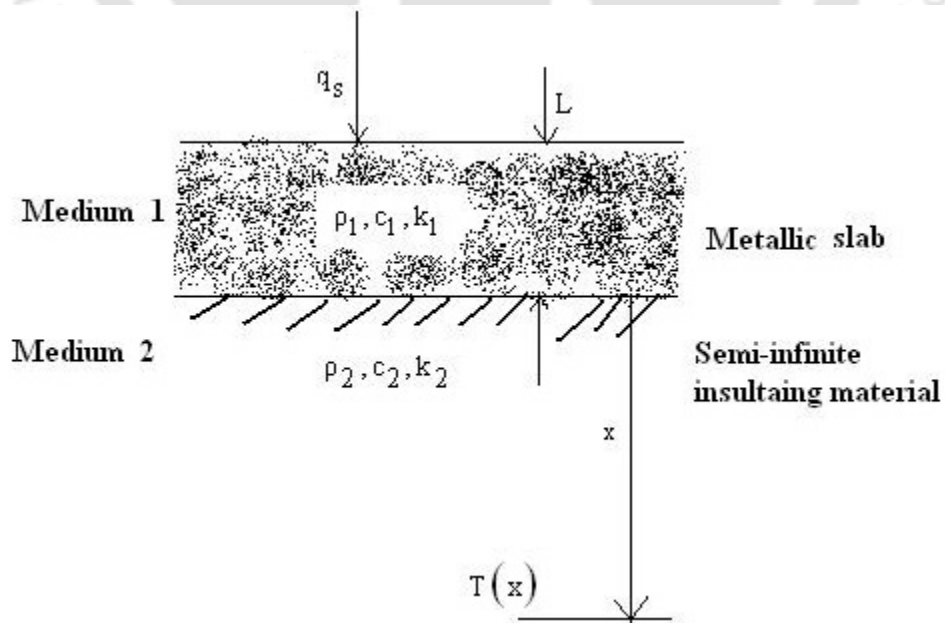


Fig. 3.8: Heat conduction analysis of heat transfer gauge

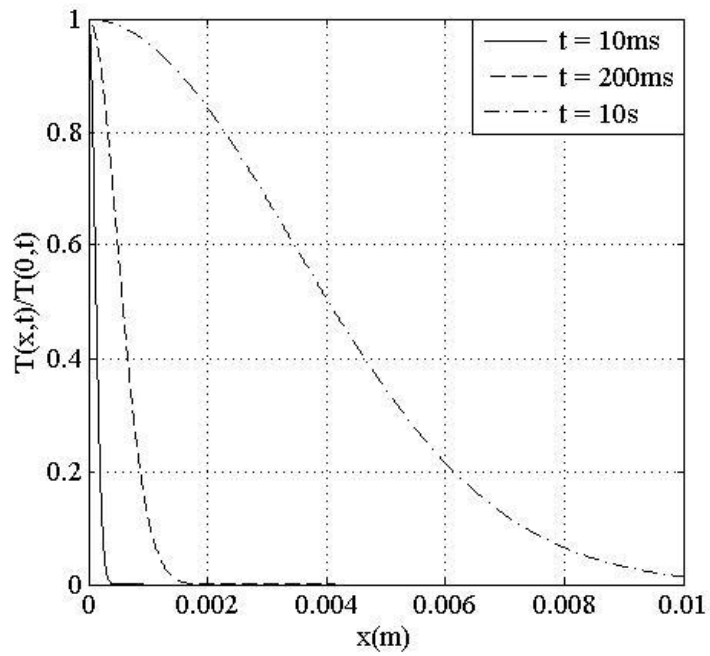


Fig. 3.9: Determination of substrate thickness for semi-infinite assumptions with pyrex substrate

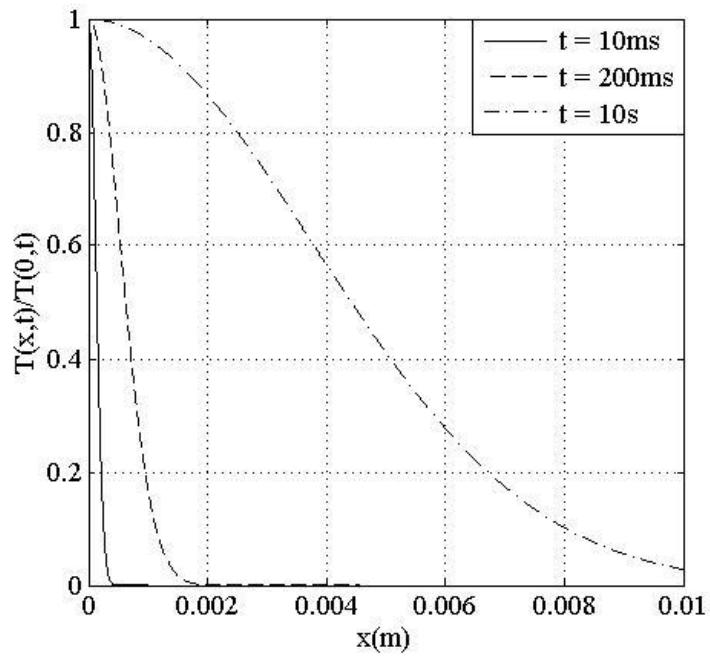


Fig. 3.10: Determination of substrate thickness for semi-infinite assumptions with Macor substrate

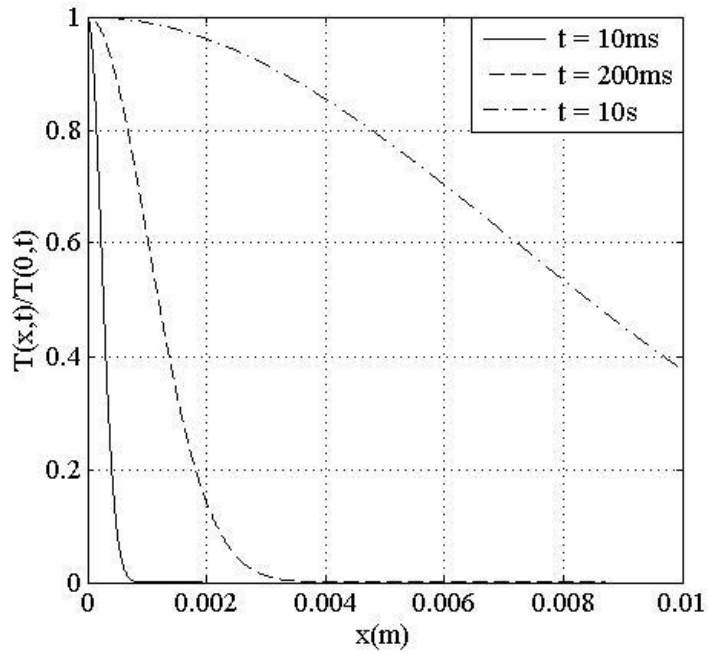


Fig. 3.11: Determination of substrate thickness for semi-infinite assumptions with chromel substrate

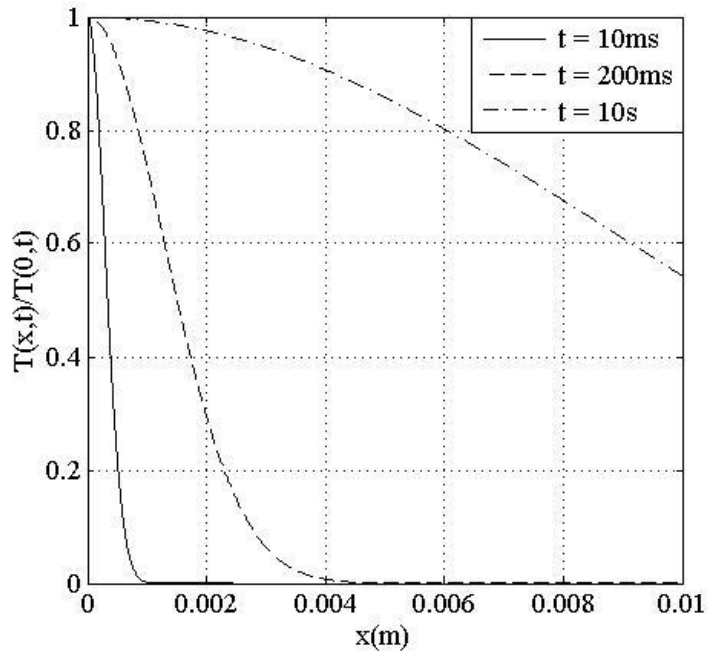


Fig. 3.12: Determination of substrate thickness for semi-infinite assumptions with alumel substrate

3.5 Summary

The fabrication method of heat transfer gauges started with initial trial and error phase of construction process and only about 10% of the heat transfer gauge produced had the desired resistance. Due to the rapid evaporation of the thinning essence and the inability to closely regulate the platinum contained in the brush, the final resistance values were consistently too low. Out of these 10%, nearly all were destroyed when subject to excitation voltages as low as 2V. These were caused by an inadequate amount of lead material at the contact points which resulted in burnout. After gaining a considerable amount of experience of gauge deposition and baking procedures, the success rate has increased to about 90%. Although the amount of sensing material applied could not be easily regulated, this method proved to give more consistent and reliable results. The analysis of variation of surface temperature histories for pyrex, macor, chromel-alumel materials as a function of the substrate depth for several different testing time intervals are also plotted. From the plots it can be seen that for a substrate base temperature to surface temperature ratio of less than 1%, the substrate thickness must be at least 10mm for the relatively long testing time (more than 10s). However, for reasons of mechanical strength, insulating substrate are actually over 10mm thick. From the plots it is obvious that substrates which exceed this value are satisfactory for short durations testing and well satisfied the semi-infinite assumptions for heat conduction modeling.

Chapter - 4

Static Calibration of the Heat Transfer Gauges for Transient Measurement

The heat transfer gauges are basically the resistance temperature detectors (RTD). They operate on the simple principle that changes in electrical resistance of pure metals are indicated as the linear positive change in voltage with variation in temperature. These sensors are widely used type of thermal sensor for measurement and control, and can also be used to convert a temperature gradient into voltage. The thermal coefficient of resistance (TCR) and sensitivity of these RTDs are the important parameters responsible to link the voltage variation with the temperature change of the medium. The TCR and sensitivity of these heat transfer gauges depend upon a variety of factors including the property of sensing junction or film materials, the size of the film deposition and its shapes. The weight of the sensing junction of the thermal sensor is also very important because a very small change in its weight may cause a significant change of the final value of TCR and sensitivity. It is possible criteria with rather small weights of importance to be much more critical in a given situation than that with larger weights. The purpose of this work is to statically calibrate each handmade heat transfer gauges by using oil bath based experimental technique. This experimental method is used to measure the variation of change in voltage signals with change in temperature and calculate the typical value of TCR and sensitivity of each handmade heat transfer gauges.

4.1 Introduction

Heat transfer gauges are suitable for measuring highly transient surface temperature in flows of this nature. From the time history of the surface temperature, the heat flux may be obtained. The electrical resistance of most of the materials increases with rise in temperature. This characteristic is used in electrical sciences to get the indication in voltage form for these handmade heat transfer gauges or RTD sensors. A typical thermal resistance sensor consists of a junction also known as sensing area mounted on a supporting framework and encased in a protective sheath. The junction is composed of a circuit that is connected to the output signal measuring instruments to measure the variations in the resistance across the materials. In order to increase the performance (sensitivity) of the thermal sensors and to obtain a useful signal, the change in resistance is converted into a change in voltage by using a Wheatstone bridge circuit. The voltage changed can be displayed or can be sent to a recording device for subsequent analysis. The ratio of change in voltage (physical property) and per unit change in temperature across the sensor sensing materials is also known as sensitivity of the heat transfer gauges. The sensitivity is an important parameter because sometimes, the sensitivity analysis may dramatically improve the effectiveness of the initial study and assist in the successful implementation of the final solution.

The RTD sensors are commonly used in surface heat fluxes measurement analysis because of their reliability, ruggedness and ability to cover a wide range of temperatures. Although no material is universally accepted for RTD elements, there are several factors that govern the type of material used. The material should have a high resistivity which permits fabrication in convenient sizes because any excessive bulk would degrade the response of the sensor. In addition, the thermal coefficient of resistivity and sensitivity should be a constant

quantity so that the variation of resistance with temperature becomes linear. Also, the higher values of TCR and sensitivity indicate good response and accuracy in temperature measurement. The material should be corrosion resistant and should not undergo phase changes in the temperature range of interest. For consideration into thin film gauge materials, some common materials that meet the above requirements are platinum, nickel, gold and silver (Bechwith 1995). However, platinum and nickel are exclusively used for precision thin film based heat transfer gauges. Evidence of the important and reliability platinum RTDs can be found in the international temperature scale which specifies a platinum resistance thermometer as the interpolation standard (Benedict 1984). Platinum is an ideal sensing element and can be obtained to a high degree of purity, but it is extremely sensitive to strains. Any minute impurity can alter the linear variation response with temperature (Vidal 1956). However, the thin film gauges has to be energized by constant current source to obtain the voltage change with temperature and hence called as *passive sensors*. In case of thermocouples, the commonly used materials are chromel-alumel and constantan-alumel, etc. These are the RTD sensors that can generate the voltage without any power sources and called as *active sensors*. The thermocouple elements produce an output voltage which depends on the temperature difference between the junctions of two dissimilar metal wires. It is important to note that it measures the temperature difference between two points, not absolute temperature. For practical measurement of temperatures, the junctions of specific alloys are used which have a predictable and repeatable relationship between temperature and voltage. Different alloys need to be used for certain specified range of temperatures. Properties such as resistance to corrosion may also be important when choosing a type of thermocouple material because any erosion of the metal films alters the sensitivity. Where the measurement point is far from the measuring instrument, the intermediate connection

can be made by extension wires which are less costly than the materials used to make the thermocouple sensors. Thermocouples are usually standardized against a reference temperature of 0°C. Any attempt to measure this voltage signals necessarily involves connecting another conductor to the 'hot' end. This additional conductor will then also experience the thermal/temperature gradient and develop a voltage signal of its own which will oppose the original value. Fortunately, the magnitude of the effect depends on the conducting material in use. Using a dissimilar conducting metal a complete circuit can be created in which the two legs generate different voltages, leaving a small difference in voltage available for measurement.

Industrial type RTD sensors are guarded against effects by elaborate precautions such as encasing them in probes or in plugs (Figliola and Beasley 1995). Although they come in variety of sizes and shapes most commercial sensors tend to be quite large and have a relatively slow response time (Schooley 1986). Traditionally, commercial sensors are used to monitor temperature rise or heat transfer over relatively long period of time. Applications of this nature do not normally require detailed specifications such as response time, sensitivity and self heating data. Therefore manufactures do not provide such information to qualify the product for high speed research applications. These factors render commercial sensors virtually unusable for many gas dynamic research applications. The advantage of custom built thermal sensors is that they can be shaped to the contour of the test model. However, the cost of sensor material is relatively high and the thermal sensors are usually destroyed by the harsh test environment after only a few shot runs. Replacing all the thermal sensors of a heavily instrumented model can be very expensive and impractical. Therefore, a low cost reliable method of handmade construction and the calibration of the heat transfer gauges are needed. Static calibration refers to the evaluation and adjusting the precision and accuracy of measurement equipment. It is also very

important during calibration to make sure that the measurements taken during the period is also valid. First, the handmade RTD heat transfer gauges must be calibrated for temperature to ensure that the corresponding voltage change should be as desired. It requires an accurate knowledge of the thermal properties (TCR) of the gauge materials. For example, the TCR of a heat transfer gauges depends on a variety of factors including the property of sensing material, the size of the deposition and its shape. The useful linear range also depends on a number of factors including the uniformity of the metallic layer, purity and bonding to the substrate materials. Furthermore, the value of the thermal property depends on the gauge construction and in particular the firing details of the ceramic production process. For accurate transient temperature measurements by heat transfer gauges, each sensor must be independently calibrated for temperature. Also, the heat flux estimation requires an accurate knowledge of the thermal properties of the sensing material. So, independent calibration of these handmade sensors is very much useful.

The objective of the present chapter is to calibrate the handmade heat transfer gauges for temperature. The voltage rise corresponding to a known temperature change is measured. An oil bath experimental setup is used for this purpose. This common experimental setup is useful for all types of RTDs including the in house fabricated sensors (i.e. thin film gauges and coaxial thermocouple). During the oil bath based experiment, the typical value of thermal coefficient of resistance and sensitivity are calculated. It is found that these handmade heat transfer sensors are also very sensitive to temperatures.

4.2 Working Principle of the Heat Transfer Gauges

In 1821, an Estonian physicist, Thomas Johann Seebeck, discovered that when any conducting material (such as a metal) is subjected to a thermal gradient then it will generate a voltage. The heat transfer gauges also operate on the same principle that the resistance of metal increases with

a rise in surface temperature. The method for determining surface heat transfer rates depends on the measured temperature rise during the test time and calculating surface heat flux from the data. When using heat transfer gauges, the surface temperature is determined from the change in resistance of the sensing film materials. For practical purpose the resistance of sensing materials varies linearly with temperature as

$$R(T) = R_0 [1 + \alpha_0 (T - T_0)] \quad (4.1)$$

Where, R is the film resistance at surface temperature T , R_0 the film resistance at temperature T_0 and α_0 is the TCR which must be experimentally determined for each heat transfer gauges. The thin film gauges are passive device therefore it operates usually by passing a low level current (7mA to 15mA) through the thin film gauges during experiment period with the help of constant current source as shown in Fig. 4.1. Therefore, the errors in the output signal measurements are also reduced due to initial heating, self heating and heat generation across the gauge materials of the thermal sensor. However, the thermocouples are self powered and they do not require external form of excitation while measuring the voltage difference. Using the fundamental Ohm's law, the relation between change in voltage and change in temperature signal is given by the equations,

$$(T - T_0) = \frac{\Delta V}{\alpha_0 V_0} \quad (4.2)$$

Here, ΔV is the change in output voltage and V_0 is the initial voltage at temperature T_0 applied to the heat transfer gauges. From Eq. 4.2, it is apparent that change in output voltage signal is directly proportional to the change in temperature applied to the heat transfer gauges. However, the maximum excitation voltage that can be applied to the heat transfer gauge is limited by internal heat generation.

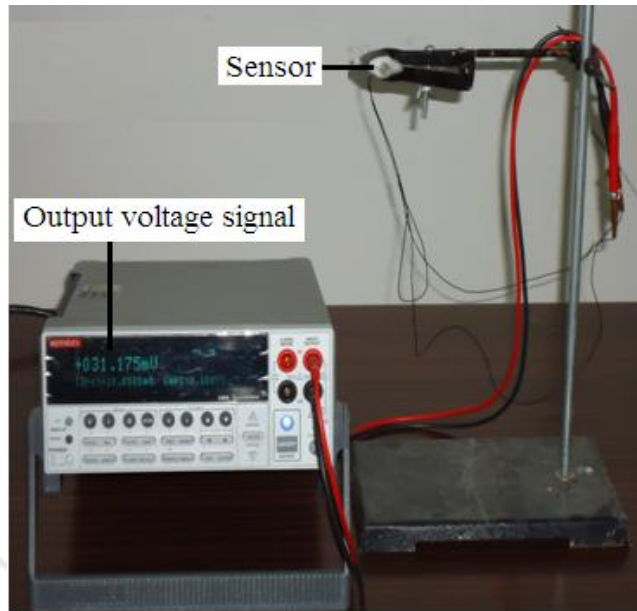


Fig. 4.1: Laboratory set up of constant current source and thermal sensor

4.3 Sensitivity Analysis of Heat Transfer Gauges

Sensitivity analysis is the study of the variation in the output of a model to different variations in the inputs. It is a technique for systematically changing variables in a model to determine the effects of such changes in the output. Here, the sensitivity of a sensor material represented as S , depends on the material's temperature and crystal structure. Typically, metals have small sensitivity because most have half filled bands. Electrons (negative charges) and holes (positive charges) both contribute to the induced thermoelectric voltage thus canceling each other's contribution to that voltage and making it small. In contrast, semiconductors can be doped with an excess amount of electrons or holes and thus can have large positive or negative values of the thermo power depending on the charge of the excess carriers. The sign of the sensitivity can determine dominance of charged carriers during the electric transport in both metals and semiconductors. If ΔT is the temperature difference and ΔV is thermoelectric voltage between the two ends of a material, then the sensitivity of a material is conventionally defined as,

$$S = \frac{\Delta V}{\Delta T} \quad (4.3)$$

The numerator of the Eq. (4.3) should be the difference in electrochemical potential while the denominator is the chemical potential and is often relatively constant as a function of temperature. For the present heat transfer sensors, the sensitivity can be increased with increase in film voltage.

4.4 Static Calibration of Heat Transfer Gauges

Determination of thermal coefficient of resistance and sensitivity of the heat transfer gauges is mandatory for inferring the temperature change and is generally obtained by using oil bath technique. Static calibration refers to the evaluation of these parameters while maintaining the precision and accuracy of output signal in measuring instruments. It is also important that the temperature range should be within the actual experimental time scale of measurement. The oil bath arrangement provides gradual step variation in the temperature fed to the sensors. The experiments are performed to check the linearity between changes in resistance or voltage signals with change in temperature across the sensing materials during heating and cooling process. Subsequently, TCR and the sensitivity of each handmade heat transfer gauges are determined. The useful linear variation also depends upon a number of factors including the uniformity of the metallic layer, purity and bonding of the sensor sensing materials.

The oil bath arrangement provides gradual step variation in the temperature fed to the gauges (Skinner 1962). In this method, hot air is produced in a beaker (where the sensor is placed), by heating oil kept in another container as shown in Fig. 4.2. The surface of the heat transfer sensors is heated in this process of indirect heating arrangements. Since the junction is not in direct contact with heating oil, it remains protected. A scientific calibrated thermometer,

the accuracy for the thermometer was $\pm 0.002^{\circ}\text{C}$ (Fluke Hart Scientific 1523 thermometer) is also mounted in the beaker along with the sensor to record manually the temperature of the air during heating and natural cooling process. The heat supplied by a constant heat flux based heating unit is utilized to heat the oil and subsequently utilized to create hot air in the beaker. Thus, the heat losses due to various sources are minimized. Once the thermal equilibrium is achieved, the bath temperature is recorded simultaneously by the sensor and thermometer. Before noting the final readings, the bath temperatures are monitored at several locations to ensure the uniform temperature gradient in the entire region of hot air beaker. An output signal measuring system is used to monitor the change in voltage across the sensor for corresponding change in temperature. The schematic diagram of the entire experimental setup is given in Fig. 4.3.

The oil bath calibration setup provides indirect way of providing temperature change across the heat transfer gauges. The heat is supplied by a constant heat flux based heating element that heats the silicon oil in the first beaker which produces hot air in another beaker containing the heat transfer gauges. Some precautions and attention is required while performing the experiments. When heat transfer gauges are placed in a temperature controlled beaker, sufficient time is allowed (several minutes) for the bath temperature to approach thermal equilibrium before any attempt to ascertain its value is made. The thermal sensors are brought to thermal equilibrium with the bath at sufficient distance from one another to avoid disturbing the flow around each other. Once this is accomplished the bath temperature can be monitored at the point of use with the smallest possibility of temperature gradient. The readings noted for several times such that no appreciable change in temperature is observed from the thermometer thereby ensuring the thermal equilibrium. The volume of bath fluid is greater than that of whatever is placed in it to avoid significant disruption of the normal flow patterns which would create non

uniformities in the temperature of the bath. With proper attention, the thermometer is used to record the temperature when the steady state is reached. The readings should be avoided, if the temperature fluctuates over intervals much longer than the response time (several tens of seconds) of the thermometers. In order to have the capacity of good control and uniformity of temperature in a liquid bath, considerable attention must be given to the selection of a properly designed bath, the controller, the sensor, the temperature range desired and the fluid to be used.

The output change in voltage signals are measured by using source meter. Since, the thin film gauges are passive device, the sensors need to be energized by flow constant current (10mA) across sensors by using a constant current source (CCS) prior to the experiments. CCS is also used to monitor the change in output voltage signals across the gauges for corresponding change in temperatures. In case of coaxial thermocouples, a data acquisition system (DAS) can directly measure output voltage signals because they are active device. The use of CCS and DAS involve gathering signals from measurement sources and digitizing the signal for storage, analysis and presentation on a PC.

4.5 Results and Discussions

The oil bath type static calibration technique of the thermal sensors provides gradual variation with thermal emf as a reference voltage at the reference temperature. The results of calibration for all the heat transfer gauges are recorded in both heating and natural cooling process, when temperature of air increases from 45°C to 85°C (from room temperature) and during natural cooling process up to 45°C. The temperature and voltage signals of the handmade thermal sensors are recorded in the step of 10°C during the heating and natural cooling process. The static calibration results of heat transfer gauges as shown in Figs. (4.4-4.6). It is seen that the temperature during heating and cooling varies linearly with voltage. It is also found that, the

voltage signals of heat transfer gauges also depend upon the heating and natural cooling process. When the temperature of air is increased and then decreased to its original value, the change of voltage or resistance signals inside the conducting materials does not follow the same path. There is a lag between the internal and the external field i.e. behavior of resistance change is different during heating and cooling. This behavior results in a loss of energy, commonly called as the “hysteresis loss” in the form of heat. However, if sufficient care is taken while recording the temperature and ensuring thermal equilibrium in the beaker, the hysteresis losses can be minimized or reduced.

It is a general practice to calculate the TCR and sensitivity for both heating and cooling experiments and use the average value to represent the TCR and sensitivity of the each heat transfer gauges. In the present experiments, the average value of TCR are found to be 0.00239 K^{-1} , 0.00336 K^{-1} and 0.064 K^{-1} for platinum TFGs, nanomaterial based platinum TFGs and coaxial thermocouples, respectively. In the same sequence, the sensitivities are $465\mu\text{V/K}$, $738\mu\text{V/K}$ and $40.53\mu\text{V/K}$ respectively. The comparative analysis of sensitivity of all the thermal sensors is shown in Fig. 4.7. Here, it is found that CNT supported platinum thin film gauges has better sensitivity as compared to conventional platinum thin film gauge and coaxial thermocouple. It is mainly because of the fact that addition of CNT improves the thermal property of the mixture. The entangled nano porous platinum-CNT structures could provide a suitable change in heat transfer rate and have large three phase boundary area. This property becomes critical when preparing good sensors with the high catalytic reactivity of platinum material. The value of sensitivity indicates that, these handmade sensors can be suitable for general purpose at high temperature testing and can be used in oxidizing environment. The temperature sensitivity of these handmade sensors are also checked regularly and it is found to be suitable for capturing the

transient temperature variations during short time scale of measurement. The main limitation is accuracy because the temperature less than one Kelvin (K) is difficult to achieve.

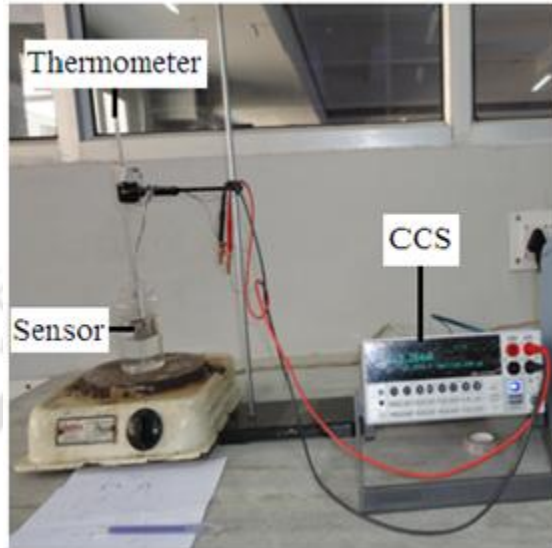


Fig. 4.2: Laboratory set up of oil bath type calibration

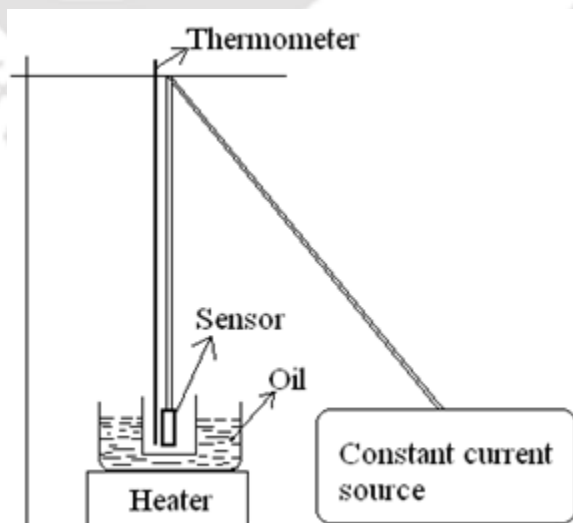


Fig. 4.3: Schematic diagram of oil bath type calibration

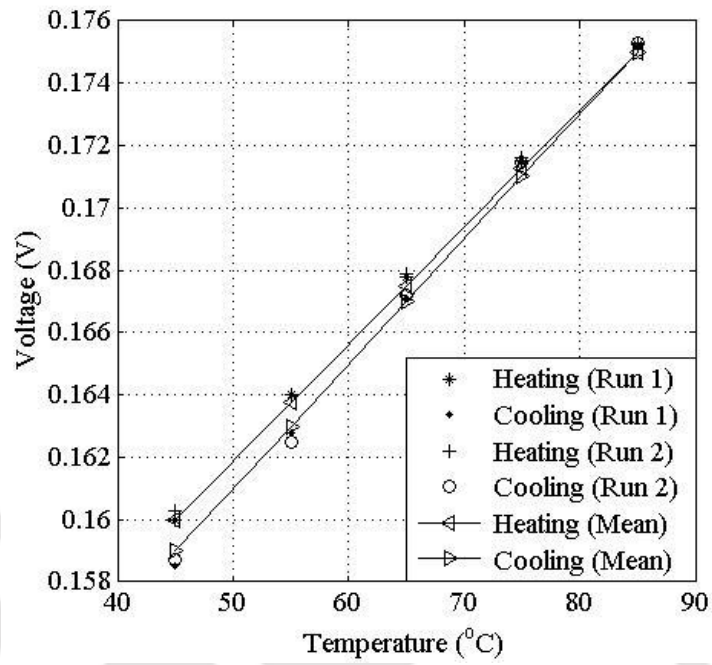


Fig. 4.4: Typical temperature - voltage signal measured from Platinum thin film heat transfer gauge

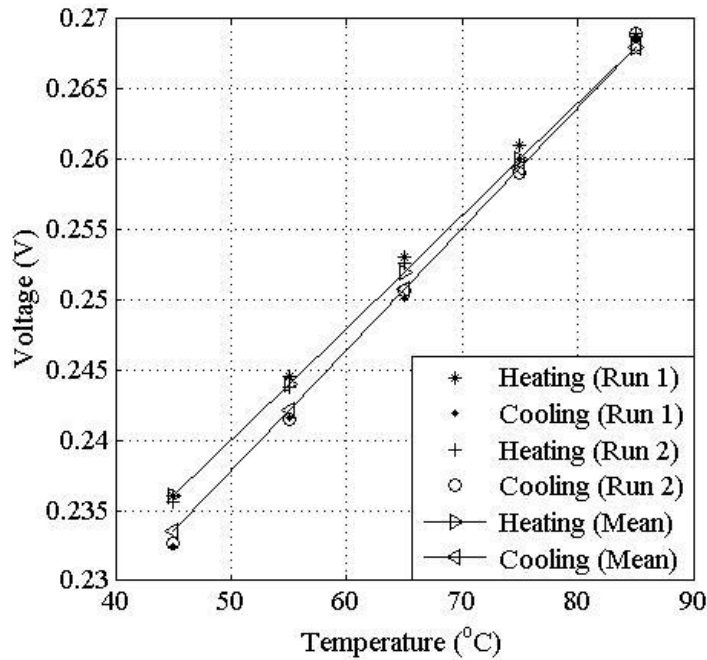


Fig. 4.5: Typical temperature - voltage signal measured from Platinum/CNT thin film heat transfer gauge

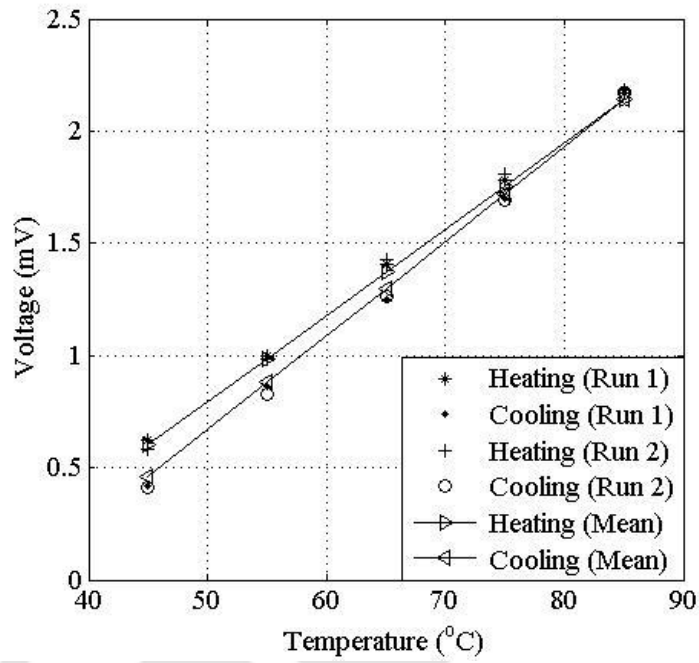


Fig. 4.6: Typical temperature - voltage signal measured from K-type coaxial thermocouple heat transfer sensor

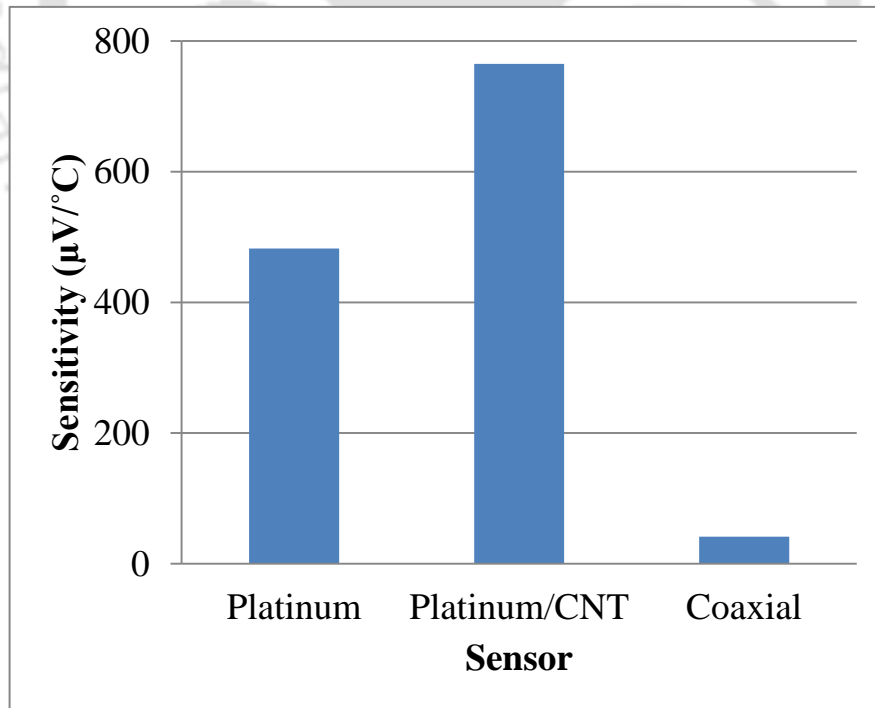


Fig. 4.7: Comparison of sensitivity between different types of heat transfer sensors

4.6 Summary

A method for static calibration of the heat transfer gauges has been presented in this chapter. The oil bath based calibration setup is used to provide gradual temperature change to the handmade sensors. Since, the sensors are not in direct contact with the heated fluid (i.e. silicon oil), they are protected. The sensitivity and TCR are calculated from the readings of thermometer used in calibration experiments both for heating and cooling. A good linear response between the change in temperature and change in voltage signals is observed for all the handmade gauges. The voltage variation with temperature shows a lag during heating and cooling which means the hysteresis loss. Even though, it cannot be completely avoided, but can be minimized by reducing the heat losses and thereby maintaining the thermal equilibrium inside the beaker. The average value of TCR are found to be 0.00239K^{-1} , 0.00336K^{-1} and 0.064K^{-1} for platinum TFGs, nanomaterial based platinum TFGs and coaxial thermocouples, respectively. In the same sequence, the sensitivities are $465\mu\text{V/K}$, $738\mu\text{V/K}$ and $40.53\mu\text{V/K}$ respectively. It is seen that CNT supported platinum thin film gauges has better sensitivity and selectivity compared to all other heat transfer gauges.

Chapter - 5

Dynamic Calibration of Heat Transfer Gauges for Transient Heat Flux Measurement

Surface temperature history and subsequent determination of heating rates are the important objectives in the present work. In the previous chapters, three different types of thermal sensors (platinum thin film, platinum-CNT thin film and coaxial thermocouple) have been successfully fabricated. Oil bath calibration experiments show the linear variation of voltage with temperature. In the entire process, the main goal for all these sensors is to predict the unknown transient heat flux. It is normally done through suitable heat conduction modeling and using the transient surface temperature data obtained from the sensors. In order to generalize this modeling, the sensors need to be calibrated experimentally for heat fluxes. The main objective of this chapter is to explore the possibility of using heat transfer gauges for short duration transient measurements with pure radiation and conduction mode of heat transfer. A simple dynamic calibration set-up has been developed and used to supply known input heat flux of different magnitudes to the handmade thermal sensors that are fabricated in-house. Experiments are carried out by applying step heat load on the sensors by using laser light and constant heat fluxes based heater of known input wattage. Recorded transient temperature data are processed for estimation of input wattage using numerical and analytical models. For the known input heating load, temperature signal is also predicted using one dimensional transient heat conduction solver using ANSYS. Encouraging agreement of these predictions has demonstrated the success of the calibration methodologies. In fact, these simple laboratory experiments can simulate the step and impulse heat loads which are encountered in high speed flow environments.

5.1 Introduction

The measurement of transient heat transfer rates is very important in the design of internal combustion engine, gun barrels and aerodynamics vehicles in high speed flow environments. In these cases, the measurement technique for accurate prediction of heat fluxes must suit for transient conditions and should have a fast response time to trace variations caused by rapidly changing flow conditions. In most surface heat transfer mapping, very fast response thermal sensors are used for dynamic temperature measurements in the flow. With respect to high speed flow environment, the response time of the temperature sensors become more crucial because the experimental time-scale of measurement is very small (~ milliseconds or less). The transient temperature measurement is usually performed by mounting the thermal sensors, embedded inside the heated material. The surface heat fluxes are then estimated from the temperature history, analytically/numerically by one dimensional heat transfers modeling.

The accurate measurement of highly transient surface temperature needs fast response temperature thermal sensors or heat transfer gauges such as thin film gauges and coaxial thermocouples. It consists of a highly conducting thin film of sensing material placed on a low conducting substrate material. During the actual experimentation, heat transfer gauges are flush mounted on the test surface or placed at appropriate location where temperature history is to be measured. When exposed to a heating environment, temperature of the surface changes that leads to the variation in the resistance of the gauge and the voltage across the sensor. Hence, measurement of voltage change across the sensing materials indicates the surface temperature from the known thermal coefficient of resistance (TCR) of the sensing film material. The measured time dependent surface temperature of the gauge with the known thermal properties of substrate material, allows the estimation of transient heat flux applied on the surface from any

source. This is generally accomplished by using theory of conduction of heat into a semi-infinite body which has an assumption that the surface heat flux does not influence the temperature of the rear end of the substrate material. It is also assumed that the temperature in the sensing material is uniform and also representative of the substrate material surface temperature. The details of methodology of the measurement using these thermal sensors and the procedure for determination of surface heat flux from the voltage signal have been described in open literatures (Vidal 1956, Carslaw and Jaeger 1959, Schultz and Jones 1973, Taler 1996 and Haldeman et al. 2005). The simple measurement technique and the analysis pathway are the key features of these heat transfer gauges. However, some other contemporary techniques have been developed for transient surface temperature measurements such as temperature sensitive paints (Mosharov et al. 2003 and Nagai et al. 2006), thin film calorimeter gauges (Miller 1981) and coaxial surface thermocouple (Sanderson and Sturtevant 2002, Mohammed et al. 2008). Nevertheless, thin film sensors are easy to fabricate, cost effective and offer instantaneous surface temperature measurements. The economical and precise measurement, higher sensitivity and most importantly rapid response times (as low as $1\mu\text{s}$) are the important traits of the thin film sensors over the contemporary measurement techniques (Sahoo 2003). The advantages of the heat transfer gauges were realized long back and this technique was implemented for measurement of surface temperatures or heat flux in internal combustion engines (Chana and Wilson 2001), gas turbine applications (Dunn and Holt. 1982, Korakianitis et al. 2002) and high speed flight experiments (Sahoo and Peetala 2010).

The heat flux measurement technique has received a promising means to obtain the transient temperatures and subsequent prediction of surface heat flux (Sahoo 2003). Moreover these handmade thermal sensors can be fabricated in-house and thus becomes cost effective as

discussed in previous chapters. However, it is necessary to dynamically calibrate the heat transfer gauges before being installed into the surface for accurate prediction of surface heat flux. The dynamic calibration methodology of such types of thermal sensors involves the basic modes of heat transfer such as conduction, convection and radiation. Smith et al. (1999) reported the convection and radiation based calibration of heat flux micro-sensors. The radiation based calibration was performed by exposing the thermal sensors to a heat lamp while convective heat flux was generated by a flow in a transonic wind tunnel. The heat flux micro sensor consisted of a differential thermopile (made out of 280 thermocouple pairs) and a resistance temperature sensor. Holmberg and Diller (1995) used similar heat flux micro RTD sensors in a convective facility to measure transient temperatures and predicted surface heat flux by using one dimensional semi-infinite heat conduction model.

With respect to application of heat transfer gauges for short duration impulse facilities, the dynamic calibration methods are not well established. In these facilities, the aerodynamic body generally experiences step heating loads for a very short duration which is in the order of few milliseconds. The transient heat fluxes are then estimated by measuring temperature history using heat transfer gauges mounted at appropriate locations on the aerodynamic body. However, before using these heat transfer gauges in the impulse facilities, it is necessary to calibrate them in the laboratory with similar nature of known heating loads in order to account for the errors in the ground based experimentation. One of the methods is to expose these thermal sensors with known input wattage and obtain the surface temperature history and compare them with theoretical and numerical results. So, the present investigations are concerned with radiation and conduction based dynamic calibration of the heat transfer gauges. Step heating loads are applied on the sensing element of the heat transfer gauges using a laser light and constant heat flux based

heater of known input wattage. Transient temperature data's are recorded for different time intervals under various step heat loading conditions in the range of 20-90kW/m² at different time intervals. This is one of the important advantages of laser based dynamic calibration where the gradual variation of heating loads is possible as compared to a heat lamp. Being highly directional, laser beams have very small divergence, thus reduces the sources of errors. The temperature histories obtained from the heat transfer gauges are then used to recover the input wattage using various numerical technique and analytical solutions. The details of dynamic calibration based experimental setup, measurement of transient temperature history and transient heating rates are described in the following sections.

5.2 Dynamic Calibration Experiments and Computational Analysis

The important objective of the present work is to establish a simple dynamic calibration based experimental set up to perform radiation and conduction based experiments with handmade heat transfer gauges. With same heating loads, finite element simulation and analytical analysis is performed for gauge substrate system using commercial package ANSYS to recover the surface temperatures. Also, one dimensional heat transfer modeling is used to recover the transient surface heat flux from the temperature histories. Subsequently, the experimental results at different step input load are compared with the simulation to justify the feasibility of radiation and conduction based measurements with heat transfer gauges.

5.2.1 Radiation based Experimental Calibration Technique

Most of the high altitude, near-realistic flight conditions are simulated in the ground based impulse facilities such as shock tunnels/expansion tubes where the test times are in the order of few milliseconds or less (Vidal 1956, Schultz and Jones 1973, Sahoo 2003, Modarress and Azzazy 1988, Simmons 1995). The convective surface heating rate measurements are performed

over the aerodynamic model by using heat transfer gauges mainly because of its high response time. Secondly, the model experiences sudden heating load in this short time scale of measurement. In order to calibrate the thermal sensors for such flow conditions, experiments are performed by applying step heat load from the laser light of known input wattage. The schematic diagram and experimental set up, especially built for this experiment is shown in Fig. 5.1 and Fig. 5.2. Continuous wave type laser (manufactured by Spectra-Physics Lasers, USA) with wave length of 514nm is used. A convex focal length of 20cm is used to focus the laser source on the heat transfer gauges. Equal distance of 20cm is maintained between the heat transfer gauges, lens and laser source. Constant current of 10mA is supplied to the thin film sensor during these experiments. Step heat load is applied to the sensing area of the heat transfer gauges by projecting laser light on the sensing element. The laser beam is enlarged by a microscope lens that provides illumination for larger area (0.22mm²) of the thermal sensors. Change in output voltage signals due to heat load across the thermal sensor has been measured for the different time duration by using a signal measuring instrument (data acquisition system) for platinum thin film gauge, nano-material based platinum thin film gauge and coaxial thermocouple and, are shown in Figs. (5.3-5.5). The raw voltage signals are digitally smoothed by using moving average filter techniques by considering suitable number of data points without distorting the trends of the signals. From the measured voltage signal, the temperature data are then obtained by using the value of thermal coefficient of resistance as discussed in the sec. 4.2 previous chapters, the comparison between transient temperature histories measured by using heat transfer gauges or thermal sensors are as shown in Fig. 5.6. This experimental procedure is repeated to conduct experiments with different input wattage values of heat fluxes at different time intervals by adjusting the input laser wattage.

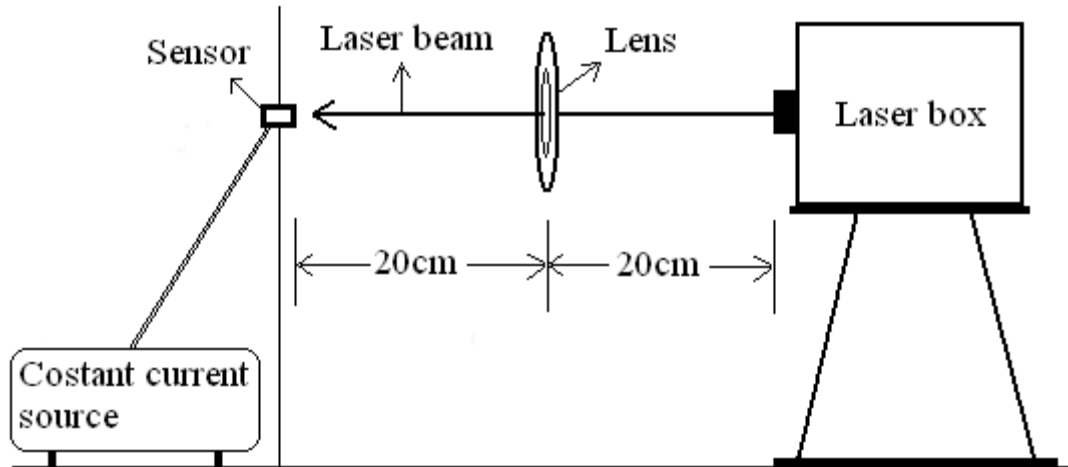


Fig. 5.1: Schematic diagram of radiation or laser based experimental setup for dynamic calibration of heat transfer gauges

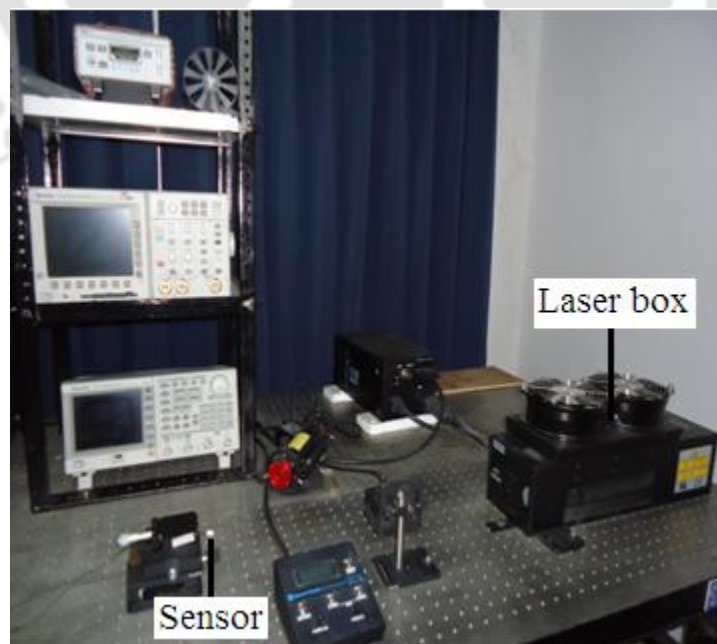


Fig. 5.2: Laboratory setup for radiation or laser based experiment

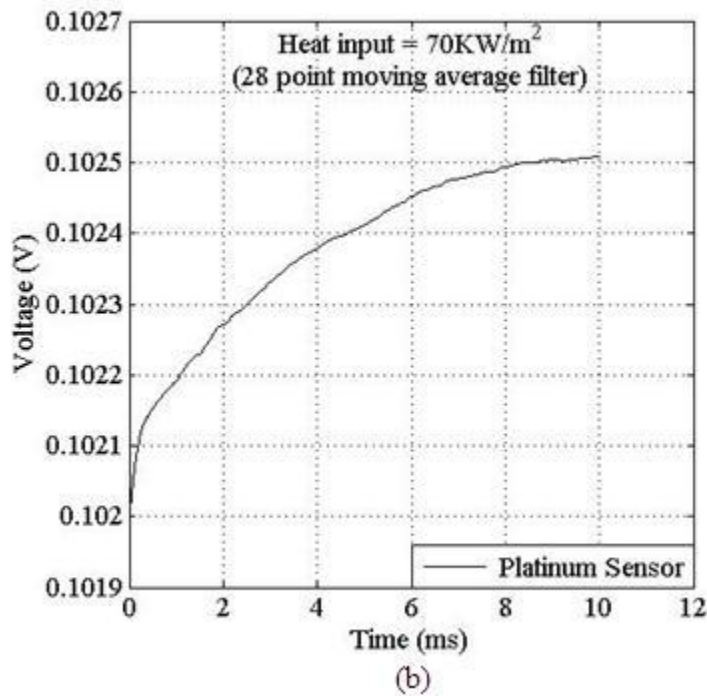
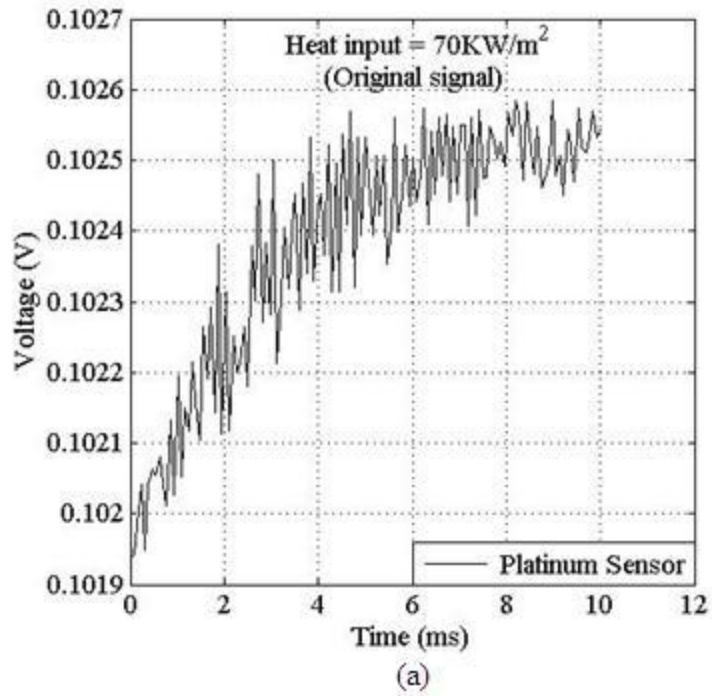


Fig. 5.3: Transient (a) original and (b) filter voltage signal for platinum thin film sensor at radiation based step heat load

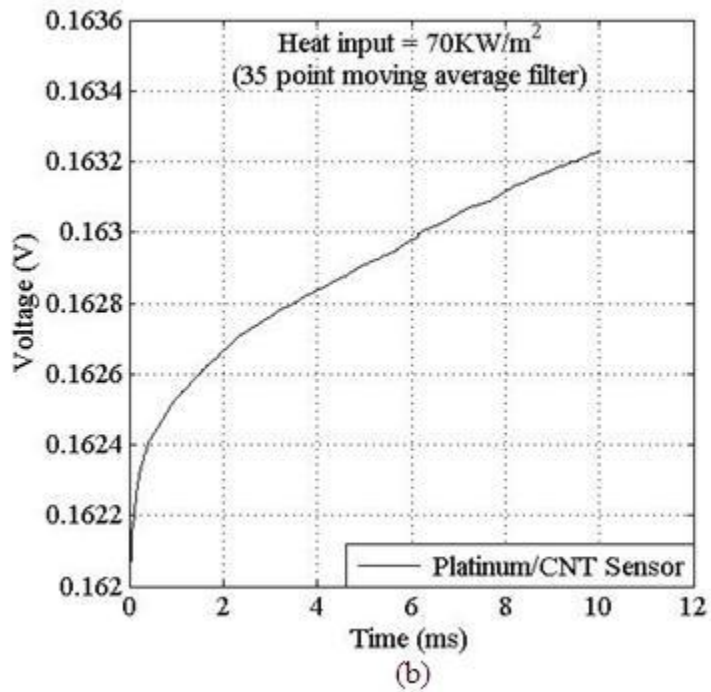
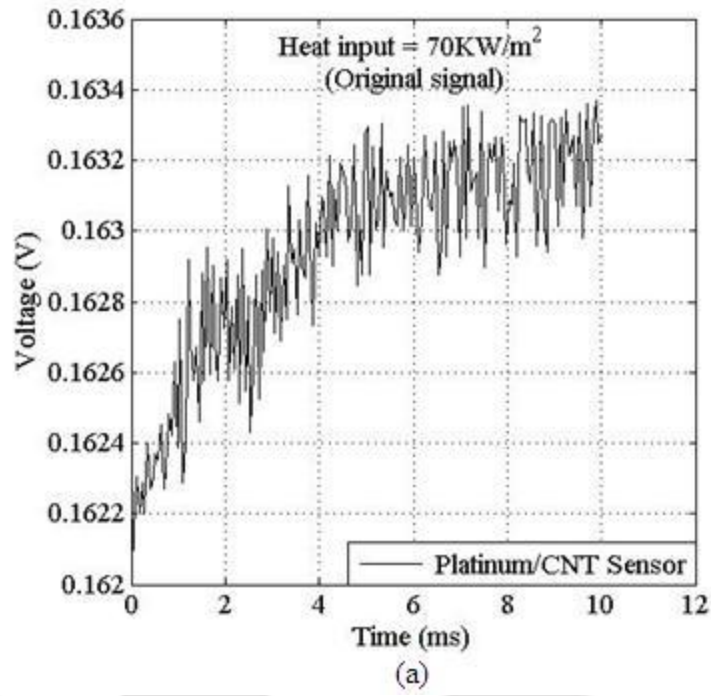


Fig. 5.4: Transient (a) original and (b) filter voltage signal for platinum/CNT thin film sensor at radiation based step heat load

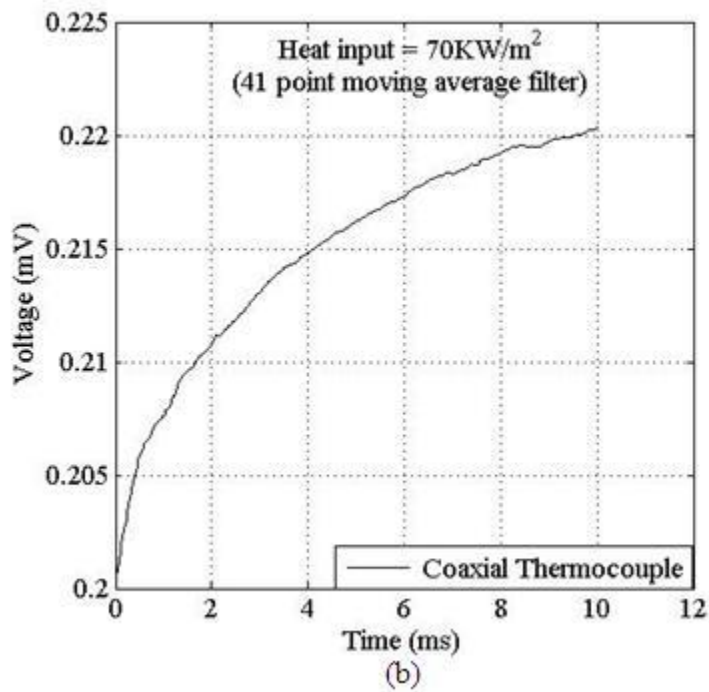
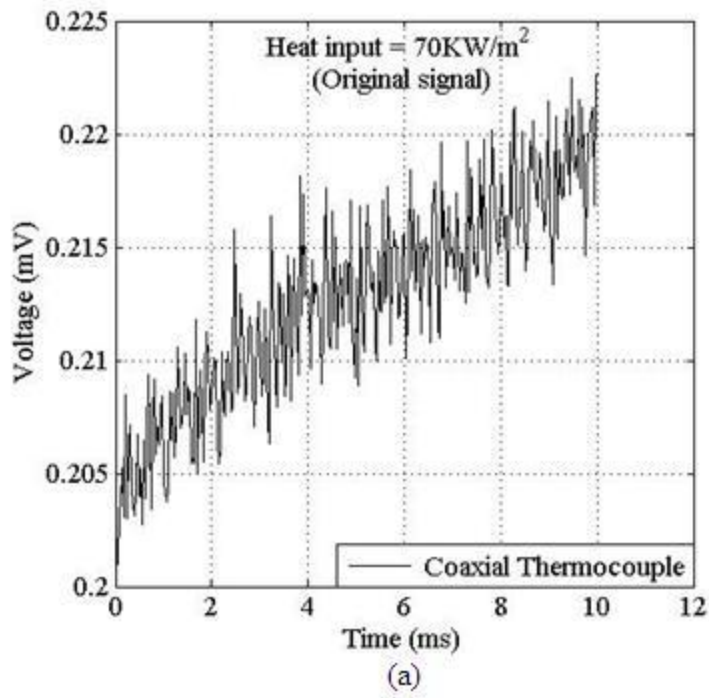


Fig. 5.5: Transient (a) original and (b) filter voltage signal for coaxial thermocouple at radiation based step heat load

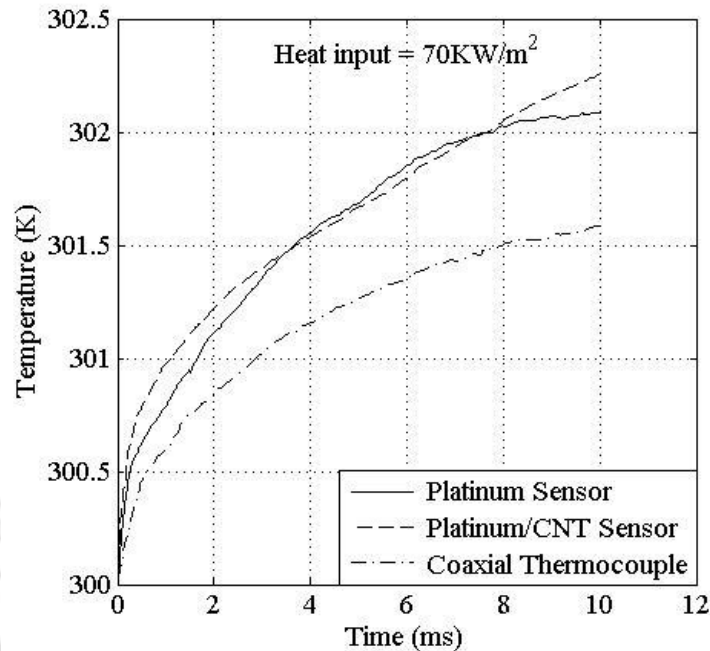


Fig. 5.6: Comparison of temperature histories for various types of heat transfer gauges at radiation based step heat loads

5.2.2 Conduction based Experimental Calibration Technique

The main task of the dynamic calibration based experimental set up is to supply constant heat flux of known input wattage to the heat transfer gauges for conduction mode of heat transfer. For this purpose, present set-up is comprised of a constant power supply source, thermally insulated metallic (copper) rod, constant current source (CCS) and computer based data acquisition system (DAS). The schematic diagram and experimental set up, especially built for this experiment is shown in Fig. 5.7, Fig. 5.8 and Fig. 5.9. The role of the constant power supply source is to give out constant heat flux to one end of the insulated copper rod. A regulator and two indicators are provided with the power source. The regulator is primarily used to control the heat flux supplied to the metallic rod surface where one of the indicators displays the same. However, the other indicator monitors the surface temperature of the metallic rod where heat is supplied through the power source. Thus, one end of the copper rod is heated while the other end is exposed to the

surroundings and all other surfaces are completely insulated with Teflon. Hence, heat is conducted from one end to the other with minimal loss through the surrounding surface. During the experiment, metallic rod achieves a constant temperature gradient along its length due to heating at one end and natural cooling at the other end for the presently used source heat flux values. Measurement of steady state temperature at the two ends of the rod gives the established temperature gradient and the steady state conduction heat flux set in the rod. This value is used as the source of known conduction heat flux applied to the heat transfer gauges. Conduction based dynamic calibration experiments are performed with different values of input heat fluxes by adjusting the input wattage. The thermal sensor which is initially at room temperature is brought suddenly in contact with the smooth surface of the copper rod to apply the step heat flux. The voltage signals are recorded for the different time duration by using a data acquisition system. With the knowledge of TCR, the transient temperature data is obtained from the voltage signal. Same procedure is repeated with all handmade thermal sensors with different step input heating loads to obtain the temperature histories for platinum based thin film gauge, nano-material based platinum thin film gauge and coaxial thermocouple. The schematic diagrams are shown in Figs. 5.10(a-d), Fig. 5.11 and Fig. 5.12(a-d).

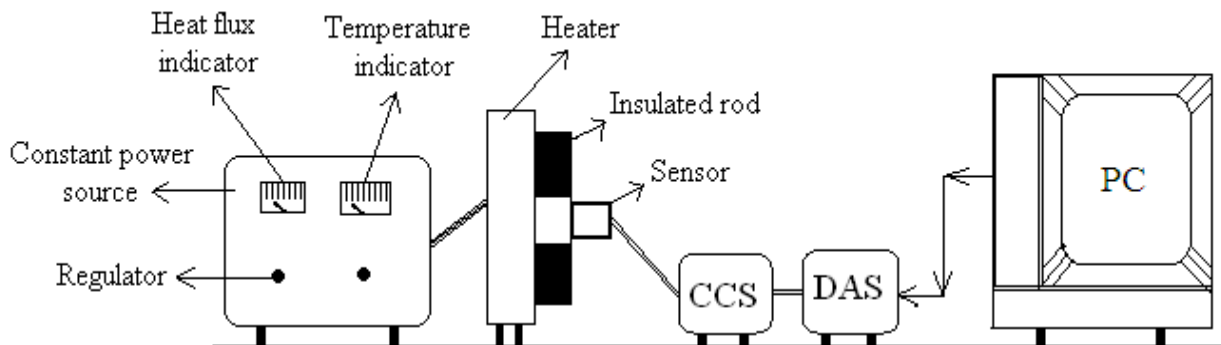


Fig. 5.7: Schematic diagram of an experimental setup for conduction based calibration of heat transfer gauges



(a)



(b)

Fig. 5.8: Laboratory set up for (a.) Constant heat flux type heater and (b.) PC based data acquisition system

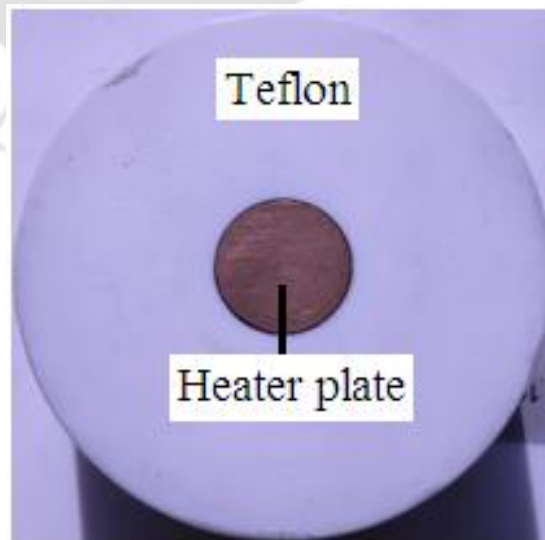
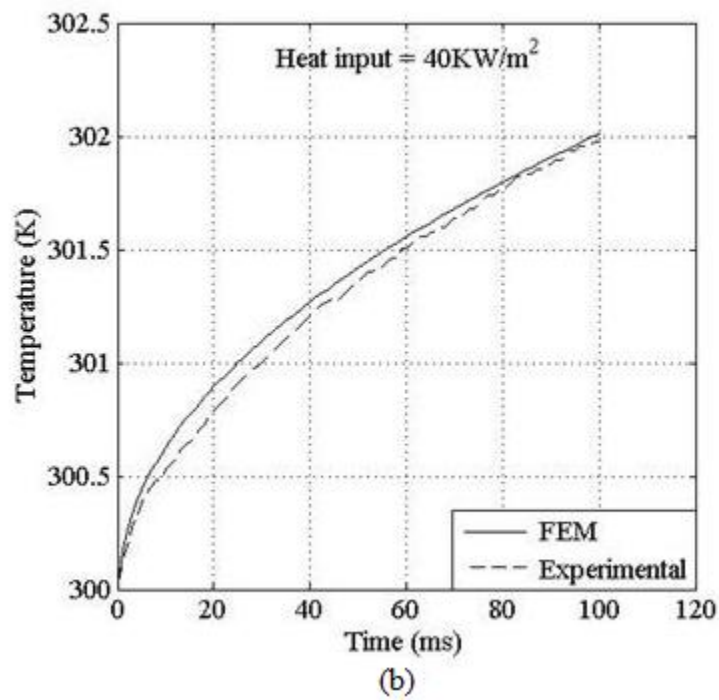
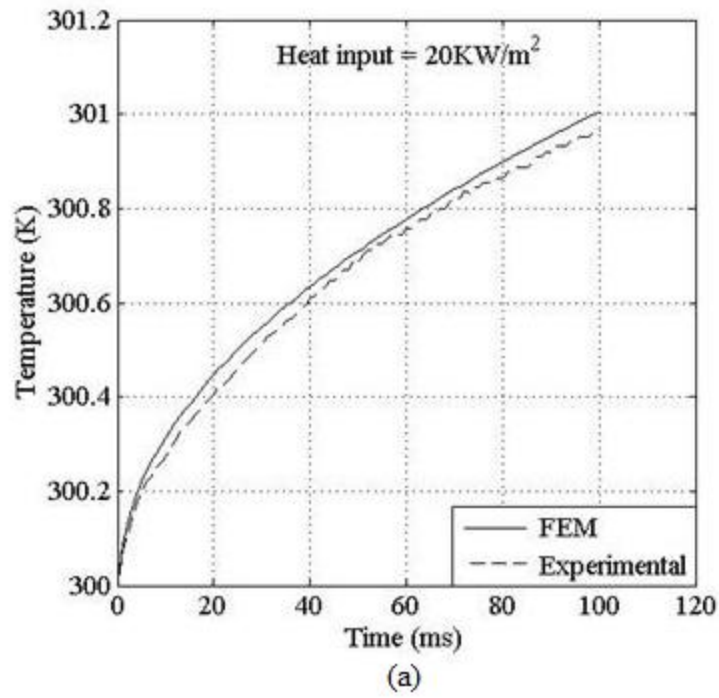


Fig. 5.9: Heater plate surface



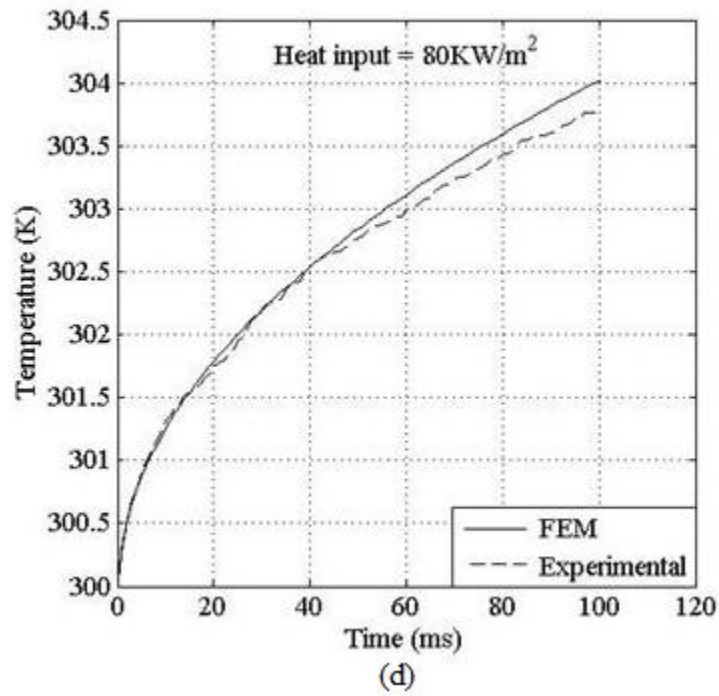
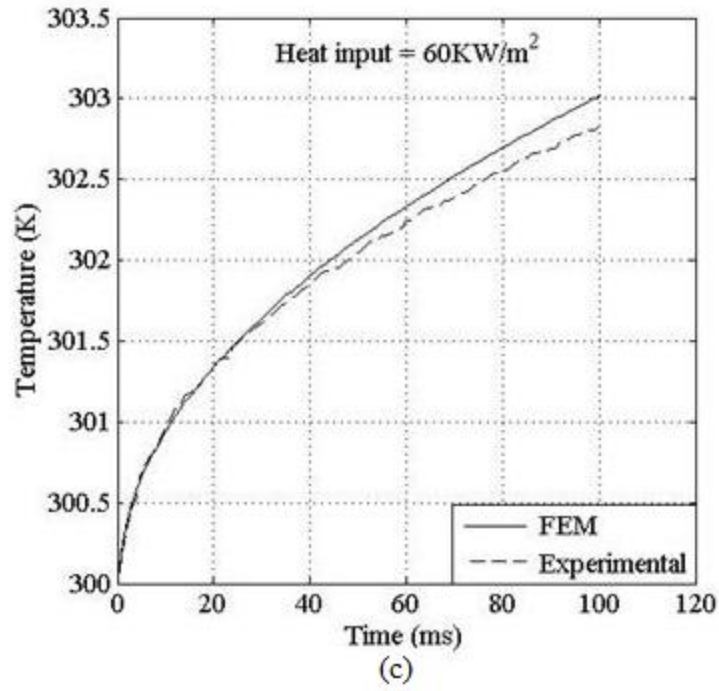


Fig. 5.10: Transient temperature signals for platinum thin film gauge at conduction based step heat load

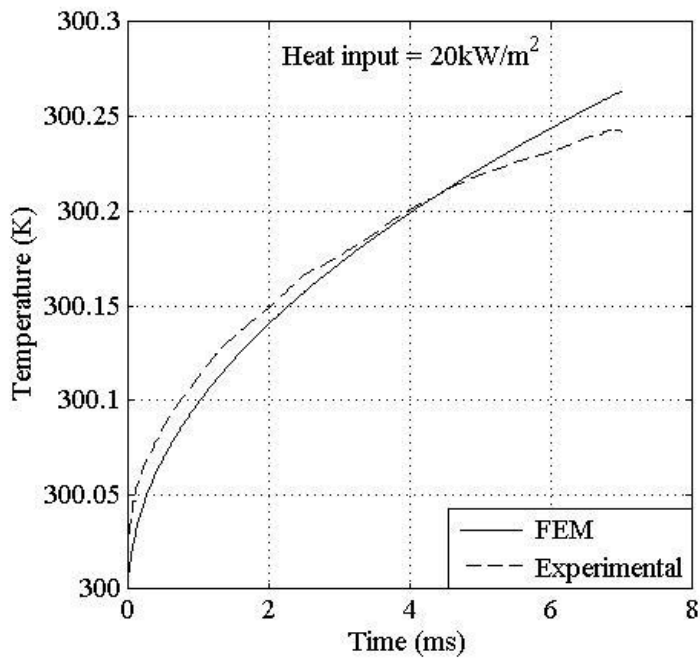
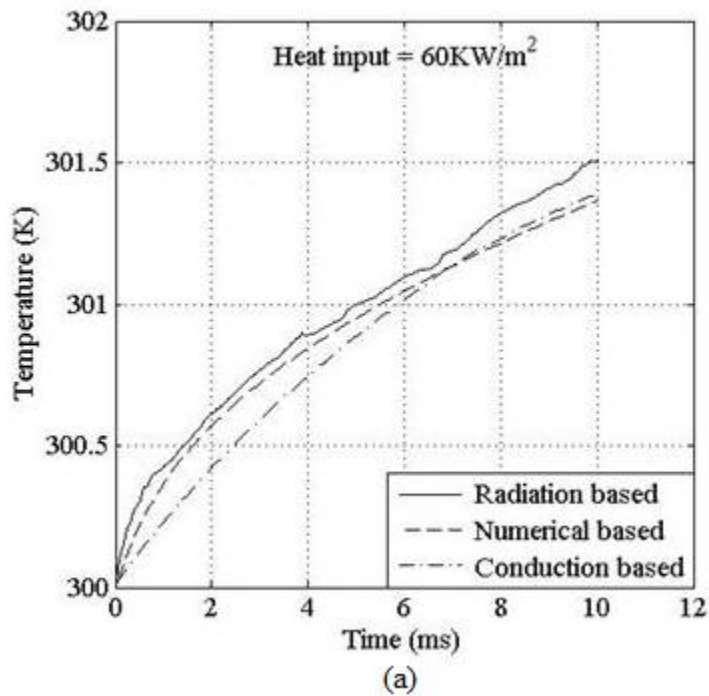
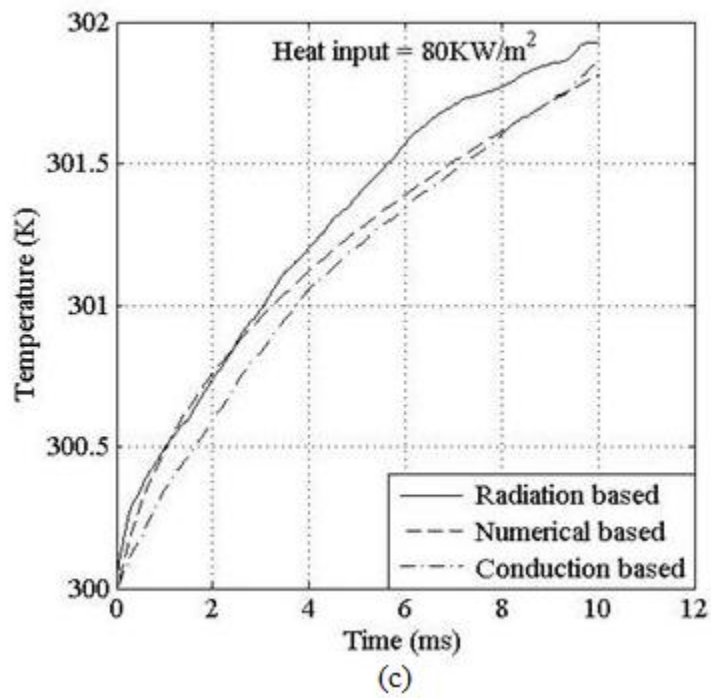
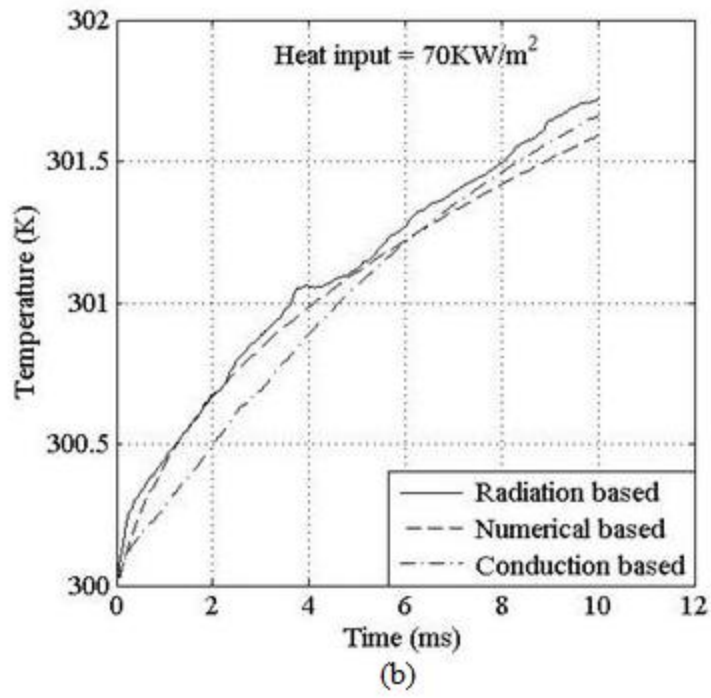


Fig. 5.11: Transient temperature signals for platinum/CNT thin film gauge at conduction based step heat load





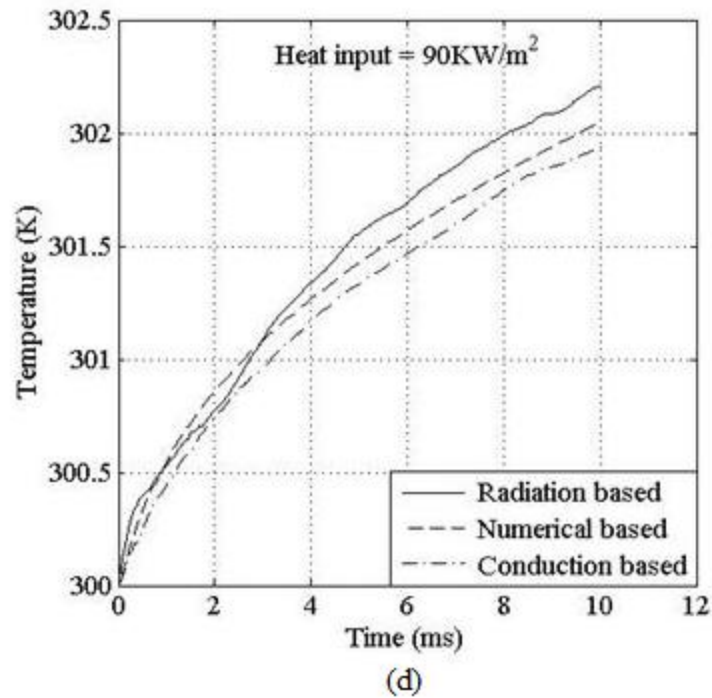


Fig. 5.12: Transient temperature signals for coaxial thermocouple at radiation and conduction based step heat load

5.2.3 Finite Element Simulation

Computational analysis has also been carried out for the dynamic calibration experiments using commercial package ANSYS. It is mainly aimed at validating the experimentally obtained transient surface temperatures for both the methods by comparing them with the numerically simulated surface temperature histories for same values of step input heat loads at same time intervals. For this purpose, the FE model of platinum based thin film gauges, platinum/CNT based thin film gauges and coaxial thermocouple sensor models are prepared in the ANSYS workbench for the geometrical configuration where the thickness for sensing film material is $10\mu\text{m}$. The backing material (substrate) has a base diameter of 6mm and thickness 10mm, respectively. During the experimental time scale of 11s as discussed in the sec. 3.4, these dimensions are sufficient to justify the assumption of one dimensional semi-infinite body (Vidal

1956, Schultz and Jones 1973). The schematic diagrams consisting of sensing junction and substrate material are as shown in Fig. 5.13 and Fig. 5.14.

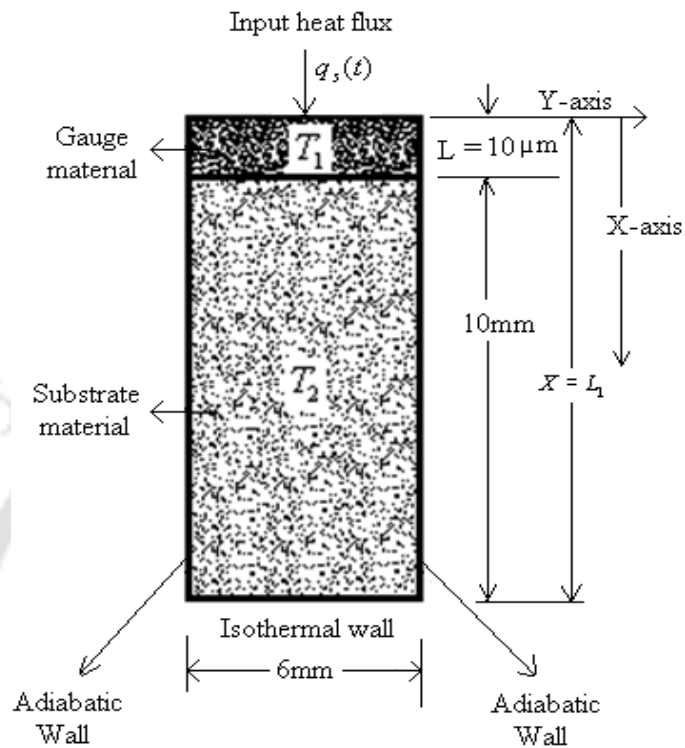


Fig. 5.13: Schematic diagram of thin film gauge used for computational study

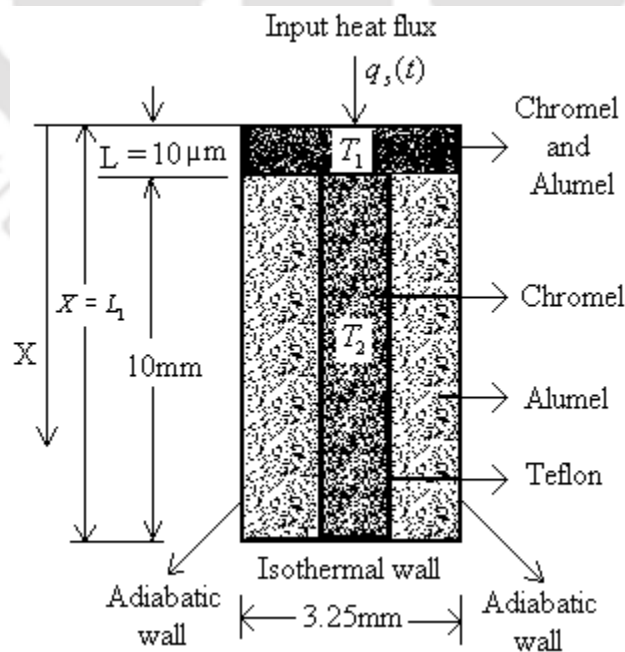


Fig. 5.14: Geometric configuration of the coaxial thermocouple sensor

The mesh generation for this dimension has been the important task since the sensing material thickness part of the model is too thin compared to thickness of the substrate material. Uniform square mesh of edge length $0.25\mu\text{m}$ has been selected in the entire computational domain consisting of sensing junction area and the substrate material after successful mesh independent studies. The computational model along with the finite element mesh and boundary conditions are as shown in Fig. 5.15(a-c) and Fig. 5.16(a-c) for thin film gauge and coaxial thermocouple. Thermal properties of sensing material and substrate material used for simulation are given in Table - 1 (Appendix – II). Referring to the Fig. 5.13 and Fig. 5.14, the initial and boundary conditions used in the simulation are given below;

$$x = 0; q_s = -k_1 \frac{dT_1}{dx} \text{ for } t \geq 0 \quad (5.1)$$

$$x = L; k_1 \frac{dT_1}{dx} = k_2 \frac{dT_2}{dx} \text{ and } T_1 = T_2 \quad (5.2)$$

where, T_1 and T_2 are the temperature variations with time (t) across the sensing material and substrate material, k_1 and k_2 are thermal conductivities of sensing junction and substrate material, respectively, q_s is the surface heat flux measured at $x=0$ and the side walls of the thermal sensor is adiabatic. The thickness of sensing material is very small so that the interface thermal resistance (between sensing junction and substrate material) can be neglected (Vidal 1956, Schultz and Jones 1973). The simulation is performed by using ANSYS one dimensional heat conduction solver for various step heating loads. The step heat flux signals measured by using numerical inverse analysis for short duration 10ms is as shown in Fig. 5.17. The temperature contour for platinum thin film gauge, platinum/CNT thin film gauge and coaxial thermocouple sensor are obtained for the input heat flux as shown in Fig. 5.18 (a-d). During the

simulation time scale of 10ms, more than half of the bottom part of the gauge is seen to retain the initial temperature of 300K that clearly provides the evidence for validity of the semi-infinite assumption required for heat flux recovery for very small experimental durations. This analysis shows that heat transfer gauges satisfy the semi-infinite assumptions for short duration heat flux applied on the sensor for the step input load. This procedure is repeated at different time intervals, by adjusting the input wattage and compared with experimental results as shown in Fig. 5.10(a-d), Fig. 5.11, Fig. 5.12(a-d) and Fig. 5.19(a-d). The parabolic nature of the temperature plots ensures the nature of applied step heat flux on the heat transfer gauges (Taler 1996). The temperature histories obtained using experiment and finite element technique portray almost same trend and magnitude for a given step heat flux. Similar nature of temperature signals are obtained for different values of surface heat fluxes. The results also indicate that the trends of temperature variations in both types are same as well as all results are very much closed, very small difference occurs between them due to thermal property (thermal conductivity, density and specific heat) of the gauge and substrate materials. Initially temperature rises instantaneously and then they are completely close to each other at all values of input heat fluxes.

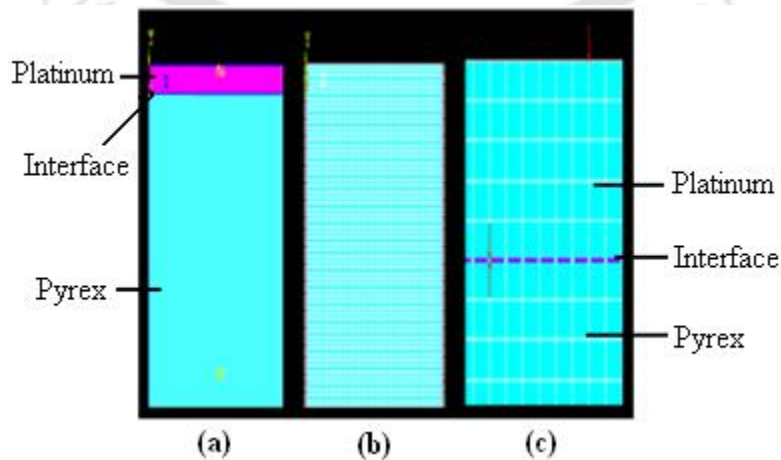


Fig. 5.15: Geometric configuration of the platinum film mounted on a pyrex substrate

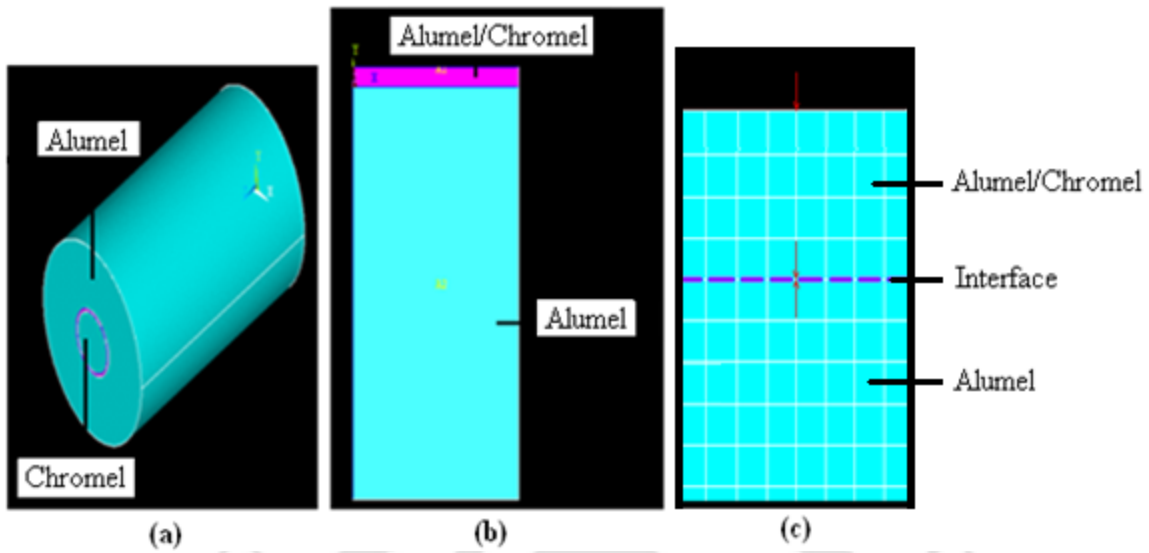


Fig. 5.16: Geometric configuration of the coaxial thermocouple (a) computational model of the thermocouple elements (b) sensing junction and substrate material (c) vertical enlarged view to show the finite element mesh

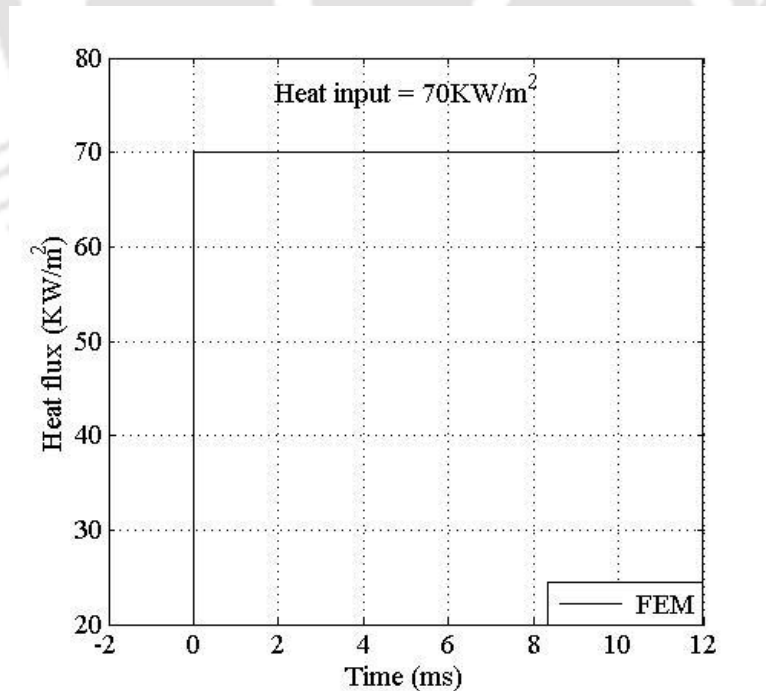
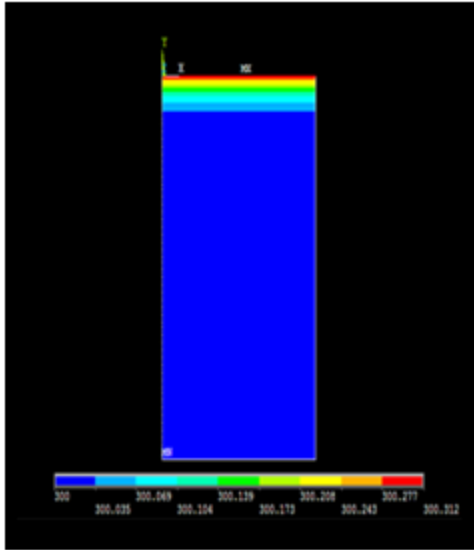
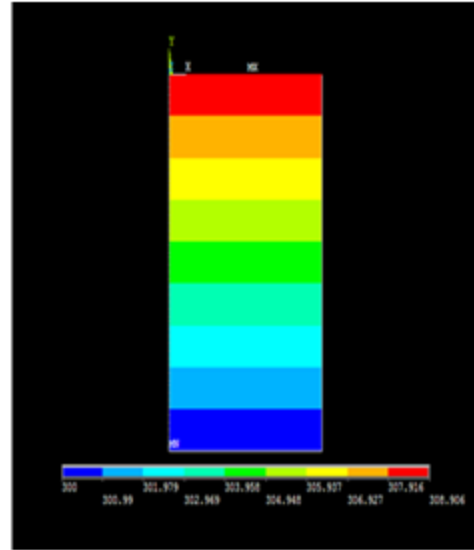


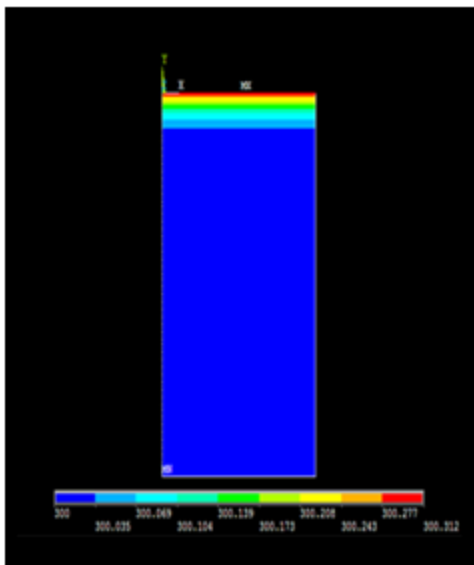
Fig. 5.17: Typical time-heat flux signal obtained from numerical inverse analysis



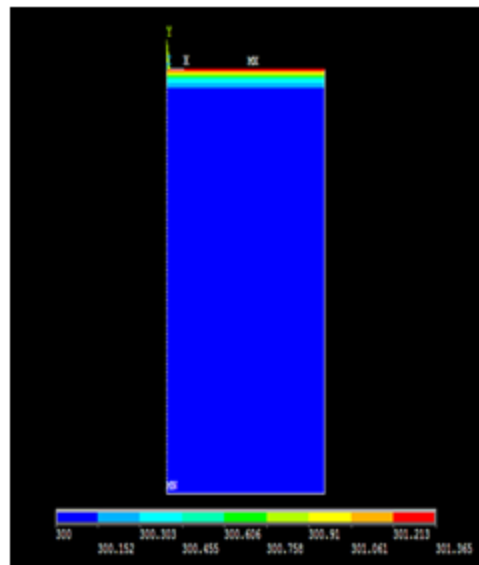
(a)



(b)

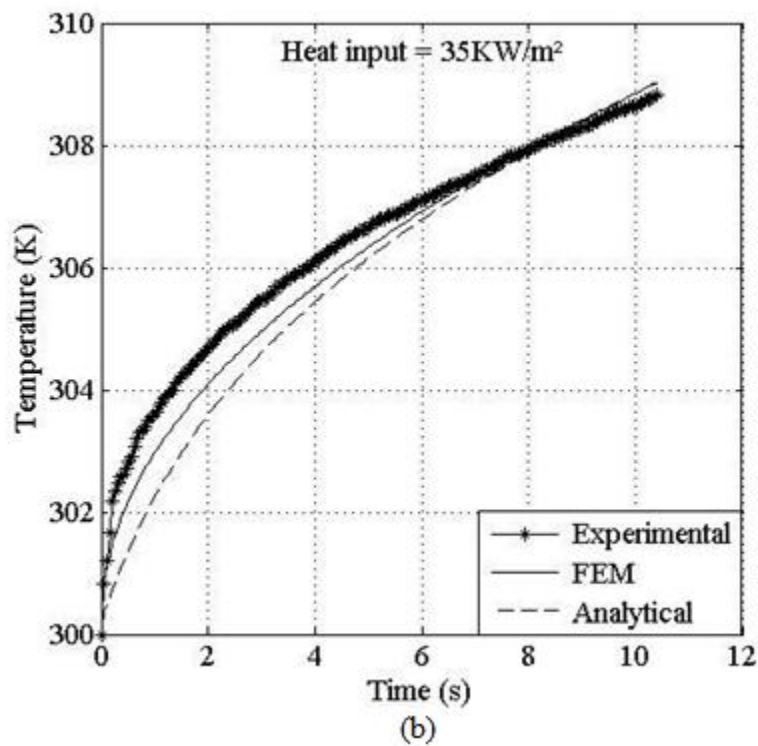
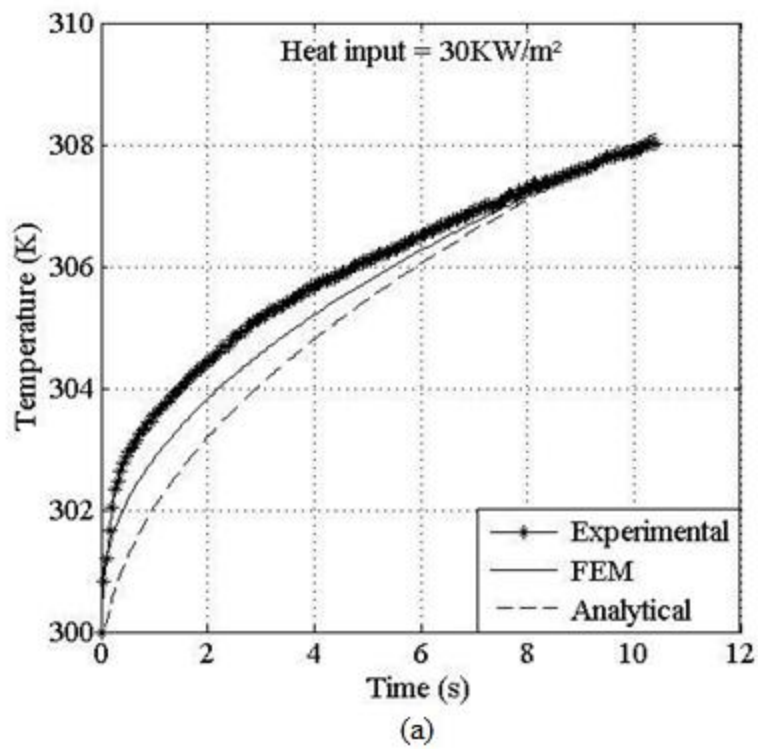


(c)



(d)

Fig. 5.18: Contours of total temperature distribution of (a) Platinum thin film gauge for 10ms duration (b) Platinum thin film gauge for 10s duration (c) Platinum/CNT thin film gauge for 10ms duration and (d) Coaxial thermocouple sensor for 10ms duration



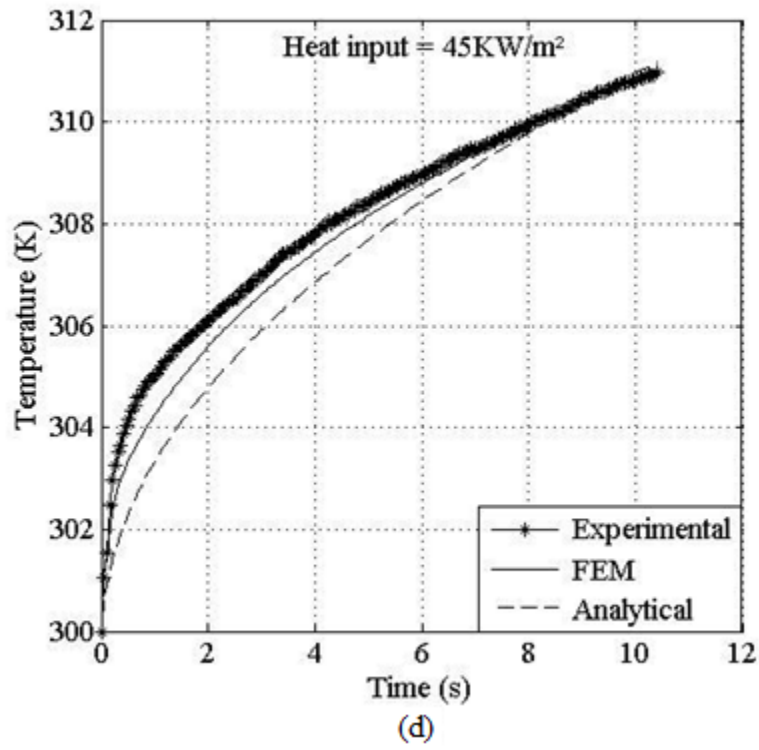
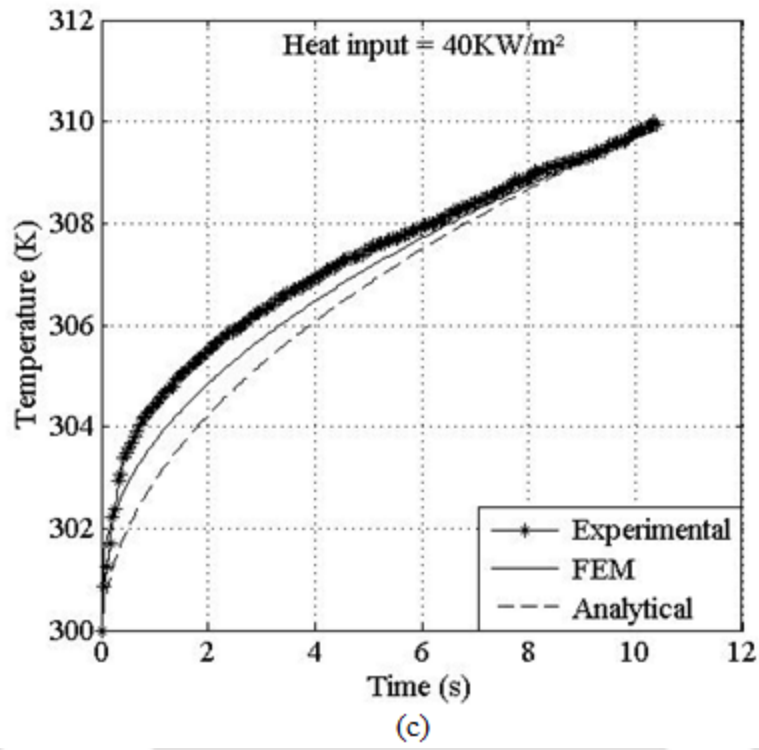


Fig. 5.19: Comparison of transient temperature signals for platinum thin film gauge at radiation based step heat load

5.2.4 Determination of Temperature History from Analytical Formulation

Transient temperature data can also be obtained from analytical formulation for the present heat transfer gauge configuration from constant heat flux by using one dimensional heat conduction equation with semi-infinite assumption for the backing material. This formulation can be obtained by solving one dimensional unsteady heat conduction equation using Laplace Transform technique (Carslaw and Jaeger 1959),

$$T_1 - T_i = \frac{2(q_s/A_s)\sqrt{(\alpha_1\tau)/\pi}}{k_1} \exp\left(\frac{-x^2}{4\alpha_1\tau}\right) - \frac{(q_s/A_s)x}{k_1} \left(1 - \operatorname{erf} \frac{x}{2\sqrt{\alpha_1\tau}}\right) \quad (5.3)$$

Where, T_i is the ambient temperature, A_s is the cross-sectional area of the sensing material, $\alpha_1 \left(= \frac{k_1}{\rho_1 c_1} \right)$ is the thermal diffusivity of gauge or sensing gauge materials and τ is the time variable. Therefore, temperature history for the step heat load on the top surface of the sensing junction material ($x=0$) as shown in Fig. 5.20 (heat transfer gauge or semi-infinite body) can be calculated from Eq. 5.3 and the expression is given by,

$$T_1 = \frac{2(q_s/A_s)\sqrt{(\alpha_1\tau)/\pi}}{k_1} + T_i \quad (5.4)$$

The temperature signals obtained from experiments for the heat loads and its comparison with simulated and analytical temperature history are shown in the Fig. 5.19(a-d). It is found that temperature rises instantaneously in the initial period and the trend of temperature variation is parabolic in all the cases. The parabolic rise of temperature plots ensures the analogous behavior with respect to the use of heat transfer gauges in transient applications. The temperature histories obtained using experiment, FEM and analytical techniques show almost same results. However,

the minor difference in the temperature signals obtained from the simulation, in comparison with the experimental signal, could be due to the use of standard thermal properties for sensing junction and substrate materials during simulation.

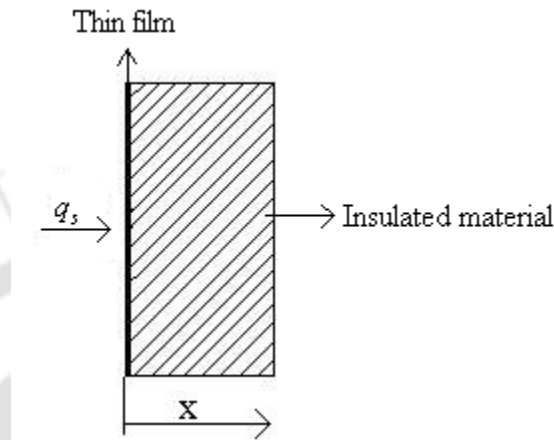


Fig. 5.20: Schematic diagram of the one dimensional semi-infinite body

5.3 One Dimensional Heat Conduction Theory

The heat transfer gauge measures the change in surface temperature of the body on which it is mounted and does not replicate the surface heating rates. The determination of the surface heat flux from the temperature signal is based on the theory of one dimensional heat conduction into a semi-infinite body (Schultz and Jones 1973, Taler 1996). However, the theory for heat conduction in non-homogeneous body can be used to relate the surface temperature history to the rate of heat transfer to the body. Since heat transfer gauge is mounted on a backing material, the gauge along with the backing material becomes a non-homogeneous body with two regions 1 (sensing junction) and 2 (substrate material) as shown in Fig. 5.13 and Fig. 5.14. For thin film gauge and coaxial thermocouple, they represent dissimilar materials with dissimilar thermal and physical properties. Since the thickness of sensing material is in the order of a few microns, its edge area would be negligible and hence the lateral heat transfer will also be small in comparison with the longitudinal heat transfer. Hence, it is possible to use a one dimensional heat conduction

model for this analysis. The backing substrate material used in this case is an extremely good thermal insulator material and considering a test time of millisecond, a 10mm thick strip of substrate material can be considered to be infinitely thick for these purposes.

The determination of the surface heat flux from the temperature signal is based on the theory of one dimensional heat conduction into a semi-infinite body. Governing equation for surface heat transfer rate is based on some assumptions: (i) Temperature measure by sensing element is identical to the temperature of surface of the substrate; (ii) There is no lateral heat conduction through the substrate and that heat is conducted only in the direction normal to the surface; (iii) Thermal properties of the substrate materials are constant during experiment, because experimental time period is very small. Using these assumptions the transient temperature distribution $T(t)$ along the depth of the sensing material (medium1) and substrate material (medium2) as shown in Fig.5.13 and Fig.5.14 can be written as in second order differential form such as,

$$\frac{\partial^2 T_1}{\partial x^2} = \left(\frac{1}{\alpha_1} \right) \frac{\partial T_1}{\partial t} \quad (5.5)$$

$$\frac{\partial^2 T_2}{\partial x^2} = \left(\frac{1}{\alpha_2} \right) \frac{\partial T_2}{\partial t} \quad (5.6)$$

The suffix 1 and 2 indicates sensing junction and substrate materials of the heat transfer gauges.

$\alpha = \frac{k}{\rho c}$, is the thermal diffusivity of the material (sensing junction material or substrate material of the RTD sensor) defined in terms of ρ , c and k are the density, specific heat and thermal conductivity of the materials. If the surface heat fluxes apply at the heat transfer gauge surface is $q''(t)$ then boundary conditions are,

$$q_s(t) = -k_1 \frac{\partial T_1}{\partial x} \quad \text{at } x=0 \quad (5.7)$$

And at the interface between regions 1 and 2 ,

$$k_1 \frac{\partial T_1}{\partial x} = k_2 \frac{\partial T_2}{\partial x} \quad \text{and} \quad T_1 = T_2 \quad (5.8)$$

For semi-infinite body extending from $x=L$ to $x \rightarrow \infty$, the boundary conditions at both the boundaries are known, i.e., $x=L, T_2 = T_2(L), (\partial T_2 / \partial x) = 0$ and $x \rightarrow \infty; T_2 = T_o$ (uniform room temperature). When solving the Eq.5.5 and Eq.5.6 for constant thermal properties of the substrate material then time dependent solution of the surface heating rates is given by the convolution integral (Taler 1996).

$$q_s(t) = \sqrt{\frac{\rho_2 c_2 k_2}{\pi}} \left[\frac{T(t)}{\sqrt{t}} + \frac{1}{2} \int_0^t \frac{T(t) - T(\tau)}{(t-\tau)} d\tau \right] \quad (5.9)$$

Where, ρ_2 , c_2 and k_2 are density, specific heat and thermal conductivity of the substrate materials are taken from Table - 1 (Appendix - II). Numerical integration of the second part of the Eq.5.9, are used to determine the transient heat transfer rate but there is a singularity at $t = \tau$ therefore the surface heat fluxes obtained by cubic spline approaches adopted to predict the surface heating rates from the temperature data namely.

An observation of the time temperature curve (Fig. 5.6) reveals that small segments of the curve can be closely approximated by cubic spline as shown in Eq. 5.10. In particular, a cubic spline is a piecewise cubic polynomial, constructed in such a way that second derivative continuity is preserved (Boor 1978). The experimental temperature is represented by a third order spline in the form of

$$\{T_2(\tau)\}_{spline} = a_{1,i} + a_{2,i}(\tau - \tau_i) + \frac{1}{2} a_{3,i}(\tau - \tau_i)^2 + \frac{1}{6} a_{4,i}(\tau - \tau_i)^3 \quad (5.10)$$

$$\text{For } \tau_i \leq \tau \leq \tau_{i+1}, i=1,2,\dots,M \quad (5.11)$$

Here, $\tau = s_t t$ is scaled time and s_t is the scaling factor. The constant appearing in this can be determined by the following expressions;

$$a_{1,i} = T(\tau_i), \quad (5.12)$$

$$a_{2,i} = T'(\tau_i) = \frac{dT_i(\tau_i)}{d\tau} = \frac{1}{s_t} \frac{dT_i(t_i)}{dt}, \quad (5.13)$$

$$a_{3,i} = T''(\tau_i) = \frac{d^2T_i(\tau_i)}{d\tau^2} = \frac{1}{s_t^2} \frac{d^2T_i(t_i)}{dt^2} \quad (5.14)$$

$$\text{and } a_{4,i} = T'''(\tau_i) = \frac{d^3T_i(\tau_i)}{d\tau^3} = \frac{1}{s_t^3} \frac{d^3T_i(t_i)}{dt^3} \quad (5.15)$$

There is a sufficient flexibility in the cubic spline approximation to ensure that not only is the smoothing spline is continuously differentiable on the interval, but also that it has a continuous second derivative on the interval. The corresponding surface heat flux is obtained from Eq. 5.9 with the help of cubic spline Eq. 5.10. The surface heat flux is given by the following expression for $M = 1, 2, \dots, (J-1)$,

$$\{q_s(t)\}_{spline} = \left[\begin{array}{l} 2\sqrt{\frac{\rho_2 c_2 k_2}{\pi}} \sum_{i=1}^{M-1} \left\{ V_i (P_i^{1/2} - R_i^{1/2}) - \frac{W_i}{3} (P_i^{3/2} - R_i^{3/2}) \right\} \\ + \frac{a_{4,i}}{10} (P_i^{5/2} - R_i^{5/2}) \end{array} \right] \sqrt{s_t} \quad (5.16)$$

$$+ 2\sqrt{\frac{\rho_2 c_2 k_2}{\pi}} \left(V_M P_M^{1/2} - \frac{W_M}{3} P_M^{3/2} + \frac{a_{4,M}}{10} P_M^{5/2} \right)$$

Where,

$$P_i = \tau_{M+1} - \tau_i; R_i = \tau_{M+1} - \tau_{i+1}; \quad (5.17)$$

$$F_i = a_{1,i} + a_{2,i} P_i + \frac{a_{3,i}}{2} P_i^2 + \frac{a_{4,i}}{6} P_i^3; \quad (5.18)$$

$$V_i = \frac{dF_i}{d\tau_{M+1}} = a_{2,i} + a_{3,i}P_i + \frac{a_{4,i}}{2}P_i^2; \quad (5.19)$$

$$W_i = \frac{d^2F_i}{d\tau_{M+1}^2} = a_{3,i} + a_{4,i}P_i; \quad (5.20)$$

Using this established procedure, the heat fluxes are predicted from the temperature history with known values of thermal properties of the substrate material, and then compared with the input heat fluxes. This procedure has been followed not only for the experimentally obtained temperature signal but also from the finite element method simulation and the analytical formulation. The one dimensional surface heat fluxes obtained from this analysis for platinum TFGs, nano-material based platinum TFGs and coaxial thermocouple are compared with input heat supply, as shown in Fig. 5.21, Fig. 5.22(a-d), Fig. 5.23, Fig. 5.24(a-d) and Fig. 5.25(a-d) at different step heating loads. Temporal nature of the heat flux and temperature traces obtained from present investigations compare well with the same reported in the literature (Billiard et al. 2002). These results show that a very good recovery of input, experimental, numerical and analytical distribution of heat fluxes data and heat fluxes varies incompletely linear fashion with time. The trends of surface heat flux obtained from semi-infinite method indicates that heat flux values first rises to critical values after that it increases linearly with time which is very much closer with input heat supply. This observation reconfirms the uni-directionally of heat transfer and semi-infinite thickness of the substrate material. So, the third order cubic-spline temperature distribution is a very good approximation of estimating a one dimensional surface heat flux for shorter and longer duration experimental data. The recovered values of surface heat flux from transient temperatures using convolution integral provide under-prediction by 1.6%, 2.4% and 4.1% for platinum based thin film gauges, platinum/CNT based thin film gauges and coaxial thermocouple from the known input heating loads supplied during dynamic calibration

experiments. Overall, the results indicate a satisfactory agreement between the applied and recovered heat flux signals in terms of trend and magnitude. Therefore, these dynamic calibration based experiments demonstrate the applicability of the heat transfer gauges for radiation and conduction based heat transfer measurement analysis. However, implementation of these heat transfer gauges or thermal sensors for particular applications like thermal property estimation needs further investigations for optimization of heat transfer gauges dimensions (thickness and diameter of gauge and substrate materials) in order to achieve proper prediction with minimum disturbance to the temperature and heat flux field in the solid domain.

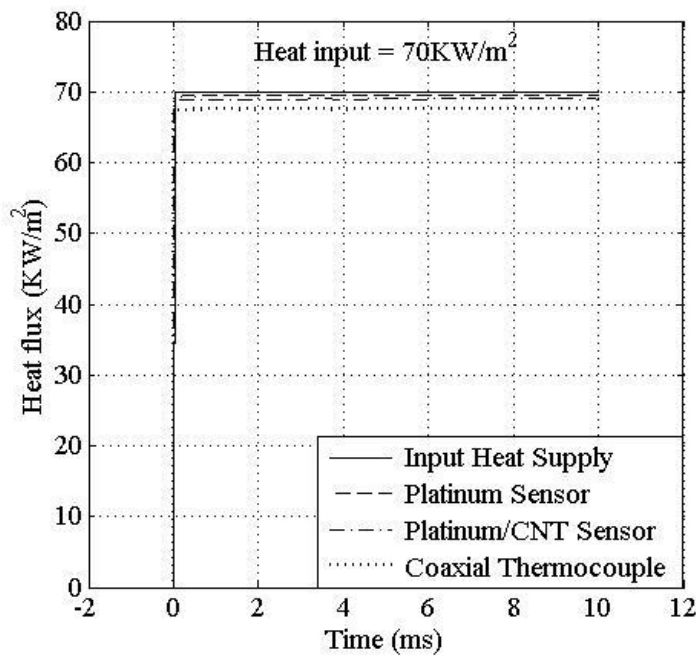
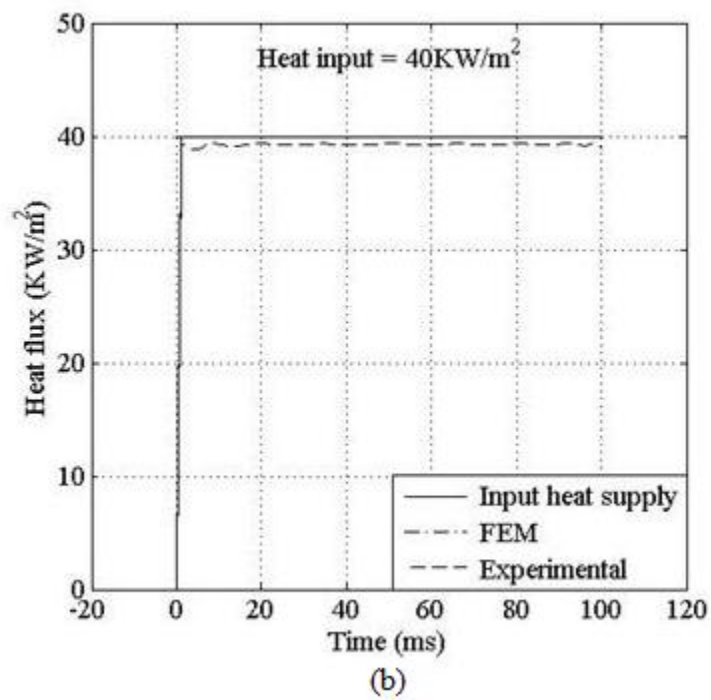
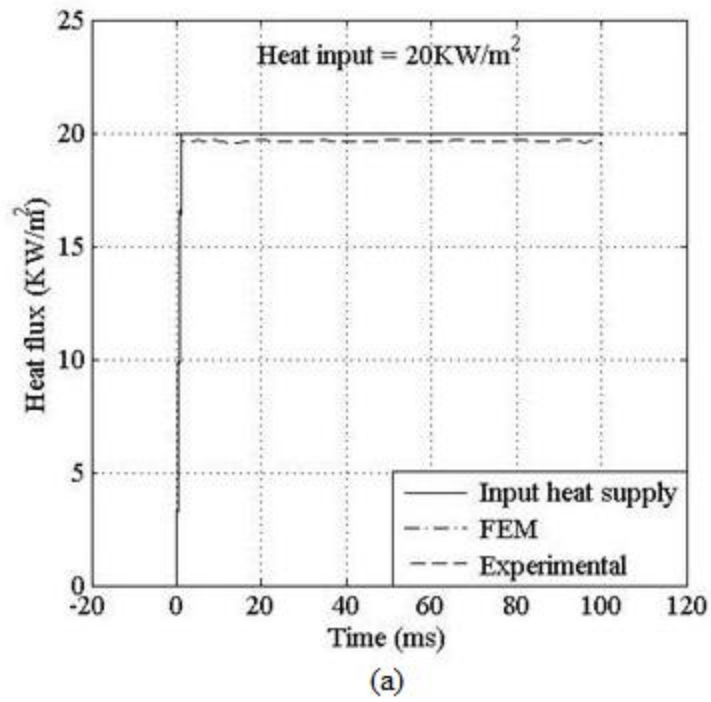
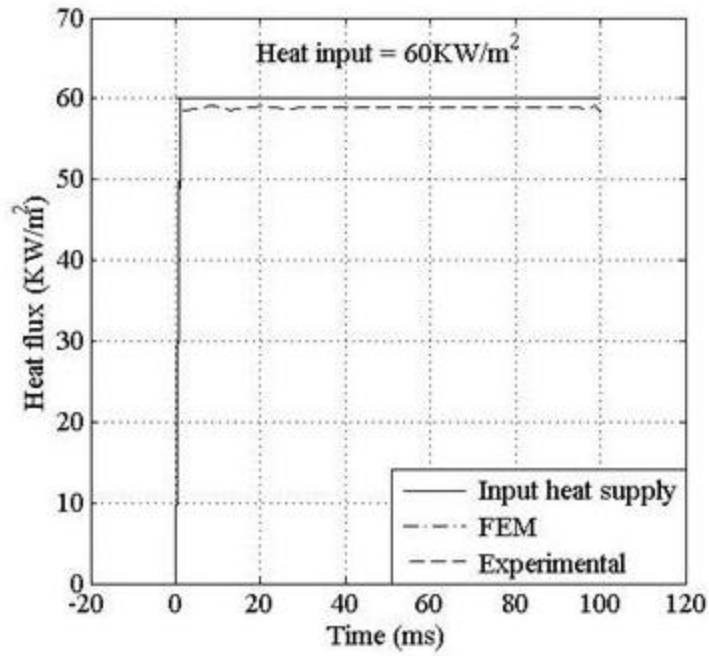
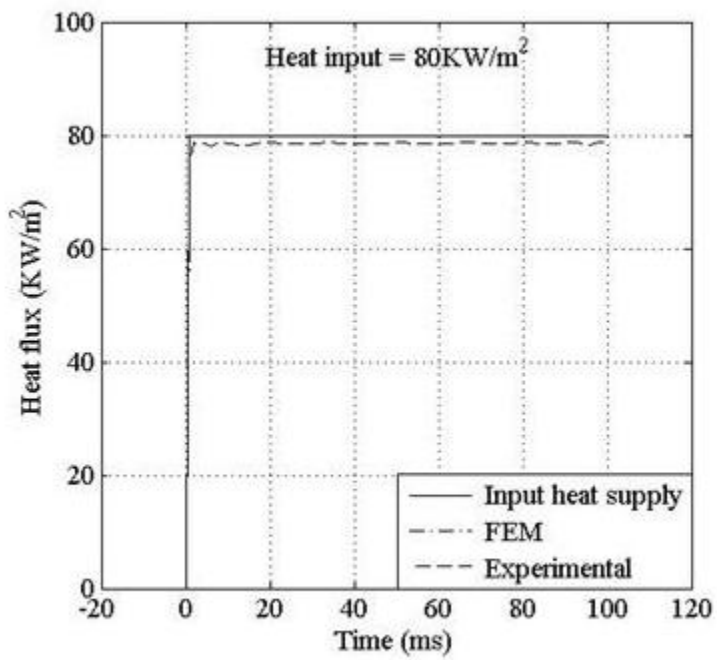


Fig. 5.21: Comparison of heat fluxes histories for various types of heat transfer gauges at radiation based step heat loads





(c)



(d)

Fig. 5.22: Transient heat flux signals for platinum thin film sensor at conduction based step heat load

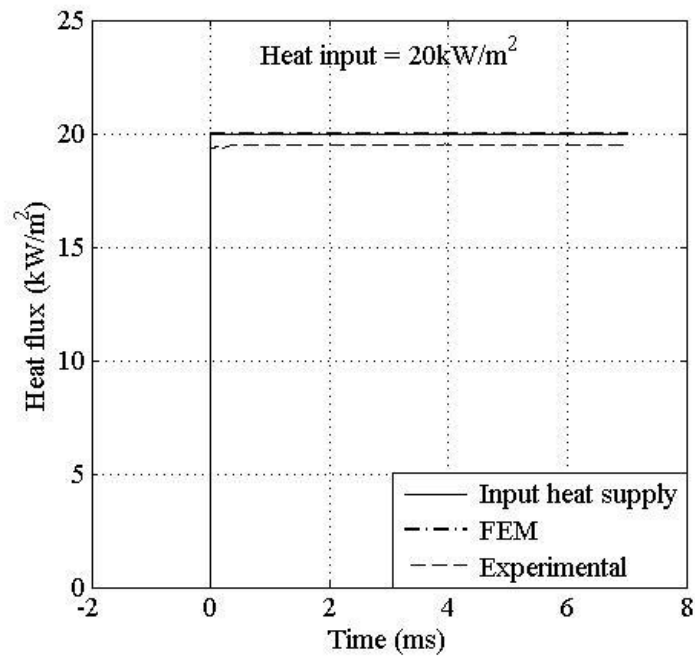
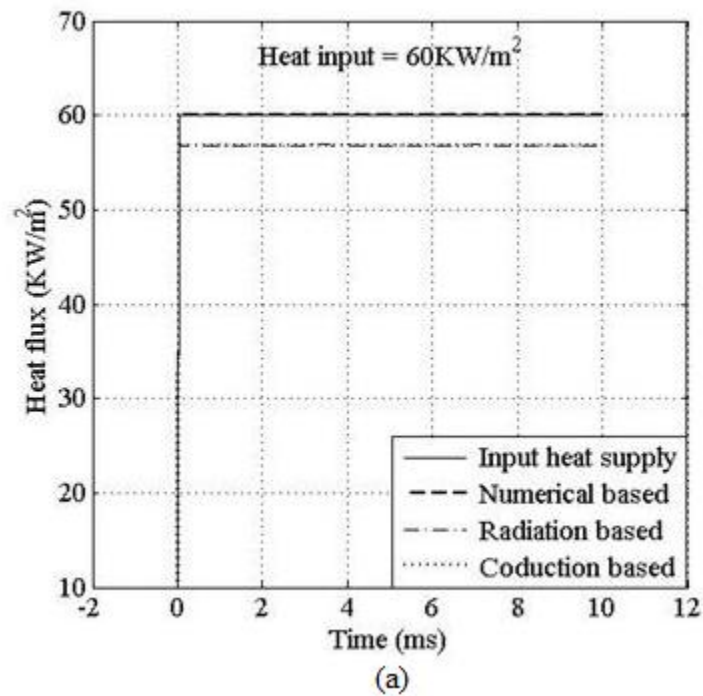
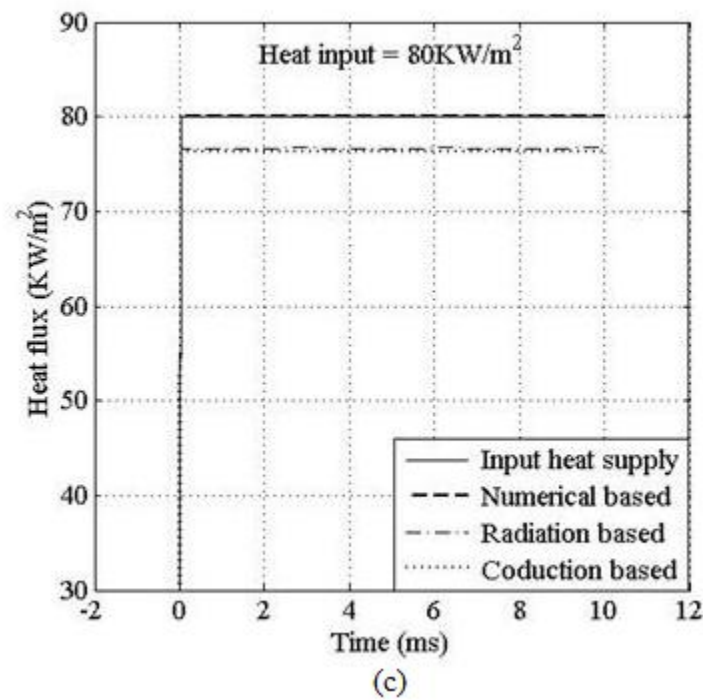
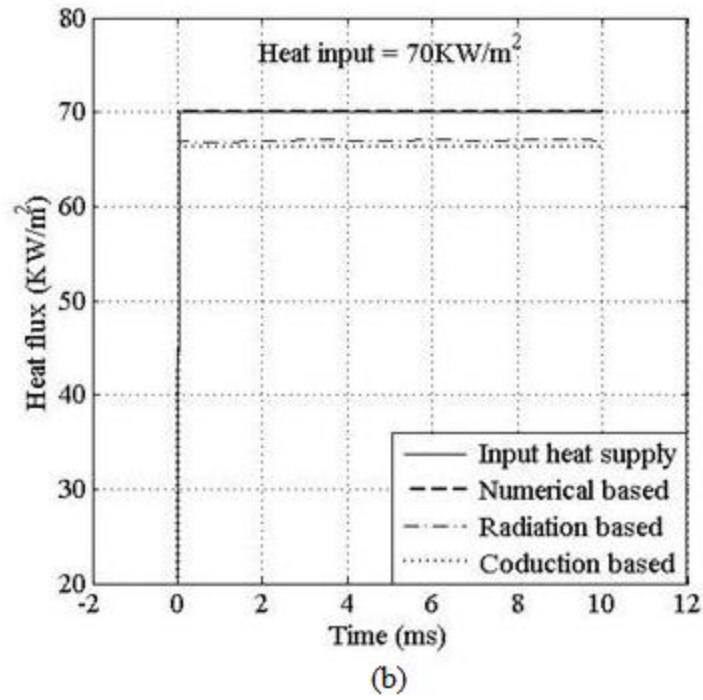


Fig. 5.23: Transient heat flux signals for platinum/CNT thin film sensor at conduction based step heat load





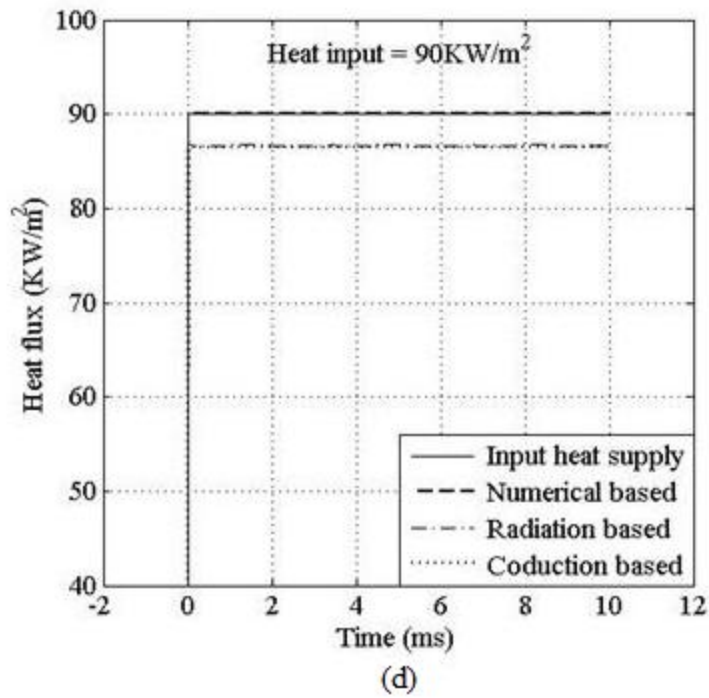
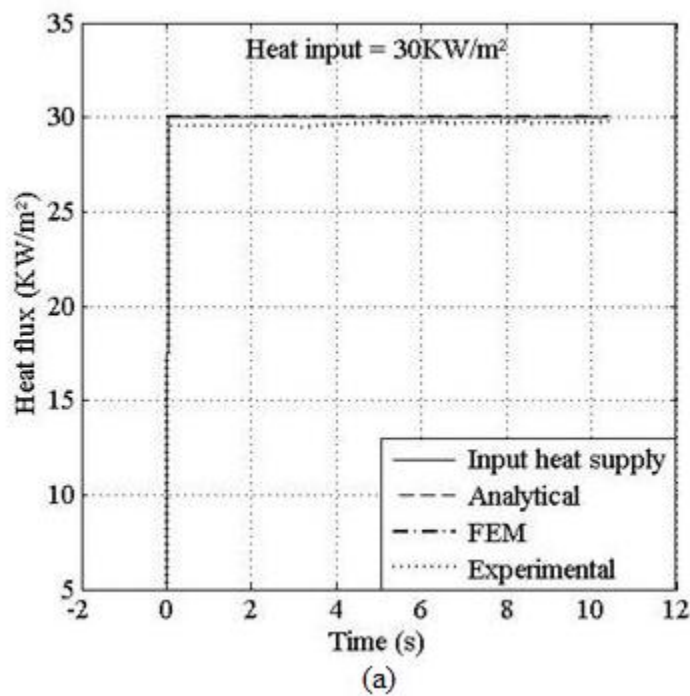
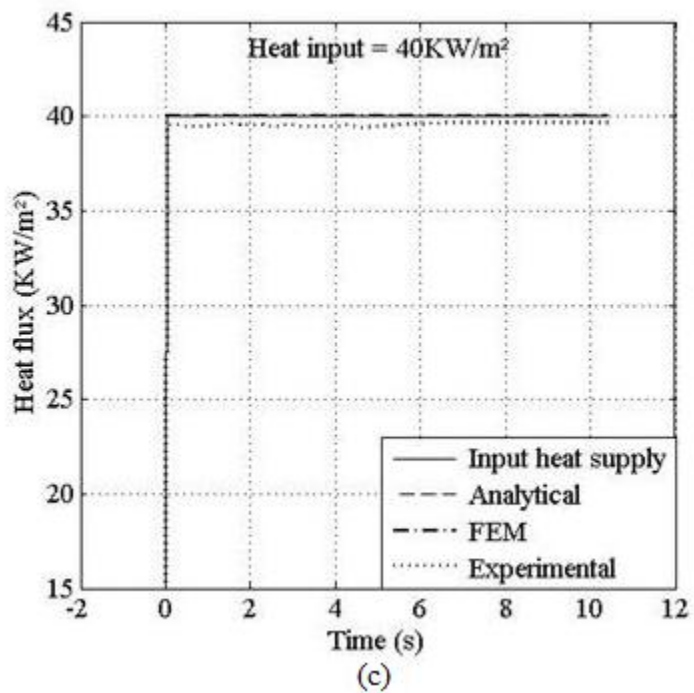
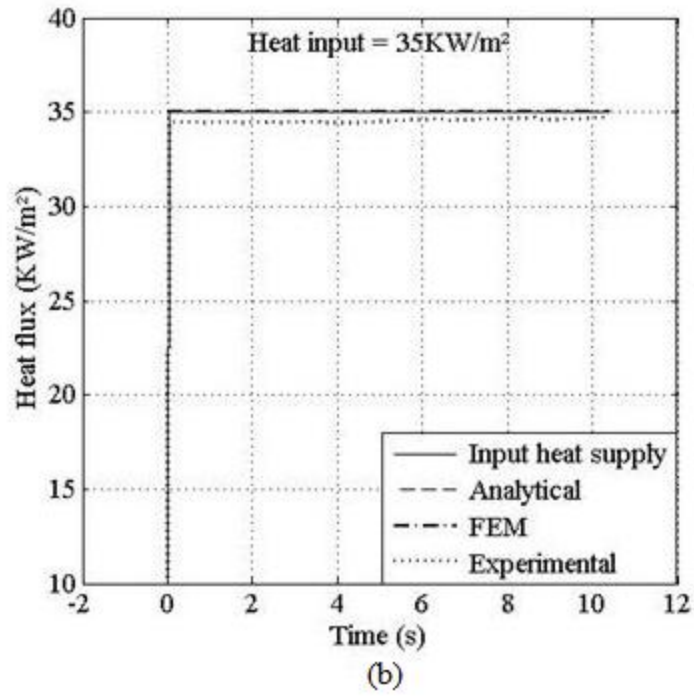


Fig. 5.24: Transient heat flux signals for coaxial thermocouple sensor at radiation and conduction based step heat load





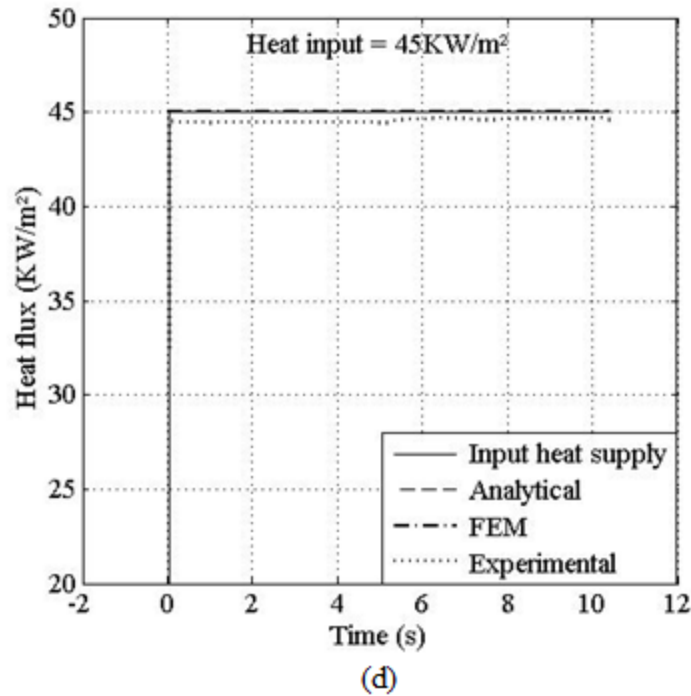
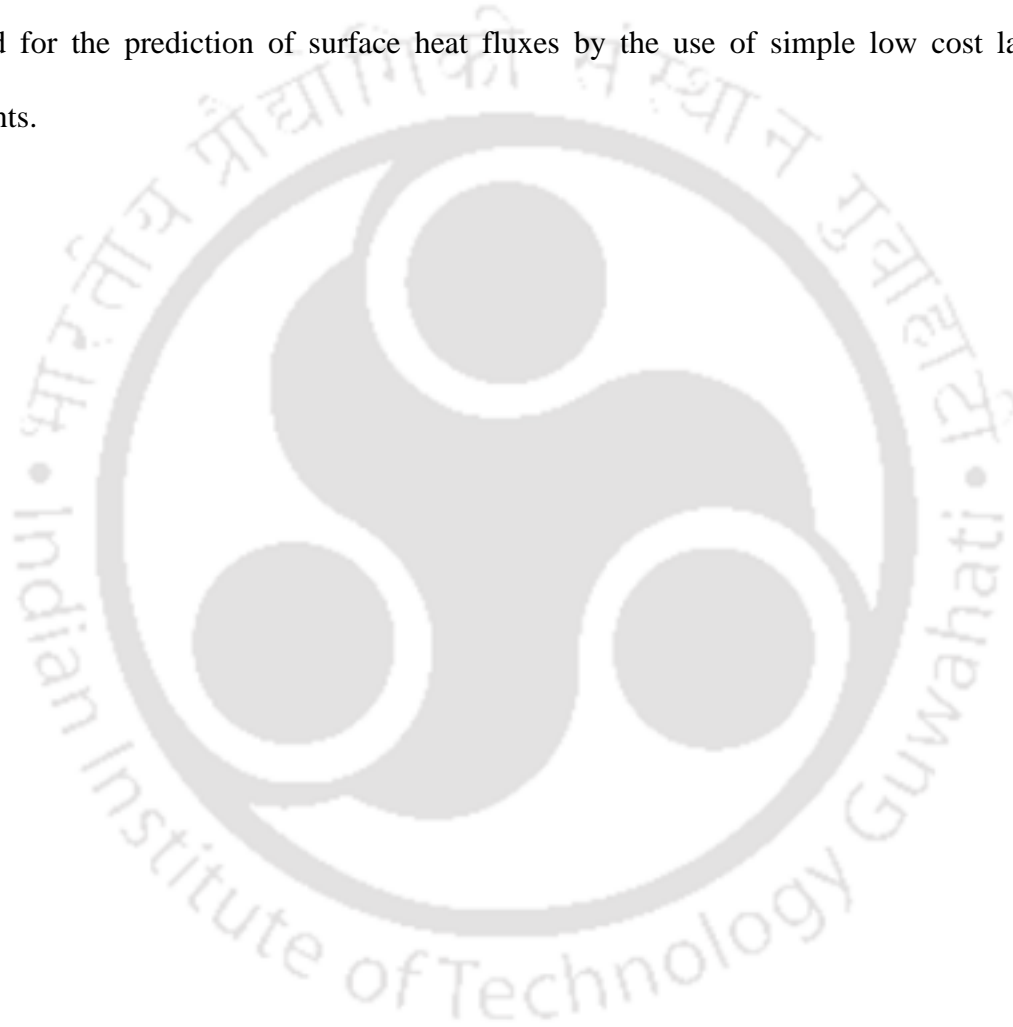


Fig. 5.25: Comparison of transient surface heat flux signals for platinum thin film sensor at radiation based step heat load

5.4 Summary

The accurate surface heat fluxes predictions from temperature history are very important for which dynamic calibrations of heat transfer gauges are required. It is also necessary to investigate the trends of thermal phenomena for the handmade heat transfer gauges. Radiation and conduction based dynamic calibration techniques are seen to be viable calibration techniques to replicate the step heat loads which is commonly encountered in high speed flow situations. The step heating load based dynamic calibration technique has proved that the handmade heat transfer gauges can be used to accurately measure the surface temperature in highly transient facilities when constant heat fluxes are applied on the sensing junction of the handmade thermal sensors. Surface heat flux is calculated from numerical and analytical analysis indicates that the distribution of surface heat flux on the gauge material varies linearly with time. While comparing

them with experimental signals, some deviations are noticed which may be due to the thermal property values used during simulation. The average value of deviation for platinum TFGs, nano-material based platinum TFGs and coaxial thermocouple are 1.6%, 2.4% and 4.1% respectively. Therefore, the well dispersed and very small sensing junction provides the ability to fabricate a highly sensitive heat transfer gauges in the laboratory. Moreover, they can be calibrated for the prediction of surface heat fluxes by the use of simple low cost laboratory instruments.



Chapter – 6

Stagnation Point Heat Flux Measurement with Heat Transfer Gauges

Measurement of surface heating rates of a fluid flow during an experiment is the most fundamental and vital to obtain certain key information of the flow field. Some important applications include wall heat transfer rates in a boundary layer, stagnation heat fluxes at the nose tip of a blunt body, rear body heat fluxes due to generation of vortices etc. With respect to aerodynamic heating point of view, the estimation of stagnation heat fluxes at the nose tip of a blunt body is very vital. In the previous sections, the author have discussed the design and fabrication procedures of heat transfer gauges, their static and dynamic calibrations under certain situations where there is a sudden increase in heat loads (such as step/ramp/impulse etc). Now, it is felt that these heat transfer gauges should be demonstrated for real time experiments to infer the surface temperature history. When a blunt body is exposed to a high speed flow, the heat transfer is expected to be the maximum at the stagnation point (i.e. the nose tip of the body). Using the techniques discussed in the previous sections, the stagnation point probes are fabricated for platinum thin films, platinum-CNT thin film gauges and coaxial thermocouple. Also, an experimental setup is fabricated to generate a heated sonic jet and all the in house fabricated gauges are exposed to this flow. The numerical technique (Fluent CFD) is used to found the exact location where maximum energy is expected and accordingly the stagnation probes are placed at that location. The transient surface temperatures recorded from these heat transfer gauges are processed through one-dimensional heat conduction modeling to infer the stagnation heat fluxes. Subsequently, they are also compared with the numerical techniques and the agreements are found to be very good.

6.1 Introduction

“Aerodynamic heating” is one of the key considerations for the design of high speed vehicles and the prediction of surface heat fluxes on the aerodynamic surfaces becomes crucial parameter. In the design aspects of high speed flow, a ‘stagnation point’ occurs at some point on the surface of the body, where the fluid is brought to rest. In other words, the fluid velocity becomes zero and all the kinetic energy is converted into heat energy. Obviously, the heat flux is the maximum at this point leading to a very high value of temperature and pressure. As a quantitative estimate, Hankley (1989) proposed the energy balance using the first law of thermodynamics, when a slug of mass (m), moving at velocity (V) is brought to rest. It leads to the fact that the entire kinetic energy is converted to heat energy (Q) as given below;

$$\frac{1}{2}mV^2 = Q \Rightarrow \frac{Q}{m} = \frac{V^2}{2} \quad (6.1)$$

For a sonic velocity of 340 m/s, the specific thermal load (Q/m) is expected to be 58kJ/kg and it is interpreted as the stagnation heating rate. If the specific heat capacities is denoted as c_p , then the above equation can be used to obtain the stagnation temperature.

$$T_0 = \frac{V^2}{2c_p} \quad (6.2)$$

Stagnation point is the location on a body that experiences maximum temperature and heat flux as compared to other locations. Normally, the temperature at the stagnation point is measured through surface thermometry methods like thin film gauges and coaxial surface junction thermocouple sensors. They provide the surface temperature history of the body, which is then used to determine the surface heat flux on to it by using the theory of unsteady, one dimensional heat conduction into a semi-infinite substrate (Rose 1958, Rumsey and Lee 1959, Trimmer and

Clark 1969). The measurements of transient heat transfer in high speed flow test facilities are normally performed with surface temperature sensing device and the time resolved data are processed to obtain surface heat flux with inverse numerical equations (Cook and Felderman 1966, Diller and Kidd 1996). Some of the resistance temperature detector sensors are thin film resistance thermometer (Miller 1981 and Wannewetsch 1985), coaxial thermocouple (Kidd 1990) and temperature sensitive paint (Mosharov et al. 2003 and Nagai et al. 2006). Different techniques to heat models prior to arrival of the test flow in blow down wind tunnels have also been discussed (Lee et al. 1994 and Martinez et al. 1995). All of these devices or methods have significant deficiencies which could possibly contribute to degradation of the accuracy of the measurement. Widhopf (1971) used a fast response calorimeter type heat transfer gauge with sputtered thin film platinum thermometer to carry out the measurements in a hotshot tunnel. Hubner et al. (2002) developed and investigate the application of high speed imaging and luminescent coating techniques to measure full field surface heat transfer rates for indented cone model. A new type of surface junction thermocouple sensor has been developed which has a response time in the order of microseconds and is suitable for measuring large transient surface heat fluxes in wind tunnels (Sanderson et al. 2002). Traditional optical methods such as liquid crystals have been attempted to measure heat transfer rates because of short test time available in impulse facilities (Merski 1998). There are other techniques used to view the thermal imaging of the full field are a, thermal paints (Asai et al. 1997), infrared thermography (Luca et al. 1995) and thermo-graphic phosphors (Micol 1995).) The thin film sensors made by vacuum deposition of thin layer of platinum on a macor substrate is used to measure the stagnation point heat flux in a shock tunnel (Reddy et al. 2009). They compared the results with analytic expressions for stagnation point heat flux value (Fay-Riddell 1958) and with numerical methods. The classical

theory of one dimensional, unsteady heat conduction into a semi-infinite medium, and design of thermal sensors with reference to dimensionless thermal penetration depth, variation of material properties like thermal diffusivity, thermal conductivity for alloys within the certain application temperature range (100-450K) may be found in the references (Schultz et al. 1973, Sundqvist 1992 and Nag 2002).

In this present work, attempts have been made to demonstrate these handmade sensors for real time experiments to acquire transient temperature data. Heat transfer measurement at the stagnation point is chosen as the location of these sensors where the heat fluxes are expected to be the maximum. For this purpose, an experimental setup is fabricated in house to generate heated air jet at sonic velocity. An insulated heavy cylinder is designed in the laboratory, which contains heated compressed air. The stagnation probes are designed and fabricated by mounting the thin film sensors and coaxial thermocouple. After exposing the probes to these sonic jets, the temperature signals are recorded. The stagnation heat fluxes are then obtained from one dimensional heat conduction analysis with the semi-infinite substrate assumption. Using the analytical expressions and computational study, the stagnation heat fluxes are also obtained and compared with experiments. The real time experiments are also simulated using commercially available software (FLUENT) to obtain the exact location of the sensor. Details of the stagnation probes, experimental setup, computations at stagnation point and the comparison of experiments are described in this chapter.

6.2 Measurement of Stagnation Point Heat Fluxes

6.2.1 Theoretical Analysis

Air is composed of molecules that are moving about in a random motion with different instantaneous velocities and energies at different time intervals. However over a period of time,

the average molecular velocity and energy can be defined and for a perfect gas, they are functions of the temperature only. In this experimental work, compressed air flow occurs through a nozzle attached to a huge reservoir or a solid cylinder as shown in Fig. 6.1. Flow exits the reservoir through the nozzle if the back pressure is less than the reservoir pressure. Further, the maximum velocity of the fluid exists at the nozzle throat where the area is smallest. When the back pressure is further decreased, fluid exits the reservoir more rapidly. Eventually, the velocity at the throat reaches the sonic velocity, for which flow Mach number is unity ($M = 1$). Further, decrease in back pressure will not increase the flow rate and the nozzle is said to be choked. This principle is used here to obtain the sonic jet by maintaining the appropriate pressure ratio (Anderson 1990). An isentropic relation for compressible flow exists to obtain the ratios of stagnation to static flow conditions for temperature and pressure.

$$\frac{T_0}{T_\infty} = 1 + \frac{\gamma - 1}{2} M^2 \quad (6.3)$$

$$\frac{P_0}{P_\infty} = \left(1 + \frac{\gamma - 1}{2} M^2 \right)^{\frac{\gamma}{\gamma - 1}} \quad (6.4)$$

$$M = \frac{V_\infty}{a} = \frac{V_\infty}{\sqrt{\gamma RT}} \quad (6.5)$$

Where, T_0 and P_0 are total pressure and temperature, T_∞ , P_∞ and V_∞ are stream temperature, pressure and velocity, γ is the specific heat ratio, a is the speed of sound in the medium, R is gas constant, M is Mach number. For air ($\gamma = 1.4$), if the sonic flow has to occur, the above equations can be simplified to obtain the stagnation to static pressure and temperature ratios as given below;

$$\frac{T_0}{T_\infty} = 1.2; \frac{p_0}{p_\infty} = 1.9 \quad (6.6)$$



Fig. 6.1: Laboratory set up for insulated solid cylinder with pressure gauge, heater and thermocouple

6.2.2 Experimental Investigation

A highly compressed air is capable of producing flow conditions to study the flow fields over a test model for durations which resembles the nature of an impulse facility. The aim of this work is to prepare an experimental setup that can provide a high speed heated air flow to the in house made heat transfer gauges and study their performances. Since, air is compressible; it can be stored in a cylinder at very high pressure as shown in Fig. 6.1. Simultaneously, it can be heated so that temperature can be increased. At this condition, the pressure and temperature inside the reservoir/cylinder is indicated as stagnation values. When it is allowed to flow out in a controlled manner through a small opening, a jet is likely to occur that expands in the atmosphere. When a minimum pressure ratio given by Eq. (6.6) is maintained, the flow will be choked and the mass flow rate can be calculated easily. In order to get the maximum advantage of the air jet, the heat

transfer gauges are to be placed in the core flow region. So, the complete experimental setup involves the design of appropriate stagnation probe and finding the appropriate locations in the flow field. Special care is taken to assure an uninterrupted supply of fresh compressed air on the junction together with the use of metals of low thermal conductivity, thus keeping heat transfer and heat dissipation losses to a minimum.

In these experiments, stagnation probes are fabricated by mounting the thin films (platinum and platinum-CNT) on the substrate material (macor). These probes resemble blunt nosed spherical shapes as shown in Fig. 6.2, while a surface junction coaxial thermocouple is shown in Fig. 6.3. These heat transfer gauges are fabricated and calibrated by same methodologies that are discussed in the previous chapters. Since the thermal sensors are exposed to high speed jets issued from the nozzle, it is necessary to electrically insulate the wire leads. Sufficient care is taken during the mounting of the sensor into the probe tip to ensure that the film is in flush with the contour of the probe.

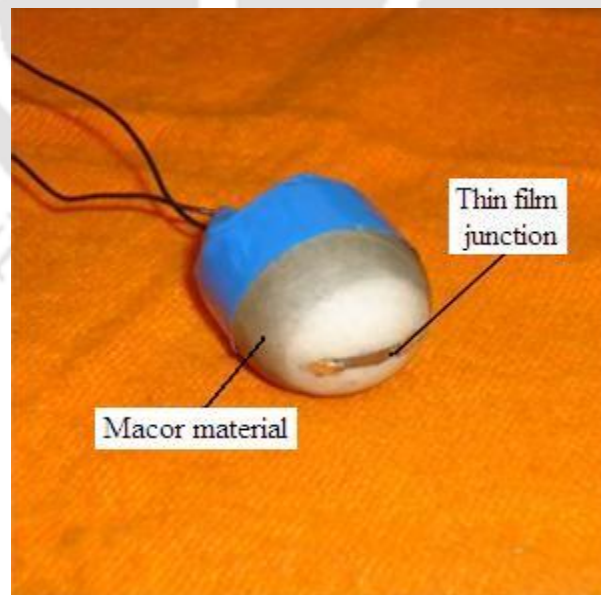


Fig. 6.2: Thin film based heat transfer gauge over a blunt shaped spherical bodies with Macor as substrate material

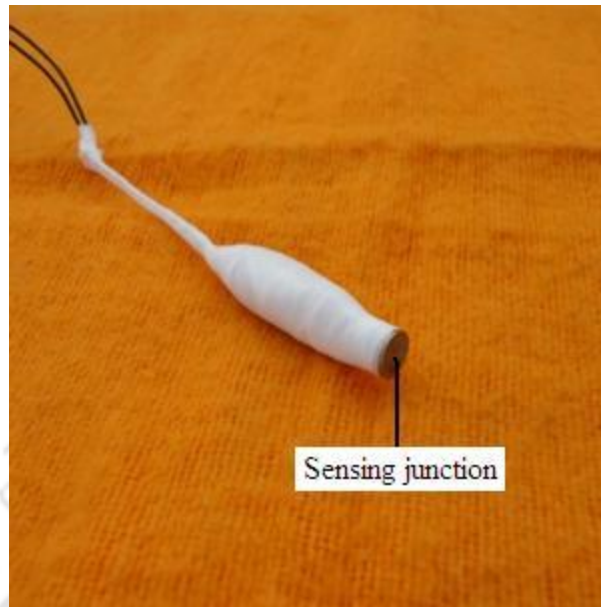


Fig. 6.3: Fabrication of coaxial thermocouple in the laboratory

6.2.3 Numerical Analysis

The ever increasing advances in computer technology have enabled many in science and engineering fields to apply numerical methods for simulating physical phenomena. Numerical analysis is the study of algorithms that use numerical approximation for the problems of mathematical analysis (as distinguished from discrete mathematics). These methods are often divided into elementary ones such as finding the root of an equation, integrating a function or solving a linear system of equations to intensive ones like the finite element method. The overall goal of the field of numerical analysis is the design and analysis of techniques to give approximate but accurate solutions for complicated problems. In the past, solving problems numerically often meant a great deal of programming and numerical based problems and the numerical stability is an important factor. An algorithm is called numerically stable if an error, whatever its cause, does not grow to be much larger during the solution or calculation. This happens if the problem is well conditioned, meaning that the solution changes marginally by a

small amount when the data are changed by a small amount. To the contrary, if a problem is ill-conditioned, then any small error in the data will grow to be a large error.

In this work, numerical simulations are intended for a sonic flow air jet expanding in atmosphere. First, it is desired to obtain the appropriate location at which the gauges are to be placed. Secondly, the flow field analysis has to be done so as to obtain expected trends of transient heat flux and surface temperatures. All these analysis needs to be done under experimental free stream conditions. For the four typical shots, the average value is taken for analysis. The two dimensional geometry of the body has been created in Gambit software and the structured grid is generated, with the number of cells being 441000. The mesh size has been kept finer near the body walls, so as to capture the gradients accurately with the minimum side of a cell. The computational analysis has also been carried out for the hot air flow based experiments using commercial package CFD FLUENT in the two stages. In the first stage, a computational domain and meshing of the cylindrical hollow pipe (20mm diameter) has been prepared in a flow field by using GAMBIT WORKBENCH as shown in Fig. 6.4, through which a highly compressed air exhausts to atmosphere. Referring to the Fig. 6.4, the boundary conditions used in the simulation are, uniform temperature of 300K at the wall surface and outlet pressure as atmospheric (1.01325 bar). The inlet pressure and temperature of hot air particles are P_∞ and T_∞ calculated by using Eq. 6.3, Eq. 6.4 and Eq. 6.5, where the stagnation pressure and temperatures are 16 bar and 347K, respectively. A pressure far field includes the free stream and inlet to the computational domain. Wall is kept as adiabatic with no slip condition. Pressure outlet includes the exit from the computational domain. The results are obtained for pressure and velocities flow fields as shown in Figs. 6.5 and 6.6. The pressure contour indicates that pressure of the fluid particle is constant through the pipe and gradually reduces when it expands. From Fig. 6.6, it is

seen that the velocity of the fluid is constant through the pipe but at a certain distance 14mm from the nozzle tip, maximum value of jet is observed. At this point, the kinetic energy is the maximum and is considered as the optimum location of stagnation probe.

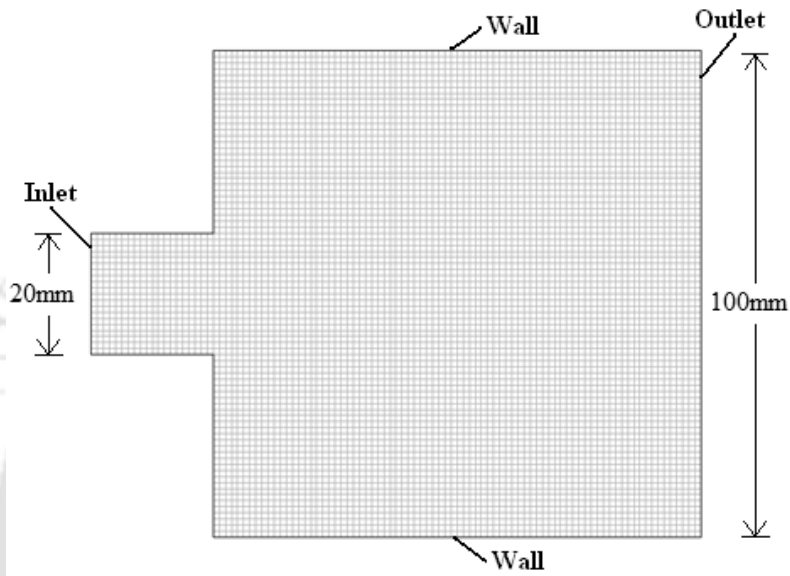


Fig. 6.4: Computational model of a flow field

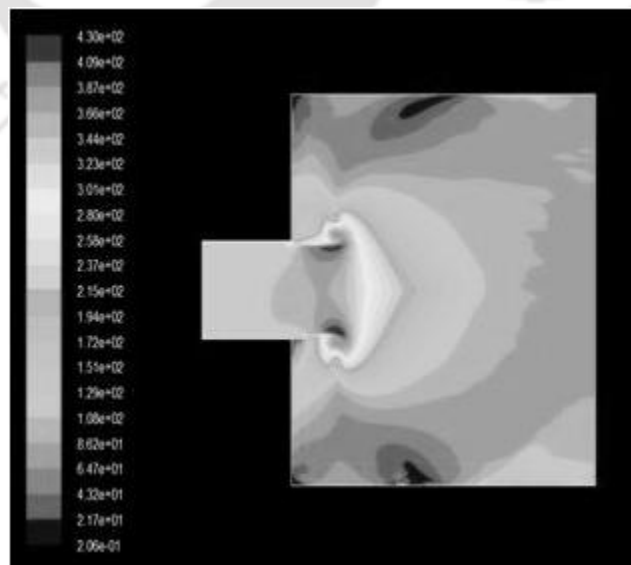


Fig. 6.5: Contour of velocity distribution along the direction of flow field

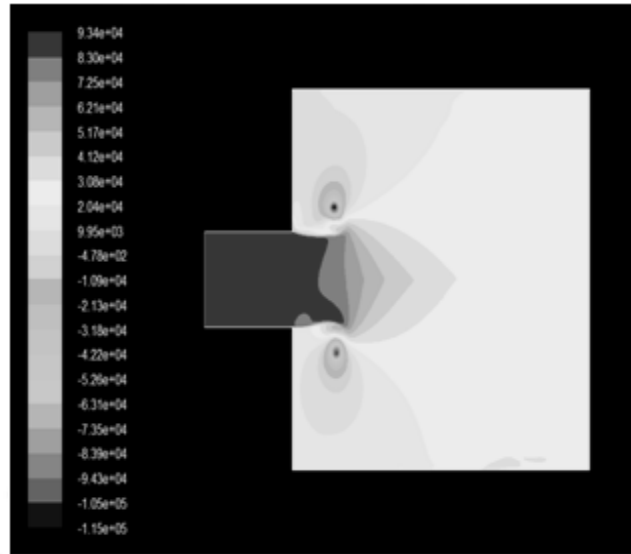


Fig. 6.6: Contour of pressure distribution along the direction of flow field

Further, the entire simulation study is repeated by placing the stagnation probe in the flow field. The model of the hollow cylindrical pipe, sensor and flow field, all are centrally placed or lies along the same axis as shown in Fig. 6.7. Here the diameter of nozzle pipe is 20mm and sensing surface of the thermal sensor is placed at a distance 14mm from the nozzle tip. The mesh generation for this dimension has been the important task, since meshing of the above part is done using square element in GAMBIT WORKBENCH software. The features for the mesh that can be used for this special problem contain very small structures inside very large structures as shown in Fig. 6.8. The boundary conditions used in the simulation are, all walls are stationary and kept as adiabatic with no slip condition, these walls maintained at uniform temperature 300K at the wall surfaces and outlet pressure as atmospheric (1.01325 bar). The inlet pressure and temperature of hot air particles are P_∞ and T_∞ calculated by using Eq. 6.3, Eq. 6.4 and Eq. 6.5, where the stagnation pressure and temperatures are 16 bar and 347K, respectively. The flow of hot air particles at inlet is viscous laminar flow. The results are obtained for velocity, total pressure and static pressure contour obtained from numerical analysis are as shown in Figs.

6.9, Fig. 6.10 and Fig. 6.11. Here, it is found that when fluid particles collide with sensing junction of the thermal sensor then velocity of the fluid particles reaches to zero value and maximum amount of heat flux occurs at the sensing junction surface of blunt shape spherical body. The velocity of air particles are also very close to zero at the sensing junction, indicate that stagnation point occurs at the head of the thermal sensor and all kinetic energy has been converted into heat energy.

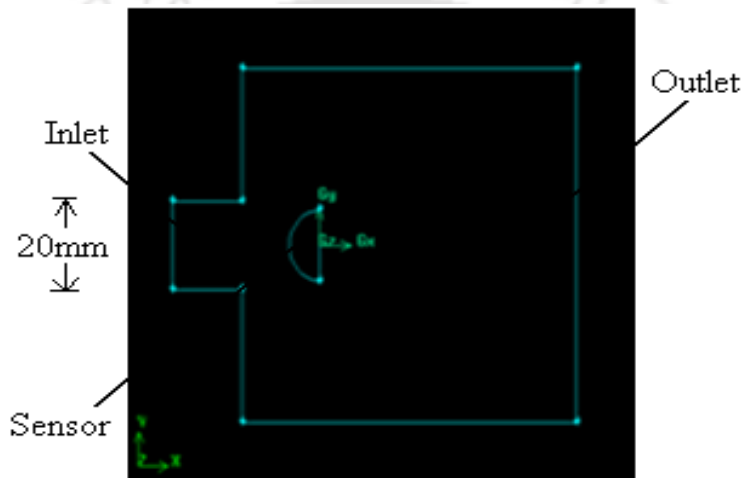


Fig. 6.7: Computational model of a blunt shaped spherical sensor in a flow field

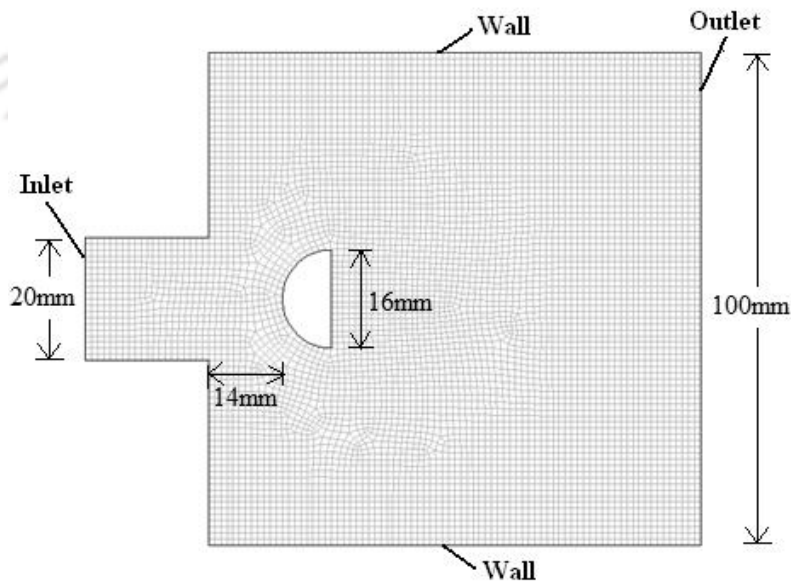


Fig. 6.8: Finite volume mesh for the flow field with blunt shaped spherical sensor

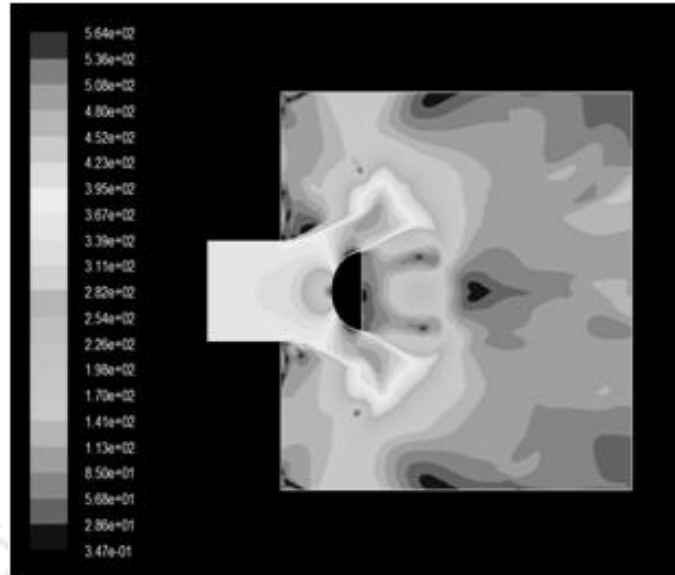


Fig. 6.9: Contour of velocity distribution along the direction of flow field

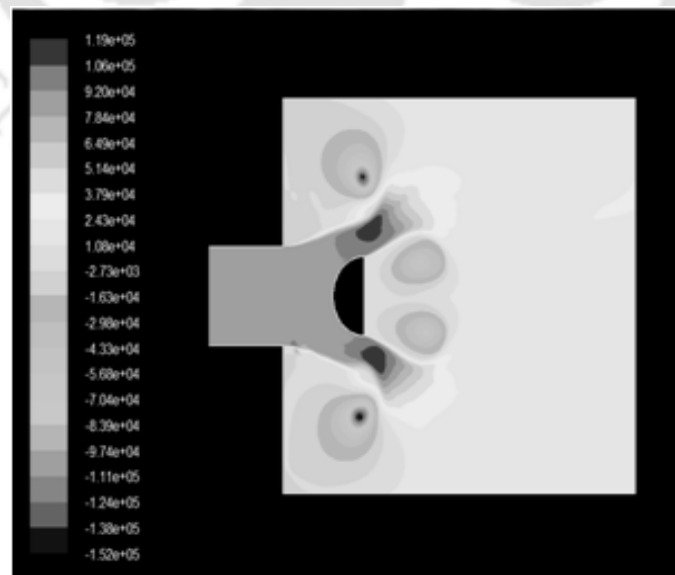


Fig. 6.10: Contour of total pressure distribution along the direction of flow field

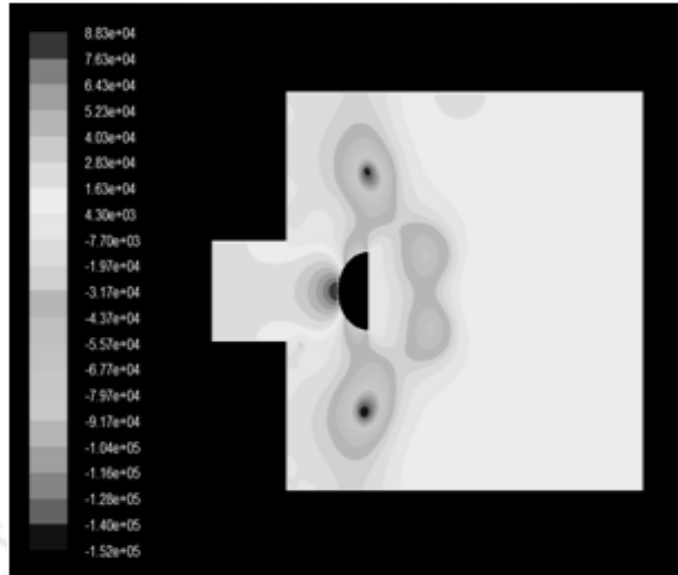


Fig. 6.11: Contour of static pressure distribution along the direction of flow field

6.2.4 Experimental Results and Discussions

With the knowledge of numerical investigations, the experimental facility for the open jet setup is designed and the schematic diagram is shown in Fig. 6.12. Here, one air compressor is used to fill highly compressed air inside the solid cylinder (the height and diameter of the cylinder is 38 cm and 21cm) and then air heated inside the cylinder with the help of a heating element. The outer part of the cylinder is well insulated (Teflon) from the surroundings so that steady state condition is reached after certain time interval. Steady state temperature of the hot air inside cylinder is measured with the help of thermocouple and the pressure gauge indicates pressure of hot air inside the cylinder. The hot air supply through the hollow cylindrical pipe is controlled by a valve as shown in Fig. 6.12. The nozzle has circular cross section with constant diameter (20mm diameter), is connected to the solid cylinder. The nozzle expands the flow up to sonic velocity where the blunt nose test model and the thermal sensor are mounted on a rake. The heat transfer gauge is directly connected from the output signal measuring instrument. During experiment the total pressure and temperature of hot air inside the cylinder is measured as 16 bar

and 347K, respectively as shown in Table 6.1. The output voltage signals from the heat transfer gauges are recorded for the duration of 200ms. Further, the voltage signals are converted to temperature-time histories with the knowledge of thermal coefficient of resistance as discussed in the previous chapters. The experiments are repeated with three types of handmade sensors (platinum based, platinum/CNT based and coaxial thermocouple) and the final temperature signals obtained from these experiments for the hot air flows indicate that temperature rises parabolic with time as shown in Figs. 6.13 (a-d). The parabolic rise of temperature plots ensures the analogous behavior with respect to the use of sensors in shock tunnel (Schultz and Jones 1973, Sahoo 2003). For all the temperature signals shown in Figs. 6.13 (a-d), the surface heat fluxes are measured. This procedure has been not only for the experimentally obtained temperature signals but also for the temperature data obtained from the numerical simulation. The inferred surface heat fluxes predicted from the temperature histories using Eq. 5.16 are shown in Figs. 6.14 (a-d). The comparison between surface heat fluxes measured by these handmade heat transfer gauges are as shown in Fig. 6.15. In these plots, the comparison between output heat fluxes measured by different types of handmade heat transfer gauges are obtained for same test conditions shows that platinum sensors are over predicting in comparison with coaxial thermocouple and numerical values. The reason for this could be the thermal property of the sensing materials or erosion of the platinum gauges that increased the resistance of the platinum thin film during a test (continuous erosion within the test duration), due to which the corresponding output was higher than the expected, considering the initial resistance of the gauge. The other reason could be shape and size of the nozzle because in this experimental work the nozzle is just a cylinder with constant diameter, it is very likely that there will be corner separations, Mach number 1 will be achieved at the vena-contracta and supersonic flow may

prevail at the exit of the nozzle. This could be also the reason why the heat fluxes recorded by the thermal sensors are all higher than the numerically predicted results. However, for stagnation point based experiments, there is a delay of 1ms for rise in surface heat fluxes. In all the cases, there is an instantaneous rise in heat fluxes resembling the nature of step load rise instantaneously.

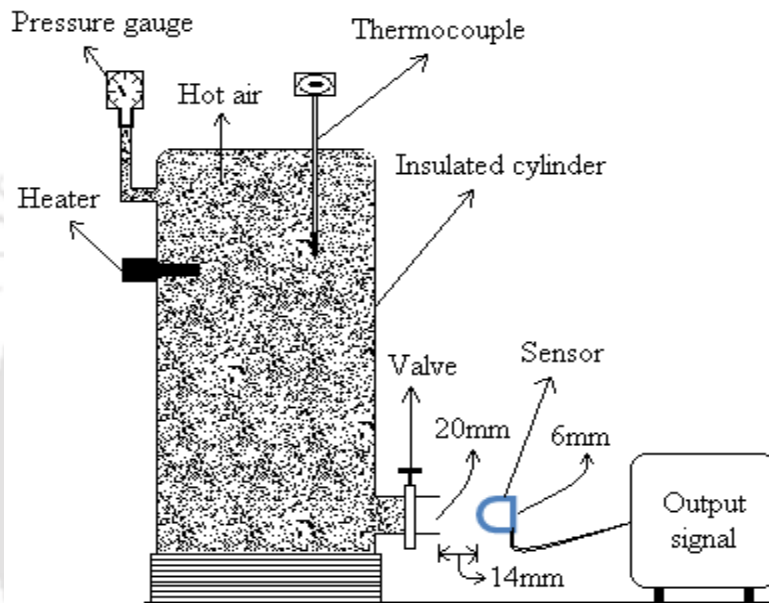
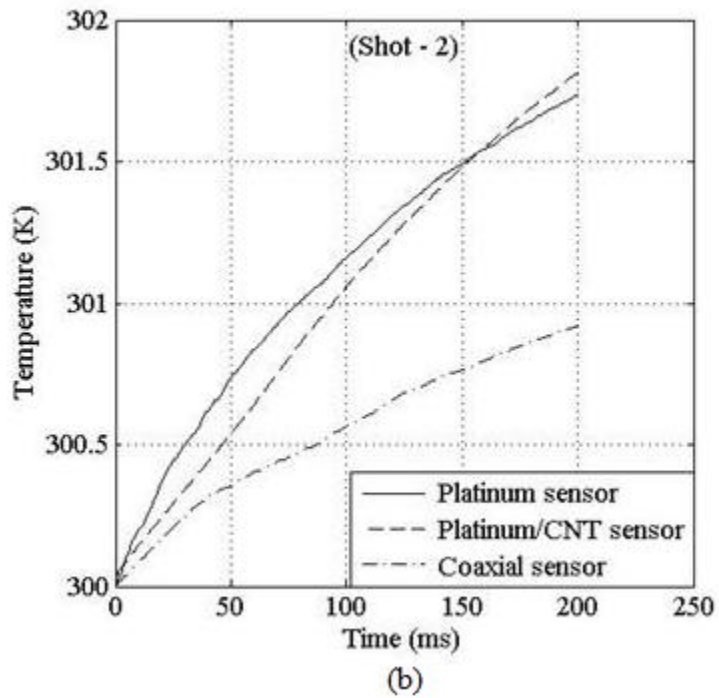
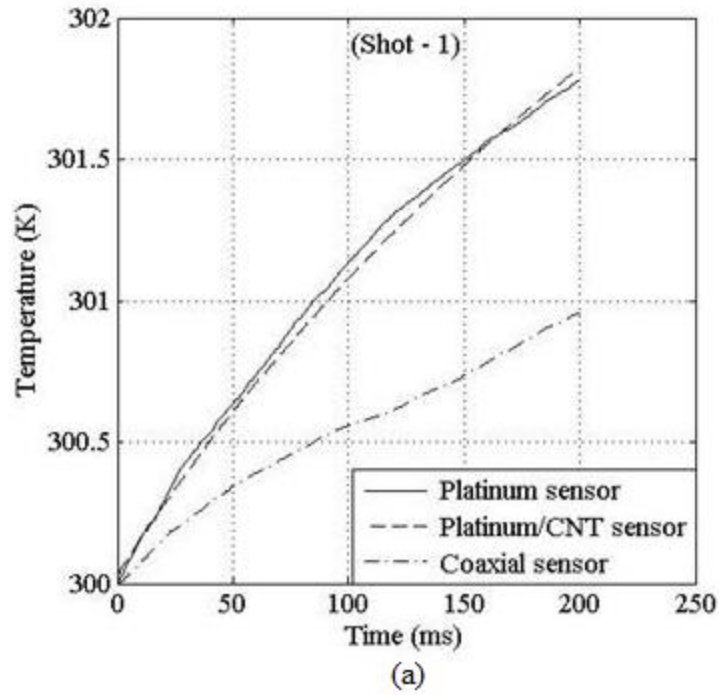


Fig. 6.12: Schematic diagram of the insulated solid cylinder with signal measuring source meter

Table. 6.1: Experimental test (flow) conditions at input

Shot – 1, Shot – 2, Shot – 3 and Shot – 4			
	Platinum based TFG	Platinum/Nanomaterial based TFG	Coaxial Thermocouple
Total Pressure (bar)	16	16	16
Total Temperature (K)	347	347	347
Mach Number	1	1	1
Time duration (ms)	10	10	10



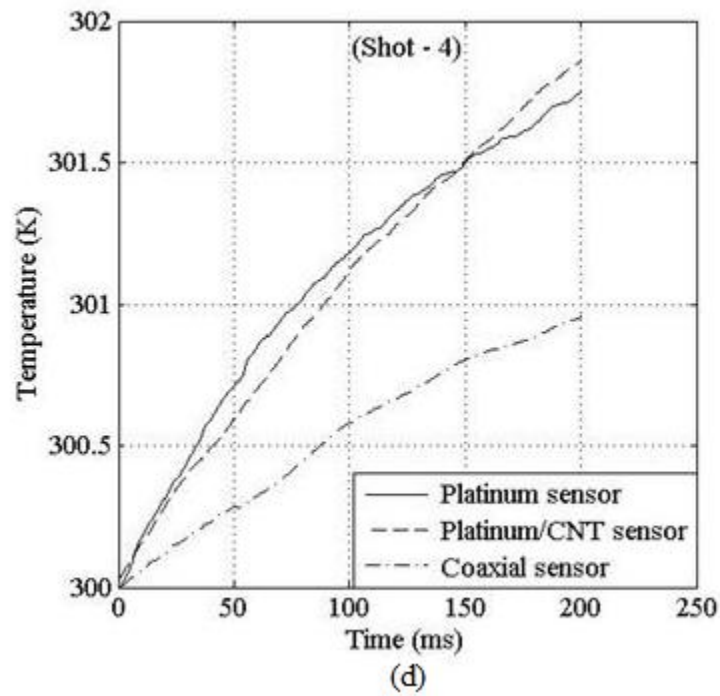
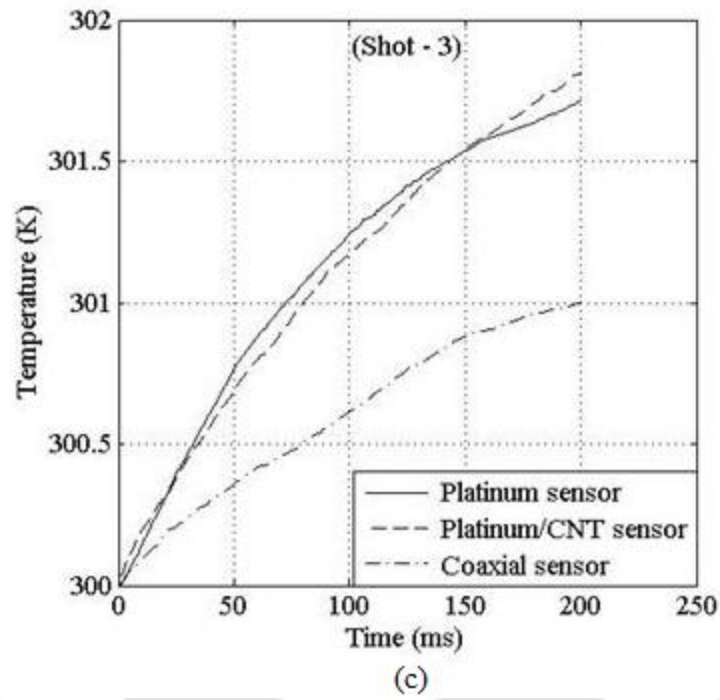
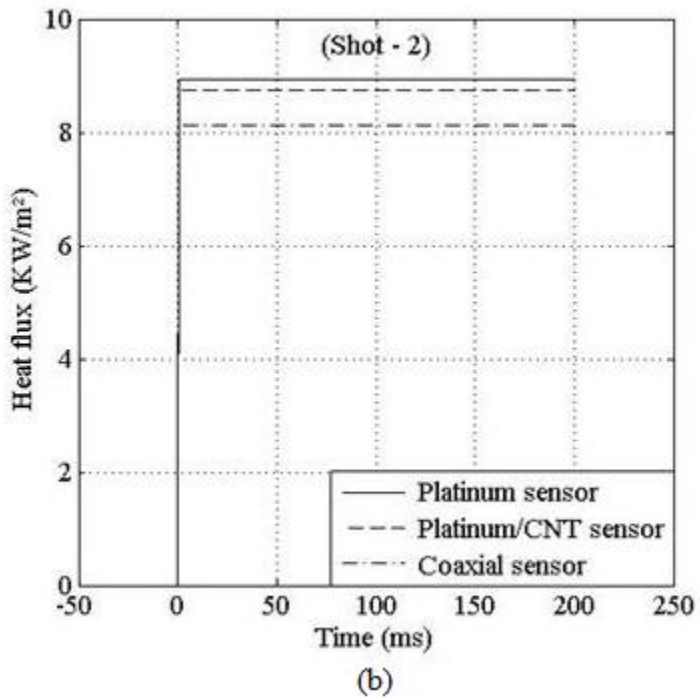
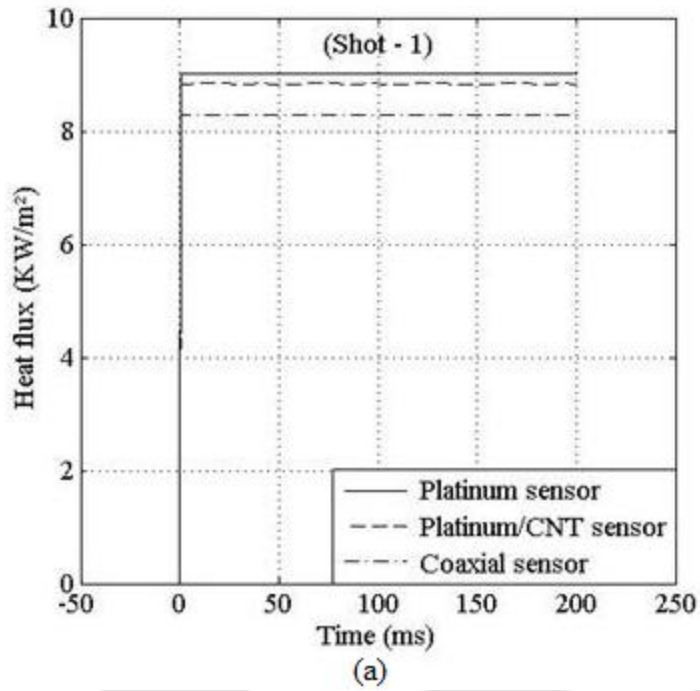


Fig. 6.13: Comparison of temperature histories for different types of heat transfer gauges



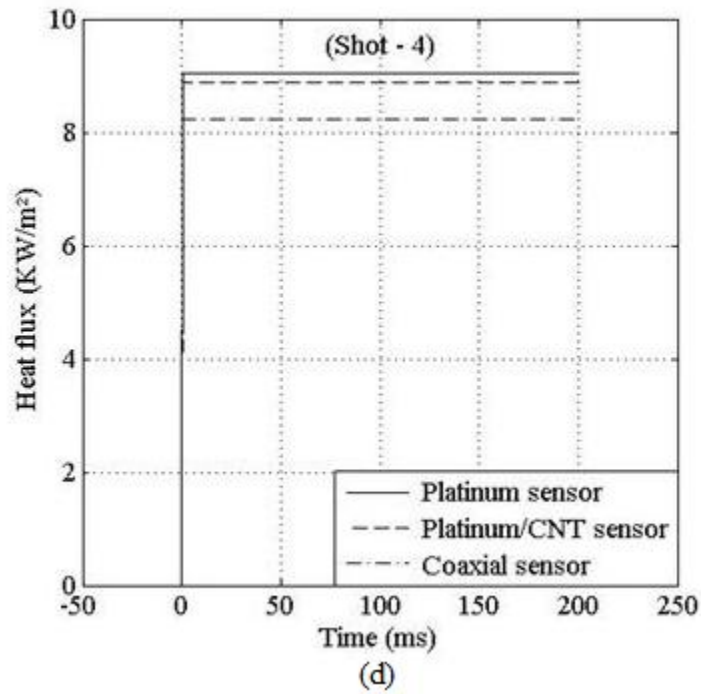
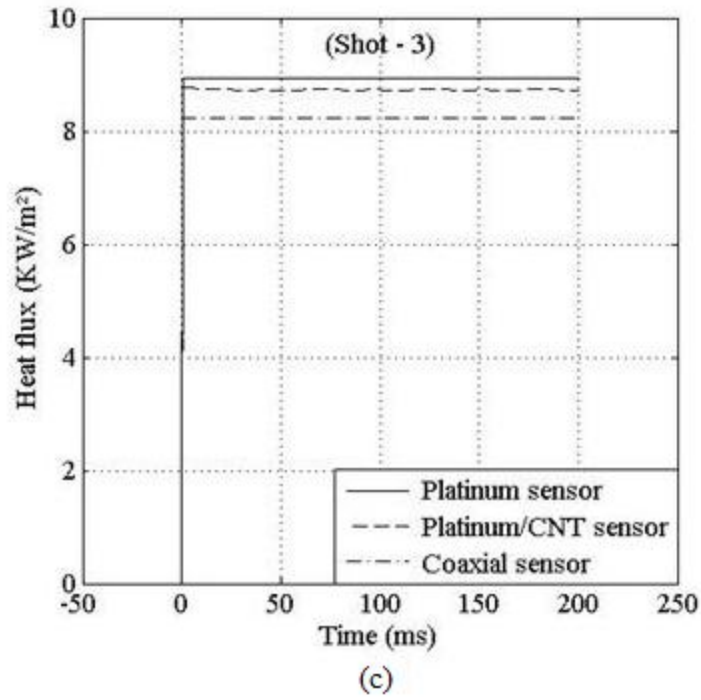


Fig. 6.14: Comparison of heat fluxes histories for different types of heat transfer gauges

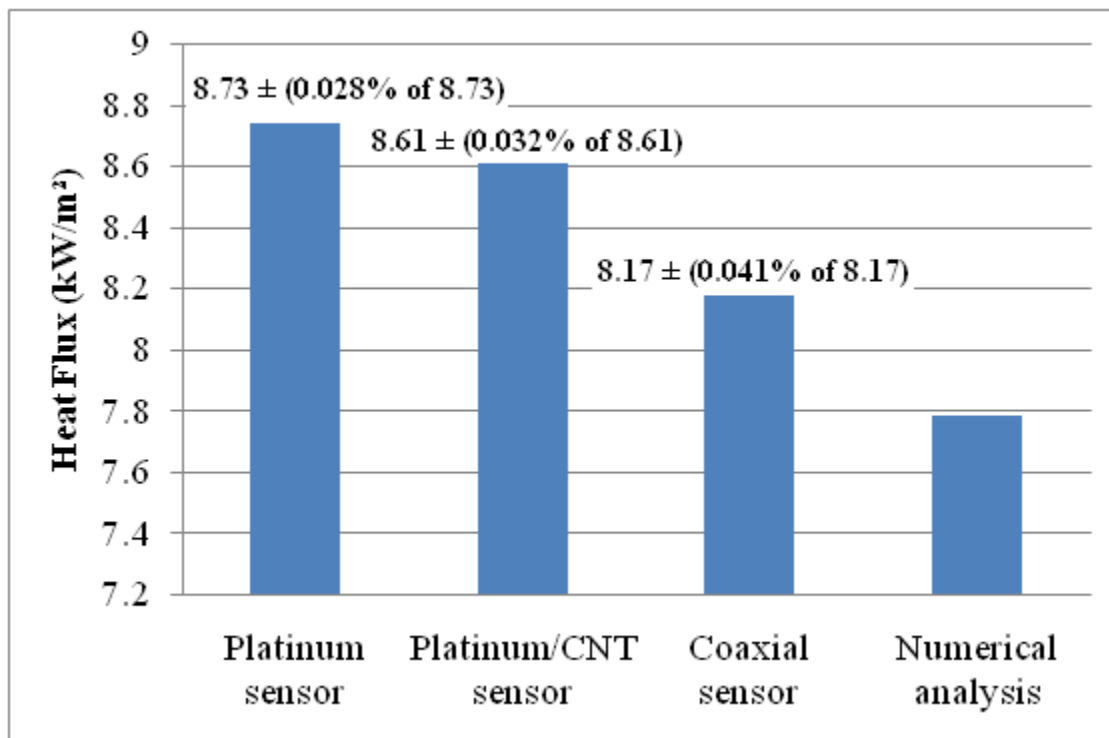
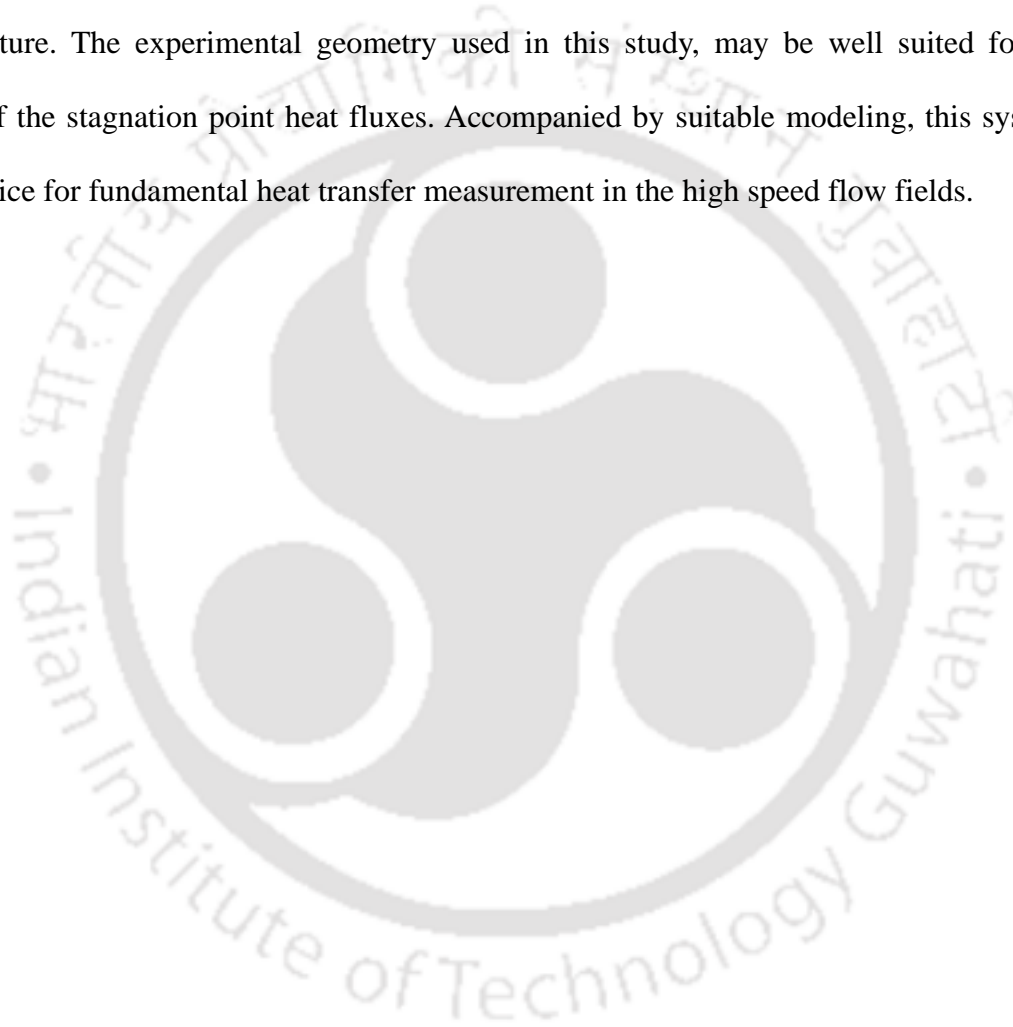


Fig. 6.15: Comparison of numerical and experimental heat fluxes measured by different types of heat transfer gauges at stagnation point

6.3 Summary

A new experimental facility of an open jet facility has been designed and successfully fabricated. It is capable of producing heated air jet at sonic velocity and expanding in atmosphere. This experimental setup is intended for stagnation point heat flux measurements of thin film gauges and coaxial thermocouples. Three types of probes are designed and fabricated and each of them has a different sensors. All these handmade sensors are calibrated for temperatures as well as for the heat flux (dynamic calibration). Then, these sensors are exposed to the heated air issuing from the open jet facility. The location of this stagnation probe is decided by exhaustive numerical analysis. All experiments are repeated four times and the statistical analysis of relative errors are calculated of each thermal sensor. This relative error is larger in the lower temperature

regime, because the temperature difference is small. The experimental results are in closed agreement with the numerical simulation. This experimental investigation demonstrates the usability of these sensors for high speed flow conditions. Moreover, the gauges respond immediately when the flow passes over the probe. At the same time, the parabolic temperature rise and step heat fluxes resemble the behaviors similar to that of a shock tunnel as reported in the literature. The experimental geometry used in this study, may be well suited for further studies of the stagnation point heat fluxes. Accompanied by suitable modeling, this system is a good choice for fundamental heat transfer measurement in the high speed flow fields.



Chapter - 7

Conclusions and Scope for Future Research

Conclusions

Thin film gauges and coaxial thermocouple sensors for short duration transient measurements have been successfully fabricated and calibrated in the laboratory. The static calibration is performed to measure TCR and sensitivity of each of the thermal sensors. Radiation and conduction based dynamic calibration is carried by exposing the thermal sensors to sudden increase in step heat load. In order to evaluate the performance of the heat transfer gauges, the experiments are performed to measure stagnation point heat flux rate. All the experimental results are validated through numerical simulation with reasonable accuracy. These heat transfer gauges find applications to capture transient temperature in the combustion chambers of internal combustion engines and gas turbine blades etc. When mounted in flush on aerodynamic surfaces, they are used to record surface temperatures of high speed air flows in short duration impulse facilities such as shock tunnels, wind tunnels etc.

The use of thin film sensors for measuring the surface heat flux has many limitations because of cost involved in making such sensors. Also, with prolonged use in high speed flow situations, the thin film can get easily worn out after a few shots, normally five or six shots. In such cases, the gauges lose the adequate resistance and need to be re-fabricated by painting the film again on the substrate surface. Besides, the thin films are passive sensors that require a constant current to energize the system. When performing the measurements at stagnation point of a body, there are experimental difficulties in mounting them exactly at the stagnation point because the sensing film has a finite surface area. Moreover, exposing the gauges repeatedly for the stagnation point may lose its resistances. With the above design and functional limitations of

the thin film sensors, it is only desirable to have an alternative i.e. coaxial thermocouple as a replacement. Since, the sensing area is a surface, the heat load any point in the surface will lead to surface temperatures. Some of the relative advantages can be highlighted as given below.

- The thermocouple wires are easily available and quite economical. They can be easily machined to form the surface junction without the need of any specialized methods like sputtering, baking etc. as case of the platinum thin film gauges.
- Coaxial thermocouples are active sensors and generate their own thermal emf. So, they do not require any external power source.
- Coaxial thermocouple sensors have rugged junction, and are generally created by sanding, abrasive paper or scalpel scratch across the thermo elements. So, they have capability to withstand harsh condition of flow situations. Any wear due to the flow creates new micro junctions on the surface. These junctions can be easily refurbished using a scalpel or sand paper to be made then ready for use again, hence giving an infinite life to each sensor.
- This type of gauge is best suited for point-measurements typically at the stagnation point on the surface.
- The only disadvantage of coaxial thermocouples is that they are an order of magnitude less sensitive than platinum thin film sensors. Accuracy becomes an important issue when they are used in the flow situations where low values of surface heat fluxes ($\sim 1 \text{ kW/m}^2$) are expected.

The overall comments from this investigation are summarized as follows:

- The handmade heat transfer gauges are rigid in construction and reusable. Moreover, they can be fabricated through simple manufacturing techniques.

- When the platinum is mixed with appropriate proportion of CNTs, the TCR and sensitivity are enhanced by two times.
- The sensitivity analysis through static calibration indicates that thin film gauges are best suited for low as well of high values of heat fluxes. However, in the flow situations where high values of surface heat fluxes ($\sim 100\text{kW/m}^2$) is expected, the adhesiveness of thin film on the substrate may reduce and they become more prone towards wear and tear. In such applications, it is advisable to use coaxial thermocouples because it is rigid in construction and sensing surface can withstand harsh flow conditions.
- The dynamic calibration tests suggest that all the heat transfer gauges can be used for short duration transient measurements for sudden increase in step heat loads.
- The stagnation point heat flux measurements ensure the capabilities of the handmade heat transfer gauges in a real experimental situations. Being small in sizes, all the sensors can be flush-mounted on the experimental surfaces.
- Due to very small response time (\sim few microseconds), it is expected that these heat transfer gauges can be implemented in the experimental facilities where the test flow durations are in the range of few milliseconds or less.
- Among all the heat transfer gauges, the coaxial thermocouple incurs least cost while platinum inks/pastes are precious materials. However, the well dispersed and very small amount of platinum supported CNTs have the ability to fabricate high sensitive thermal sensors. It may become cost effective for mass production processes.
- The handmade thin film gauges are very useful in the laboratory experiments. In case of any loss of adhesiveness of film on the substrate material, the film can be repainted on the same substrate. Many improved manufacturing techniques such as sputtering and vacuum deposition techniques are available for creating the thin film on the substrate surface.

However, these techniques need the target gauge material in solid form and become cost effective for mass production.

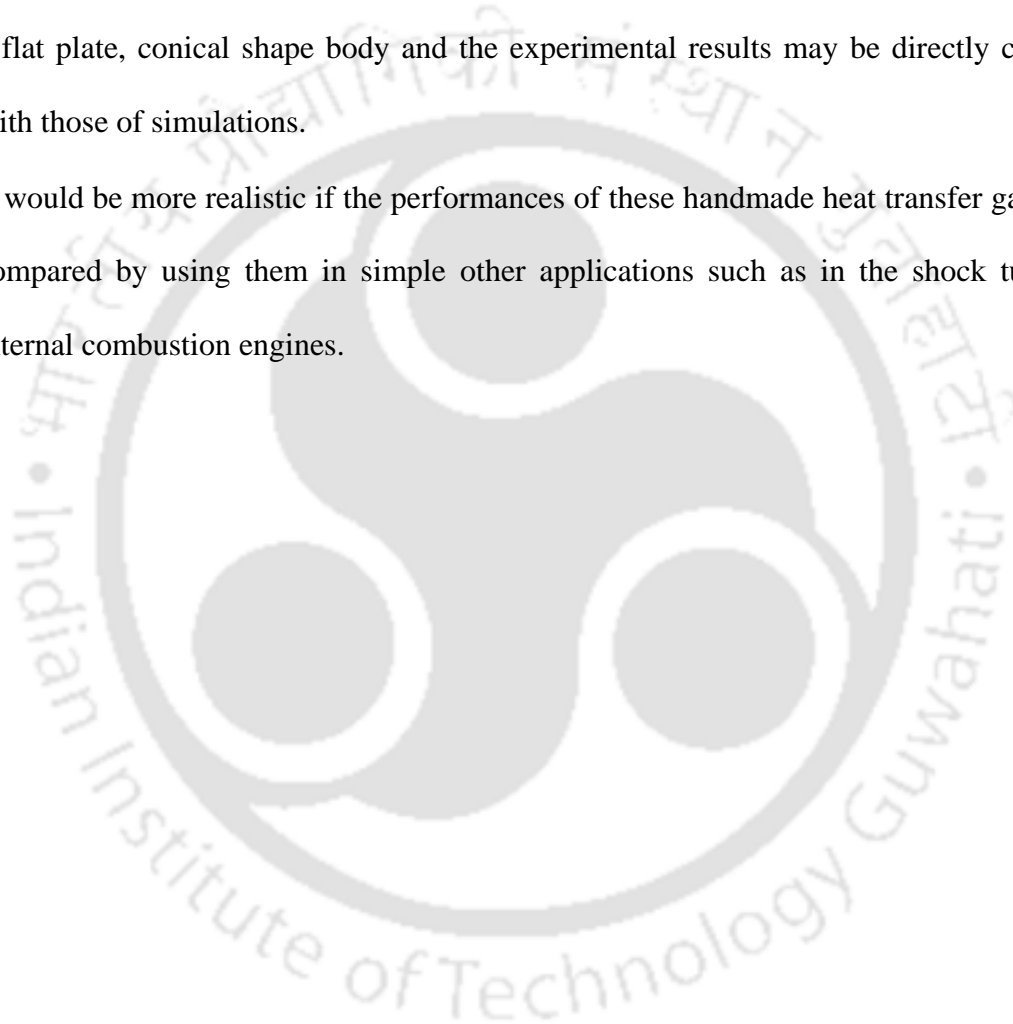
- Finally, it should be noted that extremely small thickness of co-axial thermocouple junction and thin film gauge material, has the capability of measuring heat fluxes where the available test flow durations are few milliseconds or even less. They find applications mostly in short-duration impulse facilities shock tunnels, expansion tubes etc.

Scope of Future Work

Even after the exhaustive studies on heat transfer gauges, it is felt that there are ample scopes for future research. Some of the recommendations are listed here.

- Sputtering techniques and vacuum deposition are some advanced techniques for fabricating the heat transfer gauges. The performance (such as TCR, sensitivity etc) of handmade sensors may be compared so that their usages in the laboratory scale is justified.
- The surface morphology of CNT based platinum thin film sensors needs attention because the thermal property enhancement has a definite bearing on microstructures of the sensors.
- In the similar line, the micro scratches in the surface junction thermocouple can be correlated with the response time of the coaxial thermocouple. A detailed microstructure study in this area can provide valuable information.
- The heat transfer gauges may expose to even lower enthalpy levels so that its minimum limit of performance is determined.

- The stagnation point tests should be repeated using several heat transfer gauges under several different flow velocities to confirm the reliabilities of the gauges. The ruggedness of the films should also be tested by subjecting the resistance temperature detector to flow with high Mach numbers.
- The sensor may also be used for other investigations like viscous drag determination over a flat plate, conical shape body and the experimental results may be directly compared with those of simulations.
- It would be more realistic if the performances of these handmade heat transfer gauges are compared by using them in simple other applications such as in the shock tubes and internal combustion engines.



References

- Acharya H, Sung J, Shin H, Park SY, Min BG and Park C (2009) Deposition of silver nano particles on single wall carbon nanotubes via a self assembled block copolymer micelles, *Int. J. Reactive & Functional Polymers*, 69: 552-557.
- Alexander AB, Suchismita G, Wenzhong B, Irene C, Desalegne T, Feng M and Chun NL (2008) Superior thermal conductivity of single layer graphene, *Int. J. Nano Letters*, 8: 902-907.
- Alkidas AC and Cole RM (1985) Transient heat flux measurements in a divided chamber diesel engine, *Int. J. Heat Transfer*, 107: 439-444.
- Anderson JD (1989) *Hypersonic and high temperature gas dynamics*, Tata McGraw-Hill Edition.
- Anderson JD (1990) *Modern compressible flow*, Tata McGraw-Hill Edition.
- Asai K, Kunimasu T and Iijima Y (1997) Visualization of the quiet test region in a supersonic wind tunnel using luminescent paint, 17th International Congress on Instrumentation in Aerospace Simulation Facilities, The University of Michigan, USA, September 29 - October 2, 1997.
- Babinsky H and Edwards JA (1996) Automatic liquid crystal thermography for transient heat transfer measurements in hypersonic flow, *Int. J. Experiment in Fluids*, 21: 227-236.
- Baker KI and Diller TE (1993) Unsteady surface heat flux and temperature measurements, *ASME 93-HT-33*: 1-9.
- Bakken GS, Gates DM, Strunk TH and Kleiber M (1974) Linearized heat transfer relations in biology, *Int. J. Science*, 183: 976-978.
- Beck JV (1967) Surface heat flux determination using an integral method, *Int. J. Nuclear Engineering and Design*, 7: 170-178.
- Bechwith TG (1995) *Thermo resistive element, Mechanical Measurements*, Addison Wesley, Reading, 668-673.
- Belinda IRC, Enid JCJ, Marisabel LC and Michael AM (2010) Single wall carbon nano tube chemical attachment at platinum electrodes, *Int. J. Applied Surface Science*, 257: 340-353.

- Benedict RP (1984) Resistance Thermometry, Fundamentals of Temperature, Pressure and Flow Measurements, John Wiley & Sons, New York, 53-64.
- Bendersky D (1953) A special thermocouple for measuring transient temperatures, Int. J. Mechanical Engineering, 75: 117-121.
- Bertill S (1992) Thermal diffusivity and thermal conductivity of chromel, alumel and constantan in the range 100-450K, Int. J. Applied Physics, 72: 539-544.
- Billiard N, Iliopoulou V, Ferrara F and Denos R (2002) Data reduction and thermal product determination for single and multi-layered substrates thin film gauges, The 16th Symposium on Measuring Techniques in Transonic and Supersonic Flow in Cascades and Turbo Machines, September 2002, Cambridge, UK.
- Boor D (1978) A practical guide to splines, Springer, New York.
- Broheza S, Delvosallea C and Marlair G (2004) A two thermocouples probe for radiation corrections of measured temperatures in compartment fires, Int. J. Heat Mass Transfer, 39: 399-411.
- Buttsworth DR (2001) Assessment of effective thermal product of surface junction thermocouples on millisecond and microsecond time scales, Int. J. Experimental Thermal and Fluid Science, 25: 409-429.
- Caldwell FR (1962) Thermocouple materials, Applied Methods and Instrument; Temperature: Its Measurement and Control in Science and Industry, C.W. Herzfeld Edition, Reinhold, New York, 3: 81-134.
- Carslaw HS and Jaeger JC (1959) Conduction of heat in solids, Clarendon press, Oxford.
- Charles E, Lorival R, Boyer A and Malbrunot P (1984) A fast response high temperature high pressure surface thermocouple, Int. J. Heat Mass Transfer, 6: 135-142.
- Chen H, Lin S and Fang L (2001) Estimation of surface temperature in two dimensional inverse heat conduction problems, Int. J. Heat Mass Transfer, 44: 1455-1463.

- Chen JC and Hsu KK (1995) Heat transfer during liquid contact on superheated surfaces, *Int. J. Heat Transfer*, 117: 693-697.
- Chana KS and Wilson TS (2001) High bandwidth heat transfer measurements in an internal combustion engine under low load motored conditions, *Int. J. Heat Transfer and Cooling in Propulsion and Power System*, RTO-MP-069(I).
- Chu X, Duan D, Shen G and Yu R (2007) Amperometric glucose biosensor based on electro deposition of platinum nanoparticles on to covalently immobilized carbon nanotube electrode, *Int. J. Talanta*, 71: 2040-2047.
- Chung M and Brill JW (1993) Specific heats of E-type thermocouple wires, *AIP Review of Scientific Instruments*, 64: 2037-2038.
- Cook WJ and Felderman EJ (1966) Reduction of data from thin film heat transfer gauge: A concise numerical technique, *AIAA Journal*, 4: 561-562.
- David RB (2001) Assessment of effective thermal product of surface junction thermocouples on milliseconds and microsecond time scales, *Int. J. Experimental Thermal and Fluid Science*, 25: 409-420.
- Davis JP (1999) High enthalpy shock/boundary layer interaction on a double wedge, PhD Thesis, California Institute of Technology, Source DAI-B 60/01.
- Diller TE and Kidd CT (1996) Evaluation of numerical methods for determining heat fluxes with a null-point calorimeter, *Proceedings of the 42nd International Instrumentation Symposium*, ISA, Research triangle park, N. C, May 1996, 251-262.
- Doorly DJ and Oldfield MLG (1985) Simulation of the effects of shock wave passing on a turbine rotor blade, *ASME J. Eng. Gas Turbines Power*, 107(4): 998-1006.
- Doorly JE and Oldfield MLG (1987) The theory of advanced heat transfer gauges, *Int. J. Heat Mass Transfer*, 30: 1159-1168.

- Duc DL, Chi KK, Tae SJ, Yongju J, Gi HS, Jaebum C and Yong SK (2010) Platinum nano particle supported multiwall carbon nanotube electrodes for amperometric hydrogen detection, *Int. J. Sensors and Actuators B: Chemical*, doi:10.1016/j.snb.2010.11.045.
- Dunn MG, George WK, Rae WJ, Woodward SH, Moiler JC and Seymour PJ (1986) Heat flux measurements for the rotor of a full stage turbine, *ASME 31st Int. Gas Turbine Conference*, Dusseldorf, West Germany, 8-12 June, 1986.
- Dunn MG and Holt JL (1982) Turbine stage heat flux measurements, *AIAA /ASME 18th Joint Propulsion Conference*, Cleveland, Ohio, June 21-23, 16: 1282-1289.
- Duong DL, Chi KK, Tae SJ, Yongju J, Gi HS, Jaebum C and Yong SK (2010) Platinum nano particle supported multiwall carbon nanotube electrodes for amperometric hydrogen detection, *Int. J. Heat Mass Transfer*, 6: 67-75.
- Fay JA and Riddell FA (1958) Theory of stagnation point heat transfer in dissociated air, *Int. J. Aeronautical Sciences*, 25: 73-85.
- Ferry S (2003) Transient heat transfer measurements in a short duration hypersonic facility on a blunted cone using QIRT, Master's Thesis, TU Delft, 1-57.
- Figliola RS and Beasley DE (1995) Electrical resistance thermometry, *Theory and Design for Mechanical Measurements*, John Wiley & Sons, New York, 328-336.
- Gatowski JA, Smith MK and Alkidas AC (1989) An experimental investigation of surface thermometry and heat flux, *Int. J. Experimental Thermal and Fluid Science*, 2: 280-285.
- Gai SL and Joe WS (1992) Laminar heat transfer to blunt cones in high enthalpy flows, *Int. J. Thermo Physics, Heat Transfer*, 6: 433-438.
- Geim AK and Novoselov KS (2007) The rise of graphene, *Int. J. Nature Materials*, 6: 183-191.
- George WK, Rae WJ and Woodward SH (1991) An evaluation of analog and numerical techniques for unsteady heat transfer measurement with thin film gauges in transient facilities, *Int. J. Experimental Thermal and Fluid Science*, 4(3): 333-342.

- Hager JM, Terrell JP, Silverston E and Diller TE (1994) In situ calibration of a heat flux microsensor using surface temperature measurements, ISA 94-1034.
- Haldeman CW, Dunn MG, Barter JW, Green BR and Bergholz RF (2005) Aerodynamic and heat flux measurements with predications on a modern one and one half state high pressure transonic turbine, ASME J. Turbo Machinery, 127: 522-531.
- Hamilton RL and Crosser OK (1962) Thermal conductivity of heterogeneous two component systems, Ind. Eng. Chem. Fundamental, 1: 182-191.
- Hankley WL (1989) Re-entry aerodynamics, AIAA Education Series, 1- 22.
- Hiroki N, Shunsuk O, Keisuke A and Kazuyuki N (2006) Effect of temperature sensitive paint layer on global heat transfer measurement in hypersonic flow, Int. J. Visualization Society of Japan 26 (1): 201-204.
- Holmberg DG and Diller TE (1995) High frequency heat flux sensor calibration and modeling, ASME J. Fluids Engineering, 117: 659-664.
- Hubner JP, Carroll BF and Schanze KS (2002) Heat transfer measurements in hypersonic flow using luminescent coating techniques, Int. J. Thermo Physics and Heat Transfer, 16(4): 516-522.
- Huang B, Li Z, Liu Z, Zhou G, Hao S, Wu J, Gu B and Duan WH (2008) Adsorption of gas molecules on graphene nanoribbons and its implication for nanoscale molecular sensor, Int. J. Physical Chemistry, 112: 13442-13446.
- Hwang Y, Lee JK, Lee CH, Jung YM, Cheong SI, Lee CG, Kua BC and Jang SP (2006) Stability and thermal conductivity characteristics of nanofluids, Int. J. Heat Mass Transfer, 17: 70-74.
- Iijima S (1991) Helical microtubules of graphitic carbon, NEC Corporation, Fundamental Research Laboratories, 34 Miyukigaoka, Tsukuba, Ibaraki 305, Japan, 354: 56-58.

- Ijaz UZ, Khambampati AK, Kim MC, Kim S and Kim KY (2007) Estimation of time dependent heat flux and measurement bias in two dimensional inverse heat conduction problems, *Int. J. Heat Mass Transfer*, 50: 4117-4130.
- Jessen C and Snig GH (1991) A new method for manufacture of thin film heat flux gauges, *Int. J. Shock Waves*, 1: 161-164.
- Jessen C, Vetter M and Gronig H (1993) Experimental studies in the Aachen hypersonic shock tunnel, *Z. Flugwiss Weltraumforsch*, 17: 73-81.
- Johnson LP and Diller TE (1995) Measurements with a heat flux micro sensor deposited on a transonic turbine blade, *IEEE 95CH3482-7*.
- Kawale B and Sahoo N (2008) Heat transfer data analysis from thin film heat transfer gauge, *IE (I) Journal-AS*, 91: 14-18.
- Kern DQ (1997) *Process heat transfer*, Tata McGraw-Hill Edition.
- Kidd CT (1990) Recent developments in high heat flux measurement technique at the AEDC, *Proceedings of the 36th International Instrumentation Symposium*, Instrument Society of America, USA, 6-10 May, 1990, pp. 477-492.
- Kidd CT (1992) High heat flux measurements and experimental calibrations/characterizations, CP-3161, NASA, Washington, DC: 31-50.
- Korakianitis T, Papagiannidis P and Vlachopoulos NE (2002) Unsteady flow/quails steady heat transfer computations on a turbine rotor and comparison with experiments, *ASME J. Turbomachinery*, 124: 152-159.
- Kou R, Shao Y, Wang D, Engelhard MH, Kwak JH, Wang J, Viswanathan V, Wang C, Lin Y, Wang Y, Aksay IA and Liu J (2009) Enhanced activity and stability of platinum catalysts on functionalized graphene sheets for electrocatalytic oxygen reduction, *Int. J. Electrochemistry Communications*, 11: 954-957.
- Kovacs A and Mesler R (1964) Making and testing small surface thermocouples for fast response, *AIP Review of Scientific Instruments*, 35: 485-488.

- Lawton B and Klingenberg G (1996) *Transient temperature in engineering and science*, Oxford University Press, Oxford.
- Lee LYW, Chen JC and Nelson RA (1985) Liquid solid contact measurements using a surface thermocouple temperature problem in atmosphere pool boiling water, *Int. J. Heat Mass Transfer*, 28: 1415-1423.
- Lee Y, Settles GS and Horstman CC (1994) Heat transfer measurements and computations of swept shock wave/boundary layer interactions, *AIAA Journal*, 32 (4): 726-734.
- Lee S and Choi SUS (1996) Application of metallic nanoparticle suspension in advanced cooling systems, *ASME J. Recent Advances in Solid Structures and Applications of Metallic Materials*, 72: 227-234.
- Lee L, Chen JC and Nelson RA (1982) Surface probe for measurement of liquid contact in film transition boiling on high temperature surfaces, *AIP Review of Scientific Instrument*, 53: 1472-1476.
- Lei FJ, Herbert A and Will B (1998) Thin film thermocouples and strain gauge technologies for engine applications, *Int. J. Sensors and Actuators A*, 65: 187-193.
- Leenaerts O, Partoens B and Peeters FM (2008) Adsorption of H₂O, NH₃, CO, NO₂ and NO on Graphene: A First Principles Study, *Physics Review B*, 77: 125416-125421.
- Li D and Kaner RB (2008) Graphene based materials, *Int. J. Material Science*, 320: 1170-1171.
- Liu MS, Lin MC, Huang IT and Wang C (2005) Enhancement of thermal conductivity with carbon nanotube for nanofluids, *Int. J. Heat Mass Transfer*, 32: 1202-1210.
- Luca LD, Guglieri G, Cardone G and Carlomagno GM (1995) Experimental analysis of surface flow on a delta wing by infrared thermography, *AIAA Journal*, 33: 1510-1512.
- Malongoa TK, Patris SP, Macours P, Cottona FR, Nsangub J and Kauffmanna JM (2008) Highly sensitive determination of iodide by ion chromatography with amperometric detection at a silver based carbon paste electrode, *Int. J. Talanta*, 76: 540-547.

- Marr AM, Wallace JS, Chandra S, Pershin L and Mostaghimi J (2010) A fast response thermocouple for internal combustion engine surface temperature measurements. *Int. J. Heat Mass Transfer*, 34: 183-189.
- Martinez BR, Lock GD and Jones TV (1995) Heat transfer measurements in an annular cascade of transonic gas turbine blades using the transient liquid crystal technique, *Int. J. Turbo Machinery*, 117: 425-431.
- Masanori M, Hirofumi A, Wei L, Yuhichi M and Jaffar AH (2003) An analytical solution for two dimensional inverse heat conduction problems using Laplace transform, *Int. J. Heat Mass Transfer*, 46: 2135-2148.
- Menezes V and Bhat S (2010) A coaxial thermocouple for shock tunnel applications, *AIP Review of Scientific Instruments*, 81: 104905-104909.
- Merski NR (1998) Reduction and analysis of phosphor thermography data with the one dimensional heat software package, *AIAA Paper*, pp. 98-712.
- Metha RC, Jayachandran T and Sastri VMK (1988) Finite element analysis of conductive and radiative of a thin skin calorimeter, *Int. J. Heat Mass Transfer*, 22: 227-230.
- Micol JR (1995) Aero-thermodynamic measurement and prediction for a modified orbiter at Mach 6 and 10 in air, *Int. J. Spacecraft and Rockets*, 32 (5): 737-748.
- Michael AM, James SW, Sanjeev C, Larry P and Jayad M (2010) A fast response thermocouple for internal combustion engine surface temperature measurements, *Int. J. Experimental Thermal and Fluid Science*, 34: 183-189.
- Miller CG (1981) Comparison of thin film resistance heat transfer gauges with thin skin transient calorimeter gages in conventional hypersonic wind tunnels, *NASA Technical Memorandum*, 83197, December 1981.
- Modarress D and Azzazy M (1988) Modern experimental techniques for high speed flow measurements, *Int. J. Aircraft*, 26: 889-899.

- Moffat RJ (1985) Using uncertainty analysis in planning of an experiment, ASME J. Fluids Engineering, 107: 173-178.
- Mohammed H, Salleh H and Yusoff MZ (2007) The transient response for different types of erodible surface thermocouples using finite element analysis, Int. J. Thermal Science, 11: 49-64.
- Mohammed H, Salleh H and Yusoff MZ (2008) Design and fabrication of coaxial surface junction thermocouples for transient heat transfer measurements, Int. J. Heat Mass Transfer, 35: 853-859.
- Mohammed HA, Salleh H and Yusoff MZ (2010-a) Determination of the effusivity of different scratched coaxial temperature sensors under hypersonic flow, Int. J. Thermo Physics, 31: 2305-2322.
- Mohammed HA, Salleh H and Yusoff MZ (2010-b) Fast response surface temperature sensor for hypersonic vehicles, Int. J. Instruments and Experimental Techniques, 53: 153-159.
- Mohammed HA, Salleh H, Yusoff MZ (2011-a) Dynamic calibration and performance of reliable and fast response temperature probes in a shock tube facility, Int. J. Experimental Heat Transfer, 24: 109-132.
- Mohammed HA, Salleh H and Yusoff MZ (2011-b) Thermal product estimation method for aerodynamics experiments, Int. J. Engineering Physics and Thermo Physics, 84: 785-794.
- Mohammed HA, Salleh H and Yusoff MZ (2011-c) The effect of scratch technique on thermal product of temperature sensors, Int. J. Thermo Physics and Aeromechanics, 18: 51-64.
- Mosharov V, Orlov A and Radchenko V (2003) Temperature sensitive paint for heat transfer measurement in short duration wind tunnels, 20th International Congress on Instrumentation in Aerospace Simulation Facilities (ICIASF), 25-29 August 2003, 8: 351-356.
- Muthamilselvan M, Kandaswam YP and Lee J (2010) Heat transfer enhancement of copper water nanofluids in a lid-driven enclosure, Int. J. Communication Nonlinear Science Number Simulation, 15: 1501-1510.

- Mudford NR and Gai SL (1992) Stagnation point heat flux in hypersonic high enthalpy flow, *Int. J. Shock Waves*, 2: 43-47.
- Nagai H, Oumi S, Asai K and Nakaita K (2006) Effect of temperature sensitive paint layer on global heat transfer measurement in hypersonic flow, *Int. J. Visualization Society of Japan*, 26: 201-204.
- Nag PK (2002) *Heat Transfer*, Tata-McGraw Hill Edition.
- Oldfield MLG, Burd HJ and Doe NG (1980) Design of wide bandwidth analogue circuits for heat transfer instrumentation in transient tunnels in heat and mass transfer in rotating machinery, Eds. Hemisphere, New York, 15: 233-258.
- Olivier H and Gronig H (1995) Instrumentation techniques of the Aachen shock tunnel TH2, International Congress on Instrumentation in Aerospace Simulation Facilities, ICIASF95, July 18-21, 1995, Wright Patterson AFB, USA, CH3482-3489.
- Patel HE, Anoop KB, Sundararanjan T and Das K (2008) Model for thermal conductivity of CNT Nanofluids, *Indian Academy of Science*, 31: 387-390.
- Park J, Taton TA and Mirkin CA (2002) Array based electrical detection of DNA with nanoparticle probes, *Science Report*, February 22, 2002, DOI: 10.1126/science.1067003.295, 1503-1506.
- Peres NMR, Guinea F and Castro AH (2009) The electronic properties of graphene, *Int. J. Review Modeling Physics*, 81: 109-162.
- Piccini E (1999) The development of a new heat transfer gauge for heat transfer facilities, M. Sc Thesis, Department of Engineering Science, University of Oxford, Oxford, U.K.
- Piccini E, Guo SM and Jones TV (2000) The development of a new direct heat flux gauge for heat transfer facilities, *Int. J. Measurement Science Technology*, 11: 342-349.
- Pumera M, Merkok A and Alegret IS (2006) Carbon nano tube epoxy composites for electrochemical sensing, *Int. J. Sensors and Actuators B: Chemical*, 113: 617-622.

- Qu F, Yang M, Shen G and Yu R (2007) Electrochemical bio-sensing utilizing synergic action of carbon nanotubes and platinum nano wires prepared by template synthesis, *Int. J. Biosensors and Bioelectronics*, 22: 1749-1755.
- Rumsey CB and Lee DB (1959) Heat transfer measurements on a blunt spherical segment nose to a Mach number of 15.1 and flight performance of a rocket propelled model to a Mach number of 17.8, NASA, TM-X-77.
- Rainieri S, Bozzoli F and Pagliarini G (2008) Characterization of an un-cooled infrared thermo graphic system suitable for the solution of the two dimensional inverse heat conduction problem, *Int. J. Heat Mass Transfer*, 32: 1492-1498.
- Reddy KPJ, Saravanan S, Jagadeesh G (2009) Convective heat transfer rate distributions over a missile shaped body flying at hypersonic speeds, *Int. J. Experimental Thermal and Fluid Science*, 33: 782-790.
- Rocheftort A, Yang DQ and Sacher E (2009) Stabilization of platinum nano particles on graphene by non invasive functional ligation, *Int. J. Carbon*, 47: 2233-2238.
- Rose PH (1958) Development of the calorimeter heat transfer gauge for use in shock tubes, *AIP Review of Scientific Instrument*, 29 (7): 557-564.
- Rubianes MD and Rivas GA (2005) Enzymatic biosensors based on carbon nano tubes paste electrodes, *Int. J. Electro Analysis*, 17: 73-78.
- Sadik K and Anchasa P (2009) Review of convective heat transfer enhancement with nanofluids, *Int. J. Heat Mass Transfer*, 52: 3187-3196.
- Sahoo N (2003) Simultaneous measurement of aerodynamic forces and convective surface heating rates for large angle blunt cones in hypersonic shock tunnel, Ph.D. Thesis, Department of Aerospace Engineering, Indian Institute of Science, Bangalore, India.
- Sahoo N and Peetala RK (2010) Transient temperature data analysis for a supersonic flight test, *ASME J. Heat Transfer*, 132: 84503-84507.

- Sahoo N and Peetala RK (2011) Transient surface heating rates from a nickel film sensor using inverse analysis, *Int. J. Heat Mass Transfer*, 54 (5): 1297-1302.
- Saitoh H, Ishikawa M and Urao R (1995) Substrate temperature measured by a film on plate thermocouple during diamond growth using the combustion flame technique. *Int. J. Diamond and Related Materials*, 4: 1056-1060.
- Sahney R, Anand S, Puri BK and Srivastava AK (2006) A comparative study of immobilization techniques for urea on glass pH electrode and its application in urea detection in blood serum, *Int. J. Analytical Chemical Actuator*, 578: 156-161.
- Sanderson SR and Sturtevant B (2002) Transient heat flux measurement using a surface junction thermocouple, *AIP Review of Scientific Instruments*, 73 (7): 2781-2787.
- Saravanan S, Jagadeesh G and Reddy KPJ (2009) Convective heat transfer rate distributions over a missile shaped body flying at hypersonic speeds, *Int. J. Experimental Thermal and Fluid Science*, 33: 782-790.
- Schniepp HC, Li JL, McAllister MJ, Sai H, Alonso MH, Adamson DH, Home RK, Car R, Saville DA and Aksay IA (2006) Functionalized single graphene sheets derived from splitting graphite oxide, *Int. J. Physics, Chem. B*, 110: 8535.
- Schultz DL and Jones TV (1973) Heat transfer measurements in short duration hypersonic facilities, AGARD-AG-165.
- Schooley JF (1986) Resistance thermometers, *Thermometry*, CRC Press, Boca Raton.
- Sedra AS and Smith KC (1998) *Microelectronic circuits*, Fourth Edition, Oxford University.
- Shan C, Yang H, Song J, Han D, Ivaska A and Niu L (2009) Water soluble graphene covalently functionalized by biocompatible polylysine, *Int. J. Langmuir*, 20: 12030-12033.
- Simmons JM (1995) Measurement techniques in high enthalpy hypersonic facilities, *Int. J. Experimental Thermal and Fluid Science*, 10: 454-469.
- Skinner GT (1962) A new method of calibrating thin film gauge backing materials, Cornell Aeronautical Laboratory, Buffalo, New York, CAL-105.

- Smith DE, Bubb JV, Popp O, Diller TE and Hevey SJ (1999) A comparison of radiation versus convection calibration of thin film heat flux gauges, Proceedings of the ASME Heat Transfer Division, HTD, 364: 79-84.
- Stampfer C, Schurtenberger E, Molitor F, Guttinger J, Ihn T and Ensslin K (2008) Tunable graphene signal electron transistor, Solid State Physics Laboratory, ETH Zurich, Zurich, Switzerland, Research Report, 8: 2378-2383.
- Sundqvist B (1992) Thermal diffusivity and thermal conductivity of chromel, alumel and constantan in the range 100-450K, Int. J. Applied Physics, 72: 539-544.
- Taler J (1996-a) A semi numerical method for solving inverse heat conduction problems, Int. J. Heat Mass Transfer, 31: 105-111.
- Taler J (1996-b) Theory of transient experimental technique for surface heat transfer, Int. J. Heat Mass Transfer, 39: 3733-3748.
- Talib AR, Ireland PT, Neely AJ and Mullender AJ (2005) Computational study on conduction heat transfer through a thin film gauge, Int. J. Engineering and Technology, 2: 1-7.
- Tang H, Chen J, Yao S, Nie L, Deng G and Kuang Y (2004) Amperometric glucose biosensor based on adsorption of glucose oxidase at platinum nano particle modified carbon nanotube electrode, Int. J. Biochemical, 331: 89-97.
- Touloukian YS (1970) Specific heat metallic elements and alloys, In: Y.S. Touloukian, Edition Thermo physical Properties of Matter, Temperature Sensor RC Data series, IFI/Plenum press, New York, vol. 4.
- Touloukian YS (1970) Thermal conductivity metallic elements and alloys, Thermo Physical Properties of Matter, Temperature Sensor RC Data Series, Plenum Press, New York, vol. 1.
- Trimmer LL and Clark EL (1969) Stagnation point velocity gradients for spherical segments in hypersonic flow, AIAA Journal, 7: 2040-2041.

- Tsai YC, Li SC and Chen JM (2005) Cast thin film biosensor design based on a nafion backbone a multi walled carbon nano tube conduit and a glucose oxidase function, *Int. J. Langmuir* 21: 3653-3658.
- Tsai YC, Hsua PC, Lin YW and Wub TM (2009) Silver nano particles in multi walled carbon nanotube nafion for surface enhanced Raman scattering chemical sensor, *Int. J. of sensors and actuators B: chemical*, 138: 5-8.
- Tsung TT, Loa CH and Chenb LC (2005) Shape controlled synthesis of Cu based nanofluid using submerged arc nanoparticle synthesis system, *Int. J. Crystal Growth*, 277: 636-642.
- Vidal RJ (1956) Model instrumentation techniques for heat transfer and force measurement in a hypersonic shock tunnel, Cornell Aeronautical Laboratory, Report WADC TN 56-315.
- Wang X, Xu SU and Choi J (1999) Thermal conductivity of nanoparticle fluid mixture, *Int. J. Heat Mass Transfer*, 13: 474-482.
- Wannenwetsch GD (1985) Measurements of wing leading edge heating rates on wind tunnel models using the thin film technique, *AIAA Journal*, 8: 983-972.
- Westervelt RM (2008) Graphene nanoelectronics, *Int. J. Applied Physics, Science*, 320: 324-325.
- Widhopf GF (1971) Turbulent heat transfer measurements on a blunt cone at angle of attack, *AIAA Journal*, 9(8): 1574-1580.
- Wilbur LH (1989) Re-entry aerodynamics, *AIAA Education Series*, pp. 1-144.
- Wilson TS and Chana KS (2001) High bandwidth heat transfer measurements in an internal combustion engine under low load and motored conditions, *Symposium on Advanced Flow Management*, Loen, Norway, 7-11 May 2001.
- Wildgoose GG, Leventis HC, Streeter I, Lawrence NS, Wilkins SJ, Jiang L, Jones TGJ and Compton RG (2004) Abrasively immobilised multi walled carbon nanotube agglomerates: a novel electrode material approach for the analytical sensing of pH, *Chem. Phys. Chem.* 5: 669-677.

- Woodfield PL, Monde M and Mitsutake Y (2006) Implementation of an analytical two dimensional inverse heat conduction technique to practical problems, *Int. J. Heat Mass Transfer*, 49: 187-197.
- Xie H and Chen H (2009) Adjustable thermal conductivity in carbon nanotube nanofluids, *Physics Letters A*, 373: 1861-1864.
- Xie H, Yu W, Chen L and Li Y (2010) Investigation on the thermal transport properties of ethylene glycol based nanofluids containing copper nanoparticles, *Int. J. Power Technology*, 197(3): 218-221.
- Xin Y, Liua JG, Zhoua Y, Liua W, Gaob J, Xieb Y, Yinb Y and Zoua Z (2011) Preparation and characterization of platinum supported on graphene with enhanced electro catalytic activity in fuel cell, *Int. J. Power Sources*, 196: 1012-1018.
- Xuan Y and Li Q (2000) Heat transfer enhancement of nanofluids, *Int. J. Heat and Fluid flow Transfer*, 21: 58-64.
- Yang CY (2009) Direct and inverse solutions of the two dimensional hyperbolic heat conduction problems, *Int. J. Heat Mass Transfer*, 33: 2907-2918.
- Yang P, Wei W and Tao C (2007) Determination of trace thiocyanate with nano silver coated multi walled carbon nanotubes modified glassy carbon electrode, *Analytical Chemical Acts*, 585: 331-336.
- Yang H and Zhu Y (2005) A high performance glucose biosensor enhanced via nanosized SiO₂, *Anal. Chem. Acta*, 554: 92-97.
- Zhang J and Delichatsios K (2009) Determination of the convective heat transfer coefficient in three dimensional inverse heat conduction problems, *Int. J. Heat Mass Transfer*, 44: 681-690.

Appendix

Appendix - I

Materials and Instruments used for this Work

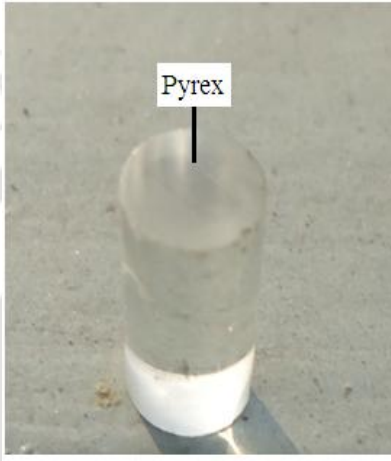


Fig. A1: Pyrex substrate material



(a)



(b)

Fig. A2: Thin film Gauge materials (a) Platinum and (b) Silver



Fig. A3: Digital Temperature Controlled Furnace



(a)



(b)



(c)

Fig. A4: Highly conducting materials (a) Platinum paste (b) Thinner and (c) CNT powder



Fig. A5: Mixture of platinum/CNT in a beaker

Tip sonicator is used to convert ultrasonic power supply 50/60 Hz into high frequency mechanical vibrations. The ultrasonic vibrations are intensified by the probe and focused at the tip where the atomization takes place. VCX digitally displays the actual amount of energy that being delivered to the probe and terminates the ultrasonics when the desired amount of energy has been dispensed.

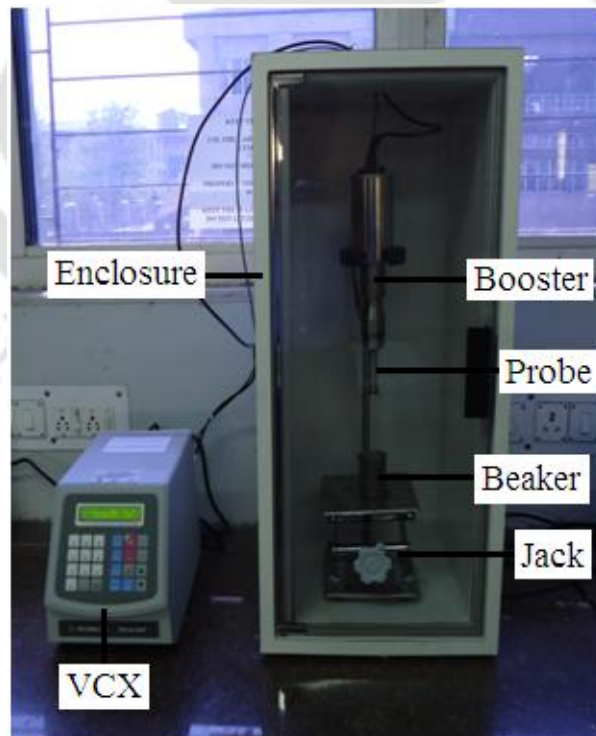
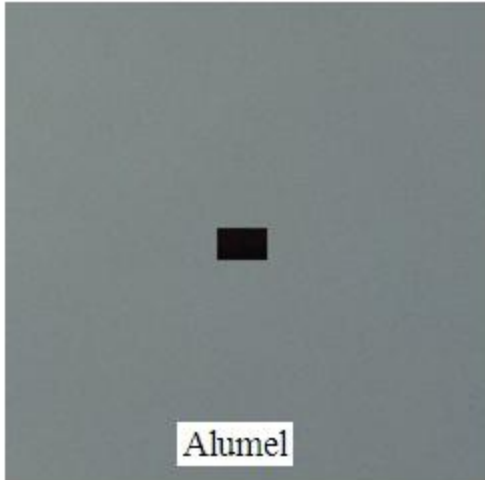


Fig. A6: Experimental set up of the tip sonicator



(a)



(b)



(c)



(d)



(e)



(f)

Fig. A7: Coaxial thermocouple wires and instrument (Grinding machine) used in this work



(a)



(b)

Fig. A8: Sensor thickness measurement analysis by using (a) Experimental setup of profilometry and (b) Dial-type Vernier Caliper

Appendix - II

Table.1: Thermal properties of gauge and substrate materials (Vidal 1956)

	Thermal conductivity (W/m.K)	Specific heat (J/kg.K)	Density (kg/m ³)
Platinum	72	130	21450
Nickel	91	540	8900
Silver	430	230	10490
Pyrex	1.1	840	2230
Macor	1.4	790	2520
Chromel	17.846	447.88	8730
Alumel	27.463	523.336	8600

Table.2: Thermal properties of nano materials (Hwang et al. 2006)

	MWCNT	Fullerene	<i>Cuo</i>	<i>Sio</i> ₂	<i>H</i> ₂ <i>o</i>	Ethylene glycol	Oil
K (W/m.K)	3000	0.4	76.5	1.38	0.613	0.252	0.107
Density (g/cm ³)	2.6	1.6	6.32	2.22	1	1.11	0.915
L	10-50 m	10 nm	33 nm	12 nm	---	---	---
D	10-30 nm	---	---	---	---	---	---

Appendix - III

Thermal Product of Chromel and Alumel Materials

Calibration of the thermocouple requires the determination of thermal product accurately. There are two different thermocouple elements with an insulator in between them. The thermal product,

$(\beta = \sqrt{\rho ck})$ of the surface junction is influenced by the weighting factor of each material's thermal property. It is reasonable to use a weighing factor of 0.5 for each element. The coaxial thermocouple wires (chromel and alumel) are purchased from the vendor in the form of chromel wire of diameter 3.25mm and constantan wire of diameter 1.25mm respectively. For determination of average thermal product of the substrate materials the following data were generated from empirical relations as discussed in section 3.3.3.

Table.3: Thermal properties of alumel and chromel materials at different temperature (Buttsworth 2001)

Temperature (K)	Thermal conductivity (W/m.K)		Specific heat (J/kg.K)	
	Alumel	Chromel	Alumel	Chromel
300	27.463	17.846	523.336	447.88
300.1	27.46598	17.84791	523.3435	447.8979
300.2	27.46896	17.84982	523.351	447.9157
300.3	27.47194	17.85174	523.3585	447.9336
300.4	27.47492	17.85365	523.366	447.9514
300.5	27.47791	17.85556	523.3736	447.9693
300.6	27.48089	17.85747	523.3811	447.9872
300.7	27.48387	17.85938	523.3886	448.005
300.8	27.48685	17.8613	523.3961	448.0229
300.9	27.48983	17.86321	523.4036	448.0407
301	27.49281	17.86512	523.4111	448.0586

Table.4: The mean value of thermal product at different temperature

Temperature (K)	Chromel (β_1) J/(m ² s ^{0.5} K)	Alumel (β_2) J/(m ² s ^{0.5} K)	Mean (β) J/(m ² s ^{0.5} K)
300	8353.306	11097.4	9725.355
300.2	8354.534	11098.771	9726.653
300.4	8355.762	11100.140	9727.951
300.6	8356.990	11101.508	9729.249
300.8	8358.218	11102.876	9730.547
301	8359.446	11104.243	9731.844
301.2	8360.673	11105.611	9733.142
301.4	8361.901	11106.979	9734.440
301.6	8363.129	11108.346	9735.738
301.8	8364.357	11109.714	9737.035
302	8365.584	11111.081	9738.333
302.2	8366.812	11112.448	9739.630
302.4	8368.040	11113.815	9740.928
302.6	8369.267	11115.182	9742.225
302.8	8370.495	11116.549	9743.522
303	8371.722	11117.916	9744.819

Appendix - IV

Uncertainty Analysis

Uncertainty analysis also measure the 'goodness' of a result and without such a measurement, it is impossible to judge the fitness of the value as a basis for making decisions relating to health, safety, commerce or scientific excellence. Some form of analysis must be performed on all the experimental data. The analysis may be a simple verbal appraisal of the results or it may take the form of a complex theoretical analysis of the errors involved in the experiment and matching of the data with fundamental physical principles. A method of estimating uncertainty in experimental results has been presented by (Moffat 1985). The method is based on careful specifications of the uncertainties in the various primary experimental measurements at different experimental setup. For example, a certain pressure reading might be expressed as

$$P = 100kN / m^2 \pm 1kN / m^2 \quad (A.1)$$

Here, \pm notation is used to designate the uncertainty, the designation is stating the degree of accuracy with which the measurement has been made. Suppose a set of measurements is made then, the uncertainty in each measurement may be expressed with the same odds. These measurements are used to calculate some desired results of the experiments, to estimate the uncertainty in the calculated result on the basis of the uncertainties in the primary measurements.

The result R is a given function of the independent variables $x_1, x_2, x_3, \dots, x_n$. Thus,

$$R = R(x_1, x_2, x_3, \dots, x_n) \quad (A.2)$$

Let w_R be the uncertainty in the result and $w_1, w_2, w_3, \dots, w_n$ be the uncertainties in the independent variables. If the uncertainties in the independent variables are all given with the same odds, then the uncertainty in the result having these odds is given as,

$$w_R = \left[\left(\frac{\partial R}{\partial x_1} w_1 \right)^2 + \left(\frac{\partial R}{\partial x_2} w_2 \right)^2 + \dots + \left(\frac{\partial R}{\partial x_n} w_n \right)^2 \right]^{1/2} \quad (\text{A.3})$$

In the experimental investigations, uncertainty assessment deals with the accuracies involved in the instruments and subsequently its effects in the global measurements. The instruments used in the present investigations include laser source, heat conduction unit, oil-bath calibration unit, data acquisition system involving amplifier and oscilloscopes. An INA 128 amplifier (eight pin, dual in-line package and three op-amp design) that operates at a power supply of $\pm 18\text{V}$ has been used in this work. This amplifier offers excellent accuracy by which the sensor output signal can be amplified by 350 times by controlling a variable resistor attached to the circuit. Also, it filters out the noise before the signal is recorded in the oscilloscope.

Based on the manufacturer's specification the accuracy for thermometer, data acquisition system, amplifier, oscilloscope, laser wattage and heat conduction unit are $\pm 0.01^\circ\text{C}$, $\pm 0.015\%$, $\pm 0.015\%$, $\pm 0.02\%$, $\pm 0.01\%$ and $\pm 0.12\%$ respectively. The uncertainty analysis has been performed by process for TCR, transient temperatures and heat flux calculations, by using sequential perturbation technique as shown in Eq. A.3 (Moffat 1985). The average value of overall uncertainties of temperature measurements and heat flux calculation, estimated in the calibration experiments for platinum TFGs, Platinum/Nanomaterial based TFG and Coaxial thermocouple sensors are as shown in Table. 5.

Table.5: Uncertainty values of handmade heat transfer gauges

	Platinum based TFG	Platinum/Nanomaterial based TFG	Coaxial Thermocouple
TCR	$\pm 0.23\%$	$\pm 0.236\%$	$\pm 0.25\%$
Transient temperature signals	$\pm 0.28\%$	$\pm 0.287\%$	$\pm 0.30\%$
Transient heat flux signals	$\pm 0.32\%$	$\pm 0.35\%$	$\pm 0.40\%$